PROJECT NO.: **NMC-1779-WRC**

NATIONAL MISSION FOR CLEAN GANGA

Ministry of Jal Shakti, Govt. of India

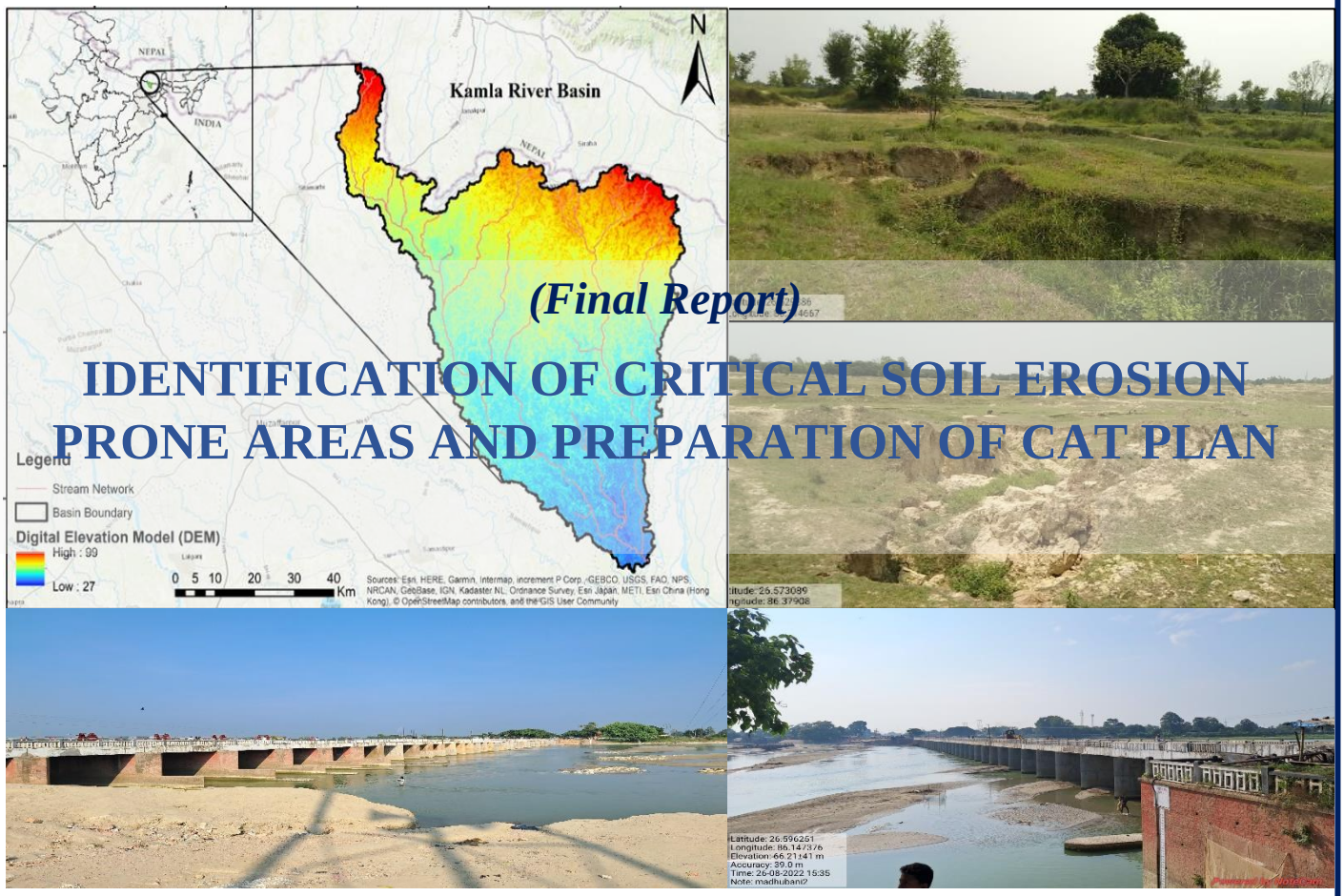

(Final Report)

IDENTIFICATION OF CRITICAL SOIL EROSION PRONE AREAS AND PREPARATION OF CAT PLAN

Submitted by

Dr. Ashish Pandey, Professor & Principal Investigator (P.I.)
Dr. Mohit P. Mohanty, Assistant Professor & Co-P.I.
Dr. Gagandeep Singh (RA), Mr. Dilip Barman (JRF)
Department of Water Resources Development and Management
Indian Institute of Technology Roorkee
Roorkee (Uttarakhand) 247667, India

March 2024

Preface

As we delve into the intricate realm of soil erosion dynamics and its far-reaching consequences on ecosystems, agricultural lands, and water resources, this project report aims to unravel the complexities surrounding soil erosion assessment and management strategies. The escalating threats posed by soil erosion prompted the need for comprehensive and sophisticated approaches, especially in sustainable land use planning.

This endeavor unfolds against the backdrop of alarming statistics; in India alone, approximately 5334 million tonnes of soil are detached annually, emphasizing the urgency to address this critical issue. The repercussions of soil erosion, closely tied to factors such as steep slopes, climatic conditions, and land use patterns, extend beyond the loss of organic matter and topsoil. It impacts water and nutrient-holding capacity, creating challenges for agricultural productivity and ecosystem health.

This study focuses on the Kamla River Basin (KRB) in the Indian subcontinent, which has long been impacted by various factors leading to extensive soil erosion and soil detachment into streams. The removal of protective soil cover, particularly through the clearing of forest vegetation, has exacerbated erosion in the catchment. In response to these challenges, the report explores three prominent soil erosion assessment models—Revised Universal Soil Loss Equation (RUSLE), Integration of Spatially Explicit Watershed Modeling with the Sediment Delivery Ratio (InVEST-SDR), and Modified Universal Soil Loss Equation (MUSLE). The synthesis of these models aims not only to evaluate the spatial and temporal distribution of soil loss in the lower region of KRB but also to establish a foundation for a targeted Catchment Area Treatment Plan, strategically managing soil erosion in the area.

The significance of the project lies not only in the exploration of these advanced models but also in their application to real-world scenarios. The objectives encompass identifying vulnerable areas, establishing the relationship between runoff and sediment yield, prioritizing sub-watersheds, and formulating a Catchment Area Treatment (CAT) plan using SYI technique for strategic soil conservation.

This report not only contributes to the body of knowledge but also provides valuable insights for policymakers and land managers. We hope the findings inspire informed decision-making and effective soil conservation strategies for a sustainable future.

TABLE OF CONTENTS

Chapter	Particular	Page No.
	Project Description	1
1	Introduction	2-6
2	Study Area and Data Description	7-23
	2.1 Kamla River Basin (KRB) at Jhanjharpur Outlet- India and Nepal	7
	2.1.1 Challenges in KRB	8
	2.2 Lower Kamla River Basin (LKRB)	9
	2.3 Data and sources	15
	2.3.1 Data used for KRB	15
	2.3.2 Data used for LKRB	18
	2.3.2.1 Land Use/ Land Cover	18
	2.3.2.2 Slope Map	20
	2.3.2.3 Soil Data	21
	2.3.2.4 Delivery Ratio (DR)	23
3	Methodology	24-38
	3.1 Soil Loss Estimation using RUSLE Model	24
	3.1.1 Database Generated for Calculating Factors of RUSLE Model	25
	3.2 InVEST Sediment Delivery Ratio (SDR) model description	28
	3.2.1 Soil Loss Estimation	28
	3.2.2 Sediment Delivery Ratio	28
	3.2.3 Sediment yield	30
	3.2.4 InVEST-SDR Model Parameter Calculation	31
	3.3 Modified Universal Soil Loss Equation (MUSLE)	32
	3.4 Silt Yield Index (SYI) and Sub-watershed Prioritization	35
	3.5 Catchment Area Treatment Planning	38
4	Results and Discussion	39-91
	4.1 Soil Loss Estimated using RUSLE Model	39
	4.1.1 Thematic Maps of USLE Factors	39
	4.1.2 Spatial Distribution of Soil Erosion	43

Chapter	Particular	Page No.
	4.1.3 Inferences- RUSLE	46
	4.2 Soil erosion simulated using InVEST-SDR model	48
	4.2.1 Calibration results	48
	4.2.2 Soil loss and sediment export	50
	4.2.3 Inferences-InVEST-SDR model	55
	4.3 Sediment Yield Estimation using MUSLE	57
	4.3.1 Data Processing for MUSLE	57
	4.3.2 Model Calibration and Verification	59
	4.3.3 MUSLE model for the Catchment (Janjharpur Outlet)	61
	4.3.4 Inferences-MUSLE	62
	4.4 SYI Model	62
	4.4.1 Composite Erosion Intensity Mapping	62
	4.4.2 Computation of Sediment Yield Index (SYI)	64
	4.4.3 Prioritization of sub-watersheds in lower KRB based on SYI	68
5	Catchment Area Treatment Plan	72
	5.1 Catchment area treatment	72
	5.2 Biological Measures	73
	5.2.1 Restoration of Degraded Areas	73
	5.2.2 Afforestation	73
	5.2.3 Fodder Plantation	73
	5.2.4 Plantation of Horticulture Crops	73
	5.2.5 Pasture Development	73
	5.2.6 Non-Timber Forest Product (NTFP) Cultivation	74
	5.2.7 Measures for Cropped Areas	74
	5.2.8 Measures for areas with Tree Cover	74
	5.3 Engineering Measures	75
	5.3.1 Field Bunding	75
	5.4 Treatment of Individual Sub-watersheds	76
	5.4.1 Sub-watershed -5	78
	5.4.2 Sub-watershed-1	81

Chapter	Particular	Page No.
	5.4.3 Sub-watershed -8	84
	5.4.4 Sub-watershed -10	87
	5.4.5 Sub-watershed -11	90
	5.4.6 Sub-watershed -12	93
	5.5 Cost Analysis of Different Works Under Plan	96
	5.5.1 Biological Measures	96
	5.5.2 Engineering Measures	96
6	Summary and Conclusions	99
	6.1 Summary	99
	6.1.1 Soil loss estimation using RUSLE	100
	6.1.2 Soil Erosion modeling using InVEST-SDR model	101
	6.1.3 Sediment Yield Estimation using MUSLE	102
	6.1.4 Sub-watershed prioritization using SYI	102
	6.1.5 Recommendations for soil conservation measures through a Catchment Area Treatment Plan	103
	6.2 Conclusions	103
	6.3 Future Scope	104
	References	105
	Annexures	108-123

LIST OF FIGURES

Figure No.	Title	Page No.
Figure 2.1	Location map of the KRB upstream of Jhanjharpur	7
Figure 2.2	Location map of the lower region of KRB	9
Figure 2.3	Annual rainfall anomaly over the period 1980-2020	10
Figure 2.4	Spatial distribution of average annual rainfall over the period (1980-2020)	11
Figure 2.5	Drainage pattern and canal system in the lower KRB	12
Figure 2.6	Soil map of the lower region of LKRB	13
Figure 2.7	Location of sampling points for estimating SSC	14
Figure 2.8	Location of gauging sites	15
Figure 2.9	Land use land cover of the Lower Kamla River Basin	19
Figure 2.10	Slope map of the study area (%)	20
Figure 2.11	Soil Map of the Lower Kamla River Basin	22
Figure 2.12	Spatial distribution of the delivery ratio	23
Figure 3.1	Methodology flowchart for RUSLE	24
Figure 3.2	Conceptual representation of the index of connectivity, adapted from Borselli et al. (2008)	29
Figure 3.3	Sigmoid function used to convert the connectivity index IC to the SDR factor. The maximum value of SDR is set to SDRmax = 0.8. The effect of the calibration is illustrated by setting kb = 1 and kb = 2 (solid and dashed lines, respectively), and IC0 = 0.5 and IC0 = 2 (black and gray dashed lines, respectively).	30
Figure 3.4	Schematic flow chart for micro-watershed prioritization using SYI	36
Figure 4.1	(a, b, and c): Spatial distribution of R-factor for the years 2000, 2010 and 2020, respectively	39
Figure 4.2	Spatial distribution of Soil erodibility factor (K factor)	40
Figure 4.3	Topographic factor of the basin	41
Figure 4.4	Spatial distribution of C and P factors for the years 2000, 2010, and 2020.	42, 43

Figure No.	Title	Page No.
Figure 4.5	Soil erosion risk map of lower Kamla basin (A) 2000 (B) 2010 and (C) 2020	45
Figure 4.6	Verification of soil erosion with Google earth pro image	47
Figure 4.7	Correlation between observed sediment and simulated sediment	49
Figure 4.8	Expected Annual Soil Loss in tons/pixel/year for 2007, 2008, 2009, 2010, 2011, and 2012	50
Figure 4.9	Expected Annual Soil Loss in tons/pixel/year for 2020	53
Figure 4.10	Box and whisker plot for the sediment data at Jhanjharpur gauging station	59
Figure 4.11	Outlier count among the daily sediment concentration observed values	59
Figure 4.12	Observed versus simulated sediment yield for the model calibration	60
Figure 4.13	Observed versus simulated sediment yield for the model verification	61
Figure 4.14	Composite Erosion Intensity Mapping Unit (CEIU) of lower KRB	64
Figure 4.16	Treatment priority for the catchment of the Lower Kamla River basin	70
Figure 4.17	(a) and (b) Agricultural fallow lands (mono-cropping pattern), (c) Gully formation, and (d) Unprotected riverbank	71
Figure 5.1 (a)	Land Use/ Land Cover map of SW-5	79
Figure 5.1 (b)	Composite Erosion Intensity Unit (CEIU) map of SW-5	80
Figure 5.2 (a)	Land Use/ Land Cover map of SW-1	82
Figure 5.2 (b)	Composite Erosion Intensity Unit (CEIU) map of SW-5	83
Figure 5.3 (a)	Land Use/ Land Cover map of SW-8	85
Figure 5.3 (b)	Composite Erosion Intensity Unit (CEIU) map of SW-8	86
Figure 5.4 (a)	Land Use/ Land Cover map of SW-10	88
Figure 5.4 (b)	Composite Erosion Intensity Unit (CEIU) map of SW-10	89
Figure 5.5 (a)	Land Use/ Land Cover map of SW-11	91
Figure 5.5 (b)	Composite Erosion Intensity Unit (CEIU) map of SW-11	92
Figure 5.6 (a)	Land Use/ Land Cover map of SW-12	94
Figure 5.6 (b)	Composite Erosion Intensity Unit (CEIU) map of SW-12	95

LIST OF TABLES

Table No.	Title	Page No.
Table 2.1	Details of inputs used in the InVEST-SDR model	16
Table 2.2	Annual Sediment load (tons) at Jhanjharpur Gauging site	17
Table 2.3	Information on the key datasets utilized for soil loss estimation based on RUSLE and GIS	18
Table 2.4	Areas under different land use/ land cover classes in the catchment	19
Table 2.5	Slope area under different classes	21
Table 2.6	Soil classes in the Lower KRB (NBSS & LUP)	22
Table 2.7	Values of delivery ratio used in the study	23
Table 3.1	Crop management factor for different land use/land cover classes	27
Table 3.2	Values of C and P factors used in the InVEST model	31
Table 3.3	Summary of MUSLE model inputs for the catchment	34
Table 4.1	Percentage of the area under different soil erosion classes	44
Table 4.2	Yearly sub-basin-wise soil erosion estimated by RUSLE during 2000-2020	46
Table 4.3	Observed and simulated sediment at Jhanjharpur for k_b=5, IC_0=-15	49
Table 4.4	Simulated results using calibrated parameters kb=5, IC0=-15 for LKRB	51
Table 4.5	Simulated results using calibrated parameters kb=5, IC0=-15 for LKRB for 2020	54
Table 4.6	Yearly sub-basin-wise soil erosion estimated by RUSLE during 2000-2012 and 2020	55
Table 4.7	Comparison of annual soil loss (tons/ha/year) estimated by RUSLE and InVEST	56
Table 4.8	Statistical metrics for the observed sediment data at Jhanjharpur gauging station	58
Table 4.9	Summary of calibration and verification of the model at Jhanjharpur gauging site	60
Table 4.10	Key factors used for evaluation of composite erosion intensity mapping	62
Table 4.11	Output key for erosion intensity mapping	63
Table 4.12	Erosion intensity classification for the study area	63
Table 4.13	Prioritized SYI value of erosion intensity rates	65

Table 4.14	Priority rating of sub-watersheds of lower KRB as per calculated SYI	65
Table 4.15	Sub-watersheds under different priority zones	70
Table 5.1	Priority category of sub watersheds using Sediment Yield Index (SYI) for different erosion intensities	76
Table 5.2 (a)	Sub-watershed wise Area (ha) Composite Erosion Intensity Unit (CEIU) in the Lower Kamla River basin	77
Table 5.2 (b)	Sub-watershed wise (%) Composite Erosion Intensity Unit (CEIU) in the Lower Kamla River basin	77
Table 5.3 (a)	Cost estimate for biological measures	97
Table 5.3 (b)	Cost estimate for biological measures	97
Table 5.4	Total cost estimate for biological measures	98

Chapter 1: Introduction

1.1 Background

The escalating threats posed by soil erosion to ecosystems, agricultural lands, and water resources necessitate comprehensive and sophisticated approaches for assessment and management. In the pursuit of sustainable land use planning, understanding soil erosion dynamics and identifying critical areas within a watershed are paramount.

In India, about 5334 m-tonnes of soil is being detached annually for various reasons (Narayana et al., 1983), and the rate of soil erosion is approximately 16.40 Mg ha^{-1} $year^{-1}$(Narayana *et al.,* 1983). Erosion levels are very high in Asia, Africa, and South America, where erosion rates vary from 30 to 40 Mg ha^{-1} $year^{-1}$ (Barrow, 1991). Erosion is triggered by a combination of factors, such as steep slopes, climate (e.g., long dry periods followed by heavy rainfall), inappropriate land use, and land cover patterns (Renschler *et al.,* 1999). Erosion ultimately leads to the loss of organic matter (Kisic *et al.*, 2018) and the loss of the topsoil that provides water- and nutrient-holding capacity (Keesstra *et al.,* 2018).

Direct field measurements of soil erosion can provide accurate runoff and net soil erosion but are time-consuming and costly to estimate large-scale soil erosion (Girmay et al., 2020). Therefore, several soil erosion models have been proposed in recent years, among which the Universal Soil Loss Equation (USLE) (Wischmeier and Smith, 1978) and the Revised Universal Soil Loss Equation (RUSLE) (Renard, 1997) are the most widely used. Many scholars have studied and refined the calculation methods of each factor of the (R)USLE model (McCool et al., 1989; Renard and Freimund, 1994; Yu and Rosewell, 1996), making the (R)USLE model applicable worldwide and validated in most regions.

In recent years, Remote Sensing data, i.e., Digital Elevation Model (DEM), satellite imageries have been widely employed to investigate and estimate soil loss for sub-watersheds prioritization and soil water conservation measures (Pandey et al., 2009; Bhattacharya *et al.,* 2020). Singh and Phadke (2006) estimated soil loss in Jamni River Basin, Bundelkhand region, India, adopting USLE using GIS and identified priority areas of the basin for future planning of watershed and its sustainable development. Pandey *et al.* (2007) identified critical erosion-prone areas in a small agricultural watershed of Karso, Jharkhand, India, using USLE, GIS, and Remote Sensing (RS). Average annual sediment yield data on a grid basis was estimated using USLE. Dabral *et al.* (2008) conducted a study on soil erosion assessment of the Dikrong river basin of Arunachal Pradesh (India). In a later work, Pandey *et al.* (2009) assessed the

sediment yield from the Dikrong river basin of Arunachal Pradesh, India, employing RS and GIS and using the Morgan-Morgan-Finney (MMF) model and USLE. Mandal and Sharda (2013) identified soil erosion risks in the eastern Himalayan region of India by integrating spatial data on prevailing erosion rates and soil loss tolerance limits in the GIS environment.

The (R) USLE model has gained new developments in recent years. The concept of sediment delivery ratio (SDR), the ratio of the amount of sediment transported at a certain section of the watershed to the total erosion of the watershed, has been introduced with the concept of runoff and sediment transport, making it possible to use (R) USLE to estimate sediment export and sediment retention (Jain and Das, 2010; Thomas et al., 2018a). Some example models are (R)USLE-SDR (Kaffas et al., 2021), WaTEM/SEDEM (Winterová et al., 2022) and SEDD (Mirakhorlo and Rahimzadegan, 2020). Different methods for estimating SDR have been studied by many scholars. Marques et al. (2019) used the USLE-SDR model to calculate the total soil erosion and sediment yield in the west-central Brazilian catchment, while Thomas et al. (2018b) estimated the gross soil erosion and net erosion of a rain shadow river basin in the southern Western Ghats based on RUSLE-TLSD.

Although the USLE model considers factors such as rainfall, topography, soil erodibility, soil conservation measures, and vegetation cover, it does not consider the ability of the land mass itself to intercept upstream sediments. Overall, the USLE model can only estimate gross soil erosion per unit area per unit of time and cannot directly calculate sediment export yield. (R)USLE models also have difficulty in predicting export sediment from a given watershed (de Vente et al., 2013).

The sediment delivery ratio (SDR) of the InVEST (Integrated Valuation of Ecosystem Services and Tradeoffs) model integrates the USLE equation and the studies of Borselli et al., 2008 and Vigiak et al., 2012 to obtain the spatial distribution of sand production in the watershed by calculating the ratio of soil erosion and sediment transport (Hamel et al., 2015). Many scholars have used the InVEST-SDR model to estimate soil erosion and sediment transport at different geographical scales with good results (Aneseyee et al., 2020; Gashaw et al., 2021).

The InVEST-SDR model combines RUSLE and Sediment Delivery Ratio using a distributed approach (pixel level analysis), and was developed to better estimate grid-wise soil loss and sediment yield from the streams. This model represents a cutting-edge approach to soil erosion assessment by integrating Geographic Information System (GIS) technologies and hydrological modeling. It enables the quantification of sediment delivery from various land

surfaces to downstream water bodies, aiding in the identification of areas most susceptible to soil erosion. As a decision support tool, InVEST-SDR contributes to sustainable land management practices by providing valuable insights into the spatial distribution of erosion risk. These advancements have significantly enhanced the accuracy and applicability of soil erosion models, enabling more effective erosion control and land management strategies.

A major limitation of the USLE model is that it was developed to estimate soil erosion at the plot and annual time scales. Therefore, its application to storm-wise sediment yields at the watershed scale may lead to substantial errors (Alewell et al., 2019). Consequently, the MUSLE was developed as a watershed-based model to estimate the sediment yield produced by individual storm events, replacing the rainfall factor from the traditional USLE with a runoff factor as a function of runoff volume (Q) and peak discharge (Q_p) (Williams, 1975). Many studies have evaluated MUSLE globally under varying conditions (Sadeghi and Mizuyama, 2007, Arekhi et al., 2012, Gwapedza et al., 2018, Gwapedza et al., 2021). MUSLE is also used as a sub-model within established models, such as the Soil and Water Assessment Tool (SWAT) (Neitsch et al., 2011), the Agricultural Catchments Research Unit (Schulze and Horan, 2007), and the Water Quality Systems Assessment Model (Hughes, 2013, Slaughter et al., 2015).

In the original MUSLE model, the soil erodibility factor (K), topographic factor (LS), cover management factor (C_m), and support practice factor (P_s) were adopted to reflect the effects of geomorphologic characteristics of soil properties, topography (such as slope length and steepness), land use and land cover, and support practice regarding sediment yield. However, few studies have considered channel characteristics that may reflect the sediment transport capacity in the MUSLE model for sediment yield prediction. For the hydrological factors, the product of runoff volume (Q) and peak discharge (Q_p) is used in the MUSLE model. It is necessary to consider runoff and peak discharge models as components of the sediment yield model to study the sediment yield in ungauged or poorly gauged watersheds. The Natural Resources Conservation Service (formerly known as the Soil Conservation Service) Curve Number (SCS-CN) method (SCS, 1972) is one of the most widely used models for estimating surface runoff. During the past four decades, many modified versions of the original SCS-CN model have been developed for various applications. (Mishra et al., 2008, Sahu et al., 2010, Babu and Mishra, 2012, Singh et al., 2015, Walega et al., 2019, Shi and Wang, 2020).

Based on the soil erosion and sediment yield modeling results, critical soil erosion-prone areas can be identified, and recommendations of best management practices can then be carried out from the soil and water conservation viewpoint considering the criteria suggested by Pandey *et al.* (2011). Therefore, management practices could effectively reduce soil erosion if the magnitude and spatial distribution of soil erosion risk areas are known. The method was found to be an effective way to map the spatial distribution of soil erosion risks in a large area.

The Catchment Area Treatment (CAT) plan pertains to preparing a management plan to treat erosion-prone areas of the catchment through biological and engineering measures (Khadse et al., 2015); however, a comprehensive CAT plan should also include the social dimensions associated directly or indirectly with the catchment. An effective CAT plan is crucial in making an eco-friendly and sustainable strategy to develop the area of interest. A detailed database on natural resources, terrain conditions, soil type of the catchment area, socioeconomic status, etc., is a prerequisite to preparing a treatment plan keeping in view the concept of sustainable development. Due to the spatial variability of the site parameters such as soils, topography, land use, and rainfall, all areas do not contribute to erosion equally. Several techniques, like a manual overlay of spatially index-mapped data, shall be used to estimate soil erosion in complex landscapes. To ensure that the latest and most accurate data is used for the analysis, satellite data shall be used for deriving land use data, and ground truth studies, too, shall be conducted.

1.2 Objectives of the study

The present study is conducted over a part of the Kamla River Basin (KRB) located within the Indian sub-continent. Unfortunately, the above state of conditions has long been disturbed in the region by several factors causing widespread soil erosion resulting in soil detachment and its transport into the streams. Primarily, removing the protective soil cover in the form of forest vegetation has resulted in the present state of erosion in the catchment. In view of the above, this study embarks on the exploration of three prominent soil erosion assessment models—Revised Universal Soil Loss Equation (RUSLE), Integration of Spatially Explicit Watershed Modeling with the Sediment Delivery Ratio (InVEST-SDR), and Modified Universal Soil Loss Equation (MUSLE). The synthesis of these models aims not only to assess the spatial and temporal distribution of soil loss in the lower region of KRB but also to lay the groundwork for a targeted Catchment Area Treatment Plan for strategic management of soil erosion.

1. The identification of vulnerable areas in the representative catchment of the Kamla River Basin using USLE/RUSLE, GIS, and remote sensing data
    - Soil loss estimation using RUSLE
    - Soil loss estimation using the InVEST-SDR model
    - Sediment yield modeling using MUSLE
    - Prioritization of sub-watersheds based on SYI
2. Preparation of Catchment Area Treatment (CAT) plan for recommendation of soil conservation measures in the vulnerable areas of the catchment

Chapter 2: Study Area and Data Description

2.1 Kamla River Basin (KRB) at Jhanjharpur Outlet- India and Nepal

Kamla River Basin, with reference to the outlet at Jhanjharpur in Bihar, India, covers a total drainage area of 3436.43 km^2. 22.69 % of this area, i.e., 779.75 km2, falls in India, and the remaining area is in Nepal. The basin has an elevation ranging from 47.84 above mean sea level (AMSL) in the south part to 2,188 above mean sea level (AMSL)in the northeast.

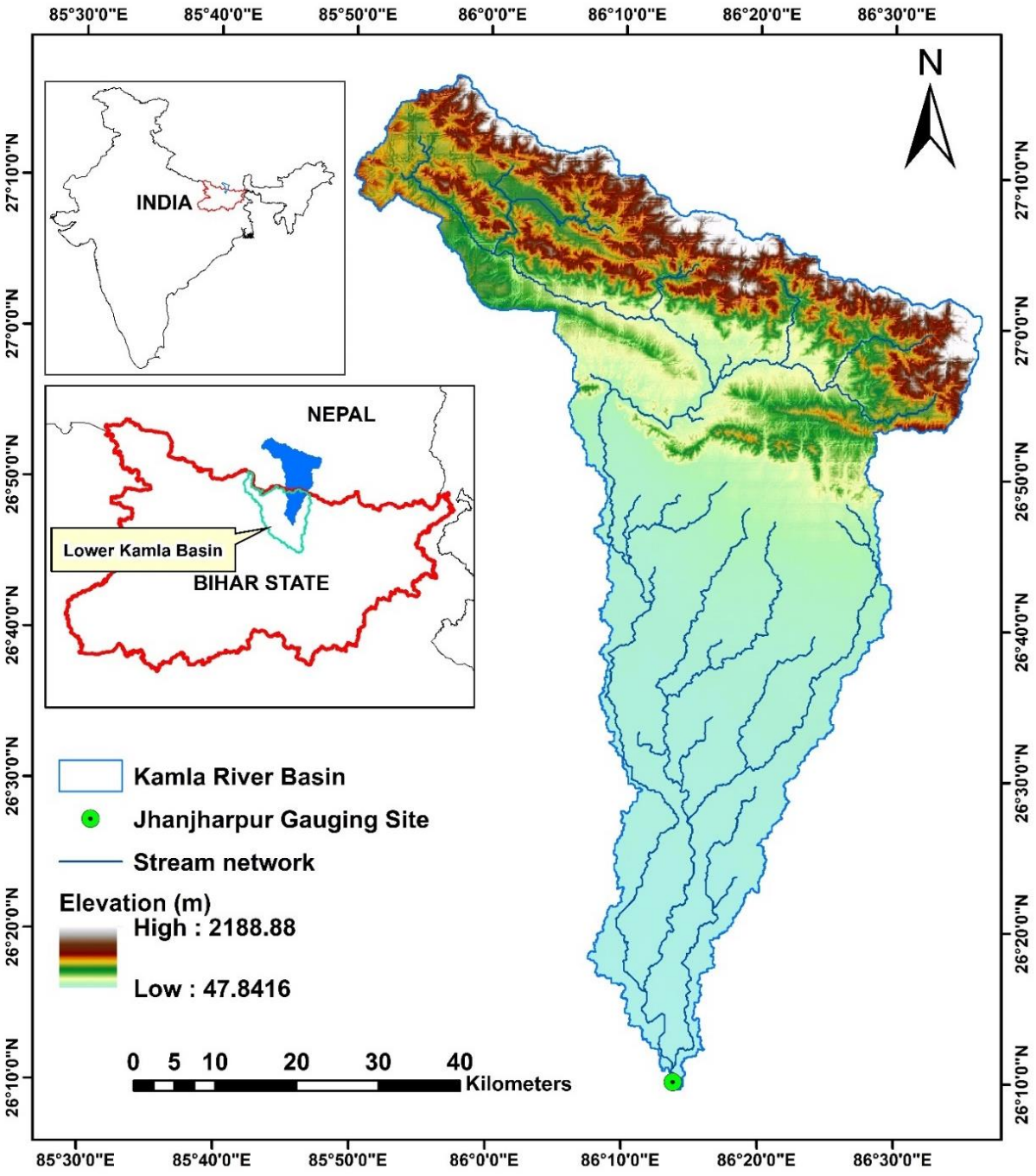

Figure 2.1 Location map of the KRB upstream of Jhanjharpur

Its soil is highly susceptible to erosion, and forests play an important role in soil and water conservation (MFSC, 2016). The Kamla region is hot and humid during the summer monsoon (June to September) and dry and temperate in the winter (December to February). High sediment loads in the Kamla Basin of Nepal cause issues for river stability and flood protection (WECS and CSIRO, 2020). The causes of sediment issues are a combination of natural processes exacerbated by human activities such as deforestation and agriculture. Management responses are particularly expensive. The Government of Nepal, in collaboration with the Government of India, invested in infrastructure projects to manage sediments and river instability in Dhanusha and Siraha with the construction of gabion embankments to control erosion in the Chure (Shivalik rang) area and embankments around the Kamala River and tributaries (WECS and CSIRO, 2020).

2.1.1 Challenges in KRB

Natural sediment processes

Due to fragile strata and loose rock formations, the Shivalik hills of Nepal are vulnerable to landslides and soil erosion (GoN, 2017). The Middle Mountains have Karst systems in addition to the predominant sandstone, mudstone, conglomerate, shale, and claystone rock types. Eroded topsoil and loose inorganic rock fragments from the upland regions are carried downstream by rainfall events. Large amounts of silt can be transported by landslides, especially during more intense episodes. Adhikari (2013) suggested that one of the primary sources of sediment load for the rivers coming from the southern part of the Basin is the Chure region.

In the valleys, braided river channels (anastomosing) with numerous in-channel features, such as sand and gravel bars, are produced by coarse and mixed texture silt, which is influenced by slope and river transit capacity. The river channels in the basin are made up of a mixture of sediments that are distributed across the river corridor, as well as boulders, gravels, sands, and finer particles. As one moves downstream, the composition of the particles shifts, going from gravel and sand to a greater amount of silts and sand. A portion of the silt is momentarily deposited on the banks of streams and along river corridors. The slope of the Kamala River decreases as it enters the Terai, and during the rainy season, it frequently changes its shape and route. Sedimentary deposition and river meandering occur naturally across the Gangetic plains, which includes the Terai region (Chakraborty et al., 2010).

Human disturbance of sediment processes

Human activities in the Kamala region disrupt the natural processes of soil erosion and sedimentation, which in turn affects the movement and structure of rivers and creates pathways for deposition. The following three major disturbances are responsible for topsoil loss and sediment erosion: 1) heavy mining of silt for the building sector in Nepal and India; 2) deforestation in the Chure Hills and in the riparian zones; and 3) growth of the unsealed road network. These disturbances are frequently linked to bed rising (aggradation), which causes lateral river migration and noticeable river widening due to streambank erosion. Riverbed levels have increased dramatically as a result of the combined factors that increase the sediment load, and within the past 50 years, about 2 metres of deposition have been recorded in some stretches of the Chure rivers (Adhikari, 2013).

2.2 Lower Kamla River Basin (LKRB)

The Kamla River originates at Sindhuli from the Mahabharata range of Nepal with a maximum elevation of approximately 1200 m and a minimum elevation of 50 m above mean sea level (AMSL) (NDRI, 2016), a tributary of the river Kosi. The river Kamla enters India near Jaynagar, Madhubani district of Bihar State. A major part of the basin is approx. 62% (4,510 km2 out of 7,232 km2) falls in India (hereafter lower KRB catchment- Figure 2.2), while the rest is in southeast Nepal. The total length of the river is 328 km of which 120 km lies in India and the remaining 208 km in Nepal (Figure 2.1).

The lower KRB catchment has many tributaries viz., Tawa, Baijnath, Mainawati, Dhauri, Soni, Balan, Trisula, Chadha, Dhauri, Soni, Balan, Gobarjai, Trishula, and Sugarwe rivers.

The basin consists of three major types of soils: sandy loam, loam, and clay. The loam soil is the dominant type of soil in the basin, mostly agricultural lands, which occupied 62% of the project area; whereas sandy loam soil occupies 26% of the basin area, mostly distributed along the riverbanks, and in the upper north-western part a small area (11%) consisted by the clay soil. The basin experiences a tropical climate with the hottest summer and the coldest winter. Usually, May and June are the hottest months in the basin with an average maximum temperature of 48˚C and a minimum of 28˚C. January is the coldest month and the temperature sometimes falls below 7˚C at some locations. The basin has experienced heavy seasonal rainfall during the South-west monsoon. The annual rainfall of the lower KRB varies from 760 mm to 2010 mm (Figure 2.3) with an average of 1230 mm (1980-2020). About 80% of rainfall occurs

from July to late September in the monsoonal months. Figure 2.4 also shows the spatial distribution of average annual rainfall in the basin (1980-2020).

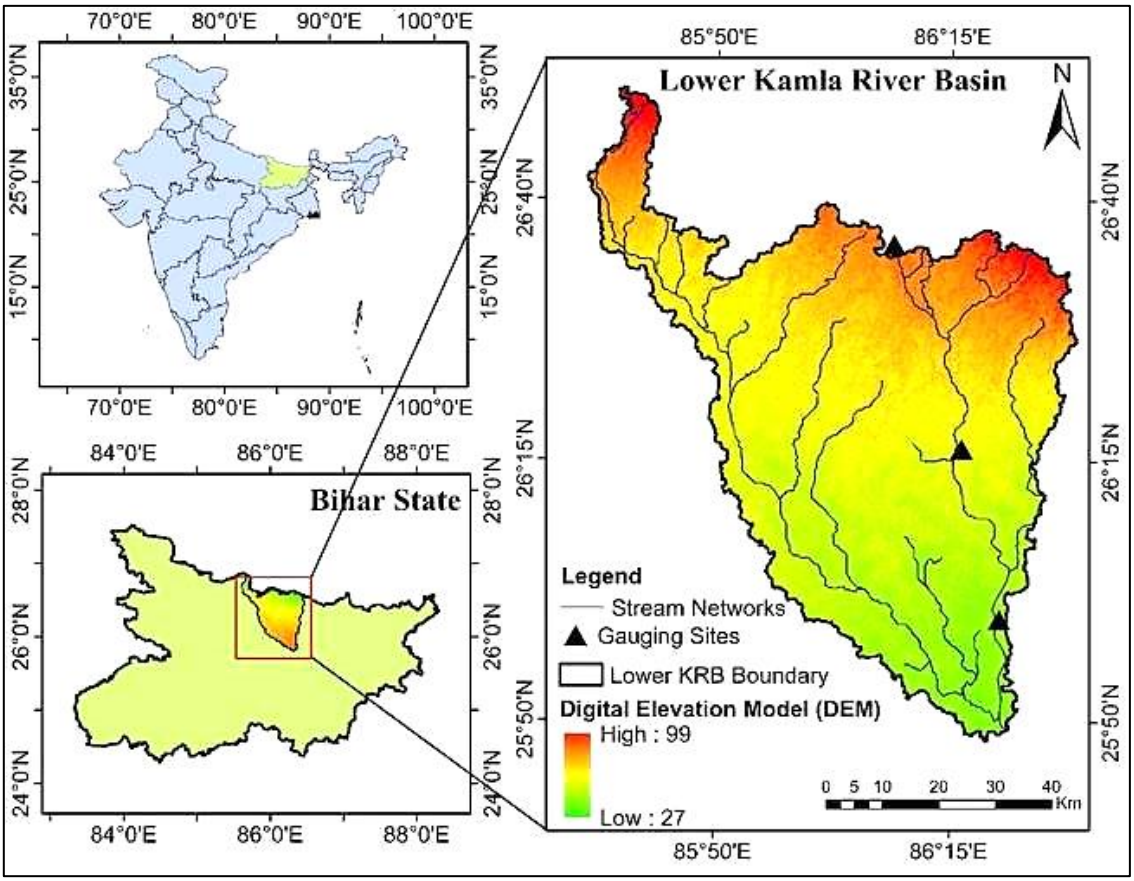

Figure 2.2 Location map of the lower region of KRB

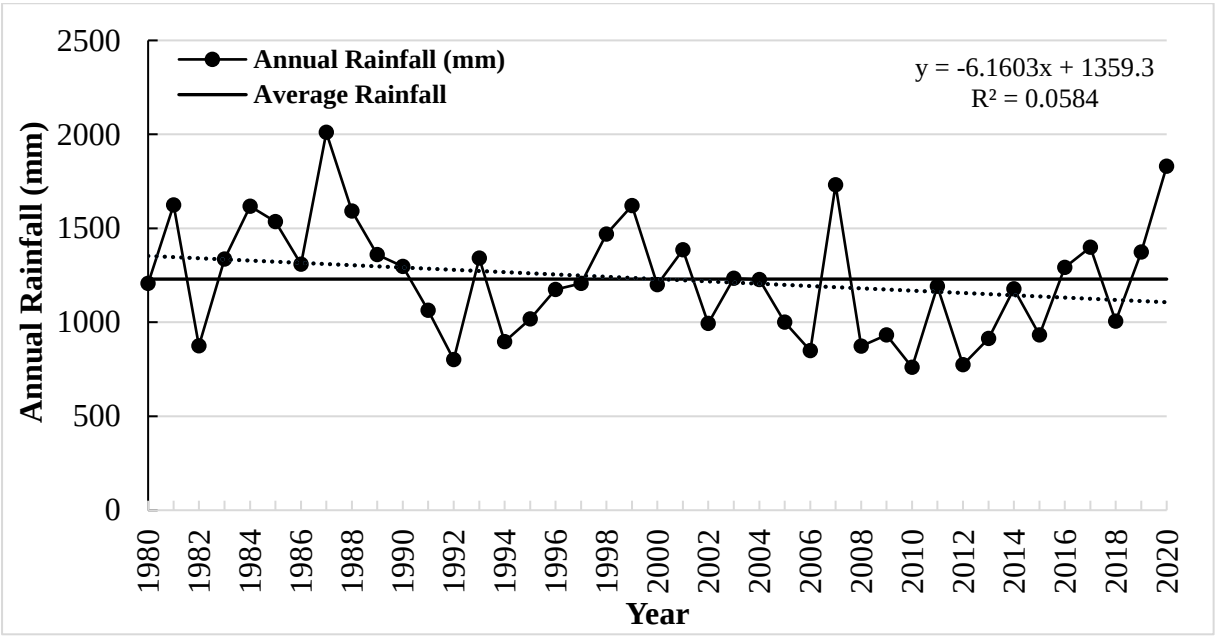

Figure 2.3 Annual rainfall anomaly over the period 1980-2020

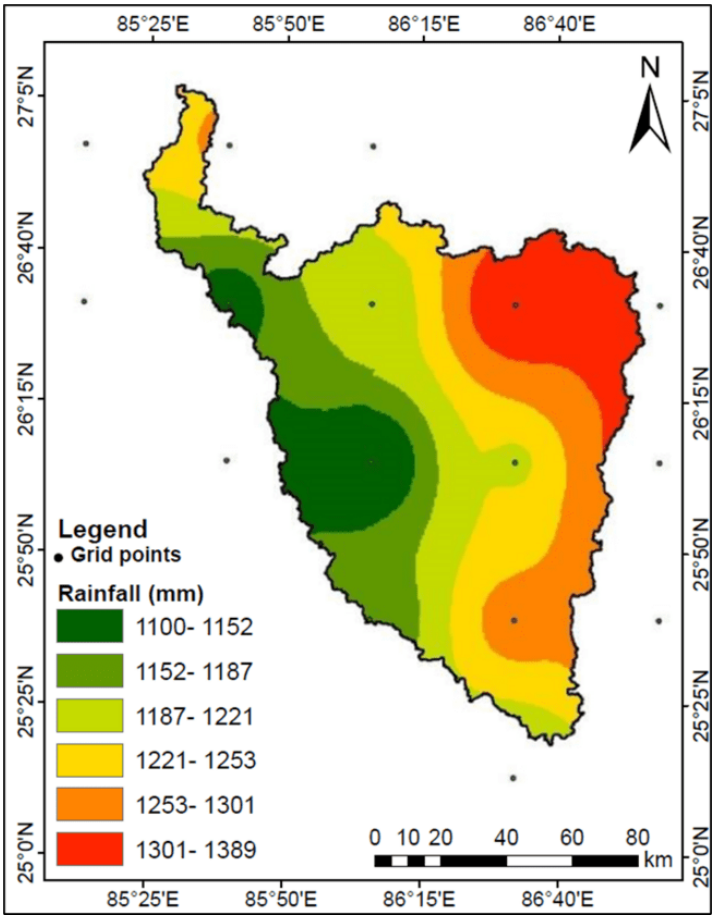

Figure 2.4 Spatial distribution of average annual rainfall over the period (1980-2020)

Cropland is the dominant land use in the region (mostly due to *Kharif* and *rabi* crops), which accounts for approximately two-thirds of its area. Anthropogenic plantations (mainly mango, bamboo, and banana) are the second most dominant land use with a covering area of approx. 17% followed by built-up area is less than 5%. The fertile soil of the basin is mainly used to produce rice, wheat, maize crops, and fruits. The major existing projects consist of the Kamla Irrigation Project, which has an Irrigation command area of 25,000 hectares; during the monsoon, the river floods, causing severe bank erosion and harming over 3.9 million people. The yearly sediment load in the basin is estimated to be around 7 million tonnes (Sehgal *et al.,* 2014).

Like the nearby Koshi River basin, it is also prone to natural hazards such as monsoonal flooding and soil erosion, which significantly negatively impact riverine ecosystem services and basin development (CSIRO and WECS, 2021). The basin experienced its first flood in 1952. Later, floods are the most frequent being experienced in the basin. On the other hand, water-induced soil erosion is also very prominent in the basin. Sah and Lamichhane (2019)

estimated that the potential soil loss was 4329 t $ha^{-1}yr^{-1}$, whereas the total potential soil loss was 1.460 million t $ha^{-1}yr^{-1}$ in the upper catchment of the basin e.g., Sindhuli of Nepal territory. Because of these hazards, the entire KRB has been significantly modified by riverbed extractions, water diversion and abstractions, and other stressors such as floods and erosion.

Drainage and Canal Networks

The river Kamla enters India near Jayanagar and flows in the north-eastern direction, finally meeting in the Kosi rivers near Ichwara, Alauli, and Khagaria districts of Bihar. It passes through the four districts of Bihar: Madhubani, Darbhanga, Samastipur, and Khagaria over a length of 120 km. This basin is located between the Bagmati River Basin and the Kosi River Basin, and annual flooding is characteristic of the basin. The flood plain is usually 0.5 to 1.5 km wide. To control this issue, a system of canals is distributed throughout the whole basin. It also plays a major role in water resource transport for irrigation water supply to crops. Figure 2.4 shows the location of major canals in the basin. The confluence points of the Kamla River with the Bagmati River near Pakariya and with river Kosi near Alauli, ultimately joining the Ganga River. The drainage pattern of the basin and distributed major canals are shown in Figure 2.5.

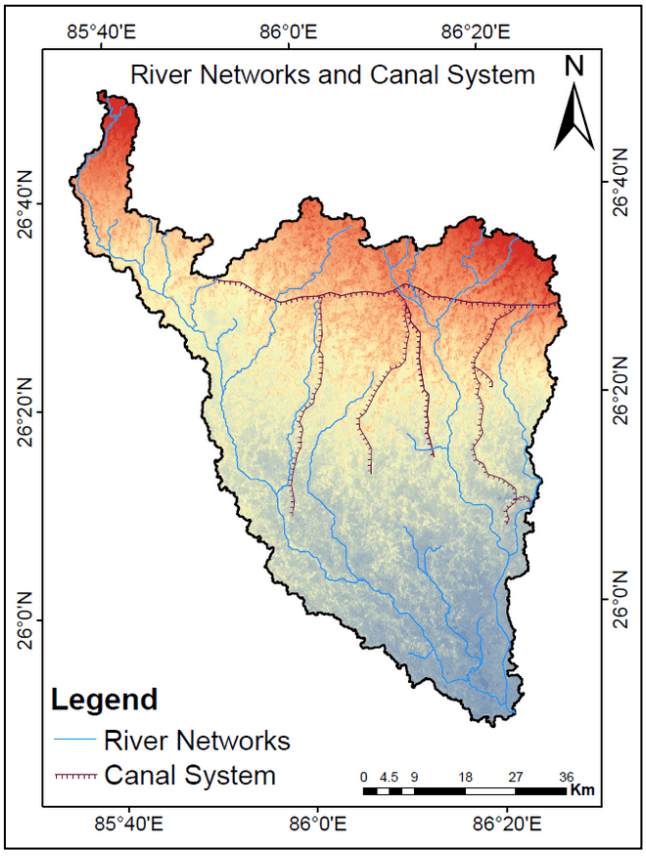

Figure 2.5 Drainage pattern and canal system in the lower LKRB

Soils

The basin consists of three major types of soils: sandy loam, loam, and clay. Figure 2.6 shows the soil map of the project area, based on the analysis of the 48 soil samples collected throughout the basin. Annexure B (Table B.1) shows the details of soil sample collection locations and analysis of soil samples. Loam soil is the dominant type of soil in the basin, occupying 62% of the project area; sandy loam soil occupies 26% of the basin area, mostly distributed along the riverbanks; and clay soil occupies a small area (11% of the basin) in the upper north-western part.

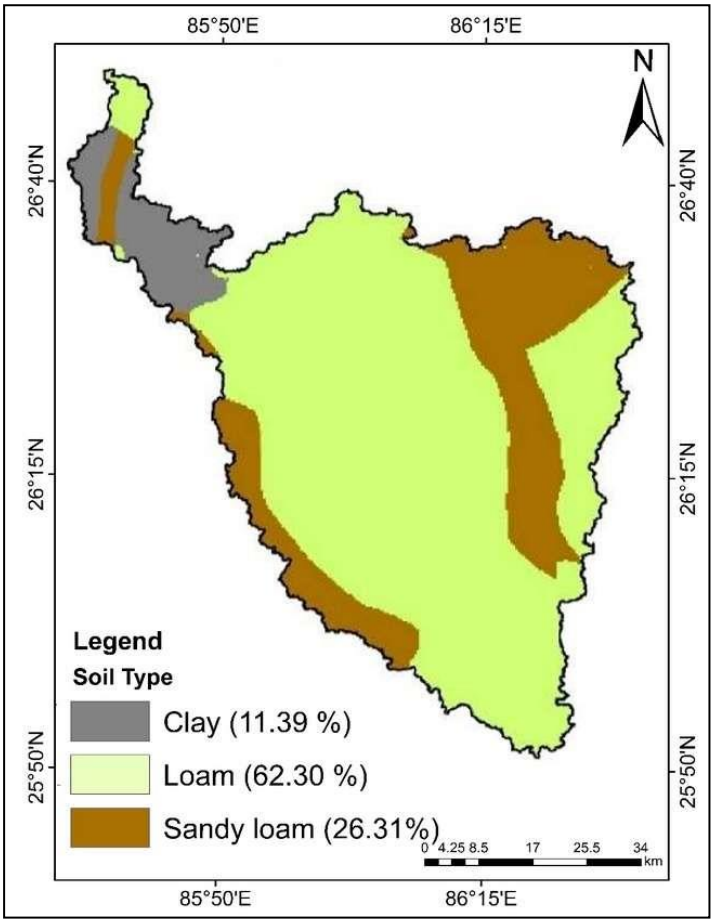

Figure 2.6 Soil map of the lower region of LKRB

Suspended Sediment Analysis

Monitoring and analysis of suspended sediment concentration (SSC) in a river system are often important to understand hydro-geological processes that are directly connected with soil erosion, land use degradation, extreme hydrological events such as floods, and ecological conditions. Therefore, SSC was also monitored at four locations in the LKRB (Figure 2.7) in

the post-monsoon season of the year 2022 using a suspended sediment analyzer. The result reports that the suspended sediment concentration varies from 231 mg/l to 300 mg/l.

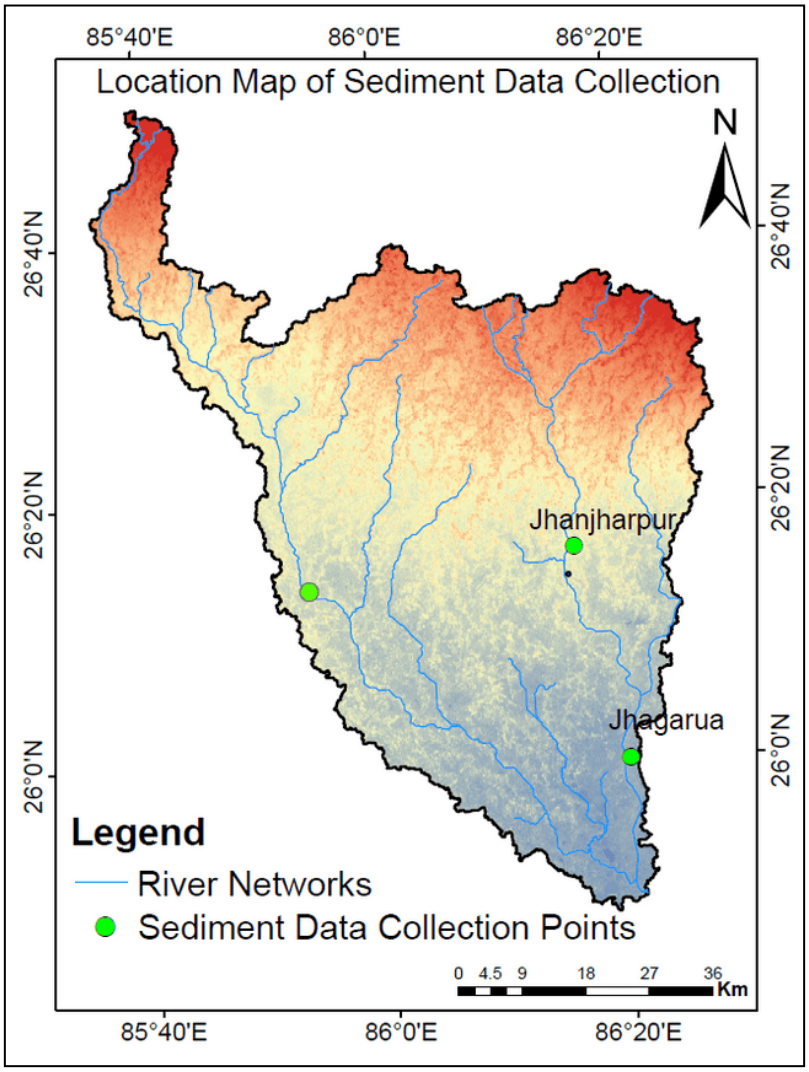

Figure 2.7 Location of sampling points for estimating SSC

Cropping Pattern

The study area is typically agricultural-based. Farmers of the site mainly follow the cereal-oriented cropping system. Wheat rice is the major dominant cropping pattern. Apart from the cultivation, the farmers are also heavily engaged with agricultural allied sectors such as dairy, goatry, and fruits like mango cultivation. For land preparation and sowing of the seasonal crops, the farmers of the district highly depend on the secondary tillage operation. Tractor-operated cultivators rotavators, and indigenous plows are the major tillage equipment used for tillage operation.

Location of Gauged Sites in the Lower Region of LKRB

There are three gauging stations, namely Jaynagar, Jhanjharpur, and Jhagarua, are available in the lower region LKRB, where regular flow is being monitored by the CWC, Lower Ganga Basin (Figure 2.8).

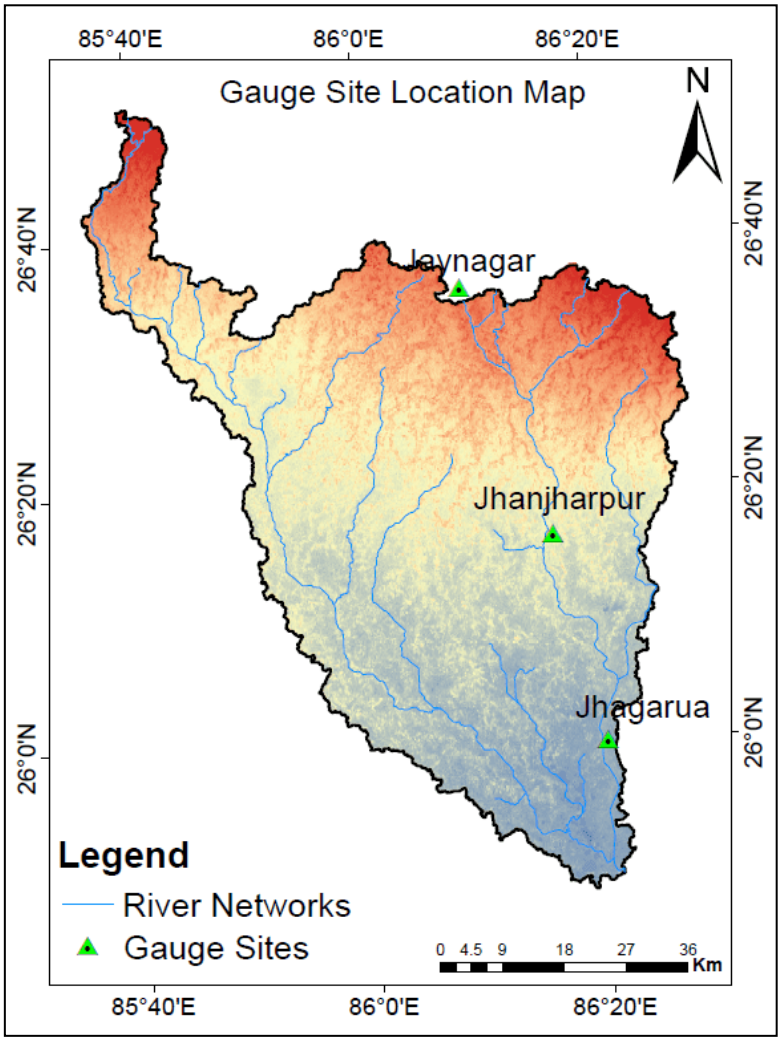

Figure 2.8 Location of gauging sites

2.3 Data and Sources

This section provided details on the datasets required for the study.

2.3.1 Data Used for KRB

All data sources and values used in the InVEST version 3.14.0 model runs are summarized in Table 2.1.

Table 2.1 Details of inputs used in the InVEST-SDR model

Input	Type	Unit of measurement	Source
Rainfall erosivity factor (R)	Raster (0.05° and resampled to 90 m)	MJ·mm/(ha·hr)	Climate Hazards Group InfraRed Precipitation with Station Data (CHIRPS)
Soil erodibility factor (K)	Raster (generated at 90 m)	ton·ha·hr/(ha·MJ·mm)	FAO
DEM	Raster (90 m)	m	MERIT DEM
Vegetation cover factor (USLE C)	Decimal	Tree cover: 0.008	USDA (1972)
		Shrubland: 0.1	
		Grassland: 0.1	
		Cropland: 0.33	
		Built-up: 1	
		Sparse vegetation: 0.18	
		Water bodies: 0.28	
		Herbaceous wetland: 0.05	
Erosion support practice factor (USLE P)	Decimal	Tree cover: 1	Yang (2003)
		Shrubland: 1	
		Grassland: 1	
		Cropland: 0.5	
		Built-up: 1	
		Sparse vegetation: 1	
		Water bodies: 1	
		Herbaceous wetland: 1	
Threshold flow accumulation	Integer	4000 pixels	-
Borselli k_b parameter	Decimal	2.0 for initiating calibration	Vigiak et al. (2012)
Borselli IC_0 parameter	Decimal	0.5 for initiating calibration	Vigiak et al. (2012)
SDR_{max}	Decimal	0.8	Vigiak et al. (2012)

Global CN raster: The GCN250 is a globally consistent, gridded dataset defining CNs at the 250 m spatial resolution from new global land cover (300 m) and soils data (250 m) (Jaafar et al., 2019).

Download link:
https://figshare.com/articles/dataset/GCN250_global_curve_number_datasets_for_hydrologic_modeling_and_design/7756202

GCN250 represents runoff for a combination of the European space agency global land cover dataset for 2015 (ESA CCI-LC) resampled to 250 m and geo-registered with the hydrologic soil group global data product (HYSOGs250m) released in 2018. The potential application of this data includes hydrologic design, land management applications, flood risk assessment, and groundwater recharge modeling. The CN values vary depending on antecedent runoff conditions (ARC), which is affected by the rainfall intensity and duration, total rainfall, soil moisture conditions, cover density, stage of growth, and temperature.

Observed sediment load at Jhanjharpur gauging site is shown in Table 2.2(provided by CWC)

Table 2.2 Annual Sediment load (tons) at Jhanjharpur Gauging site

Year	**Sediment Load at Jhanjharpur (tonnes)**	**Annual Rainfall (mm)**
2001-02	363621.74 (No Data: June, July, and August)	1385.48
2002-03	1588915.75 (No Data: March, April, and May)	993.88
2003-04	No Data Available	1233.77
2004-05	30139.54	1226.46
2005-06	1053031.07	1000.04
2006-07	1058077.15	848.60
2007-08	7682950.87	1731.26
2008-09	7393222.13	873.31
2009-10	3116236.65	932.69
2010-11	2117325.42	760.59
2011-12	4228337.06	1192.28
2012-13	920191.50	773.83
Total	**29552048.87**	-

2.3.2 Data used for LKRB

In this study, various geospatial datasets were utilized obtained from open sources, i.e., Digital Elevation Model (DEM), rainfall, soil, and land use land cover (LULC). The topographic information for the basin was derived using a DEM with a spatial resolution of 30 m acquired by the Shuttle Radar Topography Mission (SRTM). The soil's physical properties and structure were determined using the National Bureau of Soil Survey and Land Use Planning (NBSS&LUP) soil map and verified with collected soil samples during the field visit. The climate data (gridded rainfall data) of 30 years was collected from India Meteorological Department (IMD) at a spatial resolution of $0.25^{o} \times 0.25^{o}$. In addition, LULC data for 2000, 2010, and 2020 were prepared using Landsat-5 TM and Landsat-8 collections. The dataset used is listed in Table 2.3.

Table 2.3 Information on the key datasets utilized for soil loss estimation based on RUSLE and GIS

Category	**Source**	**Reference**	**Spatial resolution**
DEM	SRTM, USGS	https://earthexplorer.usgs.gov/	30 m
Rainfall data	IMD	https://mausam.imd.gov.in/	$0.25^{o} \times 0.25^{o}$
Soil	NBSS&LUP	https://nbsslup.icar.gov.in/	1: 250000
Land use/land cover	Landsat-5 TM and Landsat-8	https://earthexplorer.usgs.gov/	30 m
Slope/slope length, fill map, flow direction/flow height	SRTM DEM	https://earthexplorer.usgs.gov/	30 m
Hydro-geomorphological Data (Discharge and Sediment data)	CWC, Patna (data request under processing)	Jhanjharpur and Jaynagar gauge sites	Period: 1980-2020

2.3.2.1 Land Use/ Land Cover

The land use land cover map of the study area was obtained from the European Space Agency (ESA) with a 10 m spatial resolution. The LULC map was classified into eight classes: plantation, shrubland, grassland, cropland, built-up, bare/sparse vegetation, water bodies, and

herbaceous wetlands. Figure 2.9 shows the spatial pattern of land use/land cover in the lower KRB, which portrays nearly 67 % of the area occupied by agricultural or cropland followed by plantation (23.34 %), built-up (5.14 %), grassland (1.74 %), waterbodies (0.54), shrubland, herbaceous wetlands, and bare or sparse vegetation consisting of 0.5 %. Table 2.8 shows the area under different LULC classes and percentage distribution in the study area.

Table 2.4 Areas under different land use/ land cover classes in the catchment

LULC Class	Area (Km^2)	Area (%)
Plantation	1055.22	23.34
Shrubland	0.20	0.0044
Grassland	78.67	1.74
Cropland	3094.45	68.61
Built-up	231.76	5.14
Bare/ Sparse Vegetation	16.73	0.37
Waterbodies	24.16	0.54
Herbaceous Wetland	8.93	0.12
Total	**4510.12**	**100.00**

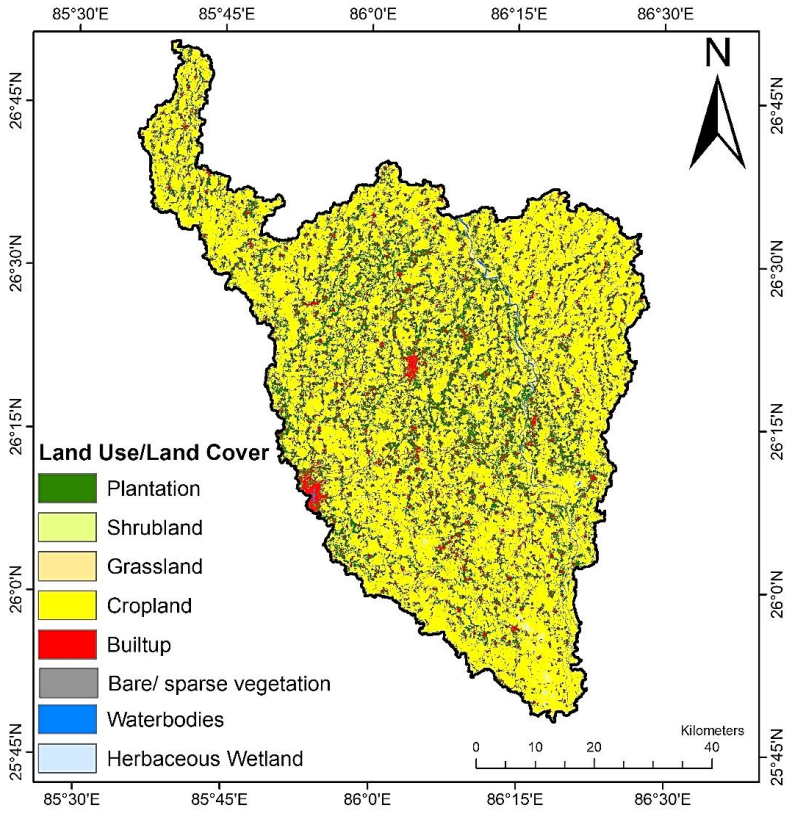

Figure 2.9 Land use land cover of the Lower Kamla River Basin

2.3.2.2 Slope Map

The slope is the most influencing parameter of the soil loss rate (Fox and Bryan, 2000). The percentage of slope determines the erosion susceptibility of soil and its class. This helps classify various land suitability classes, enabling the formulation of suitable conservation measures for the prevention of soil erosion. The slope map of the Lower Kamla River basin has been generated using the Shuttle Radar Topographic Mission (SRTM) Digital Elevation Model (DEM) of a spatial resolution of 30 m. DEM is the raster representation of a continuous surface, usually referring to the surface of the earth. The DEMs have proved to be very efficient in extracting different topographical attributes (elevation, slope, aspect, relief, curvatures, etc.). The slope was divided into five classes as recommended by AISLUS (Figure 2.10). The slope class ranges and corresponding areas for each sub-basin are detailed in Table 2.10.

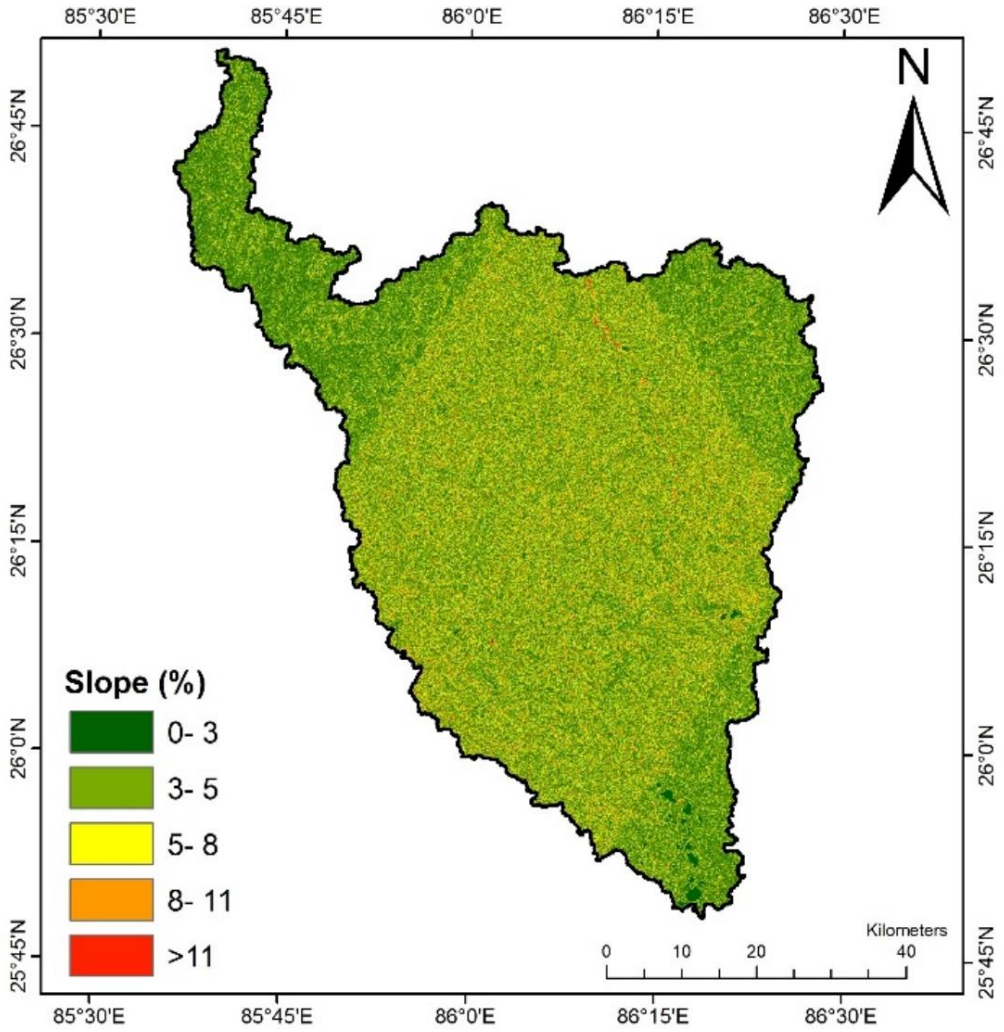

Figure 2.10 Slope map of the study area (%)

Table 2.5 Slope area under different classes

Sub-watersheds	Area (Km^2)				
	Very gentle slope (1-3%)	**Gentle slope (3-5%)**	**Moderate Slope (5-8%)**	**Strong Slope (8-11%)**	**Steep Slope (>11%)**
SW1	390.81	201.40	74.23	10.25	1.25
SW2	123.09	108.57	80.23	21.14	4.50
SW3	73.29	67.32	53.21	14.97	3.68
SW4	109.71	100.92	77.55	20.95	4.49
SW5	351.02	287.95	204.80	56.31	15.40
SW6	188.99	138.67	85.20	21.61	4.94
SW7	173.36	155.94	117.78	32.02	7.54
SW8	67.68	61.08	48.32	14.87	4.47
SW9	169.45	130.66	87.86	23.60	6.08
SW10	113.13	95.57	67.88	17.87	4.48
SW11	77.90	52.62	28.33	6.10	1.36
SW12	29.95	12.68	5.32	0.90	0.24

2.3.2.3 Soil Data

Soil texture is an essential parameter considered for soil loss estimation. The soil map of the lower KRB was obtained from NBSS & LUP with a 1:500,000 scale (Figure 2.6). The soil map of the study area portrays loam soil as the dominant type of soil in the basin, mostly agricultural lands, which occupied 62% of the study area; whereas sandy loam soil occupies 26% of the basin area, mostly distributed along the riverbanks, and in the upper north-western part a small area (11%) consisted by the clay soil. Higher weighted values have been assigned for sandy loam soils because these can be eroded easily in comparison to other soil types in the study area. Table 2.11 provides a comprehensive overview of the diverse soil types present within the designated study area.

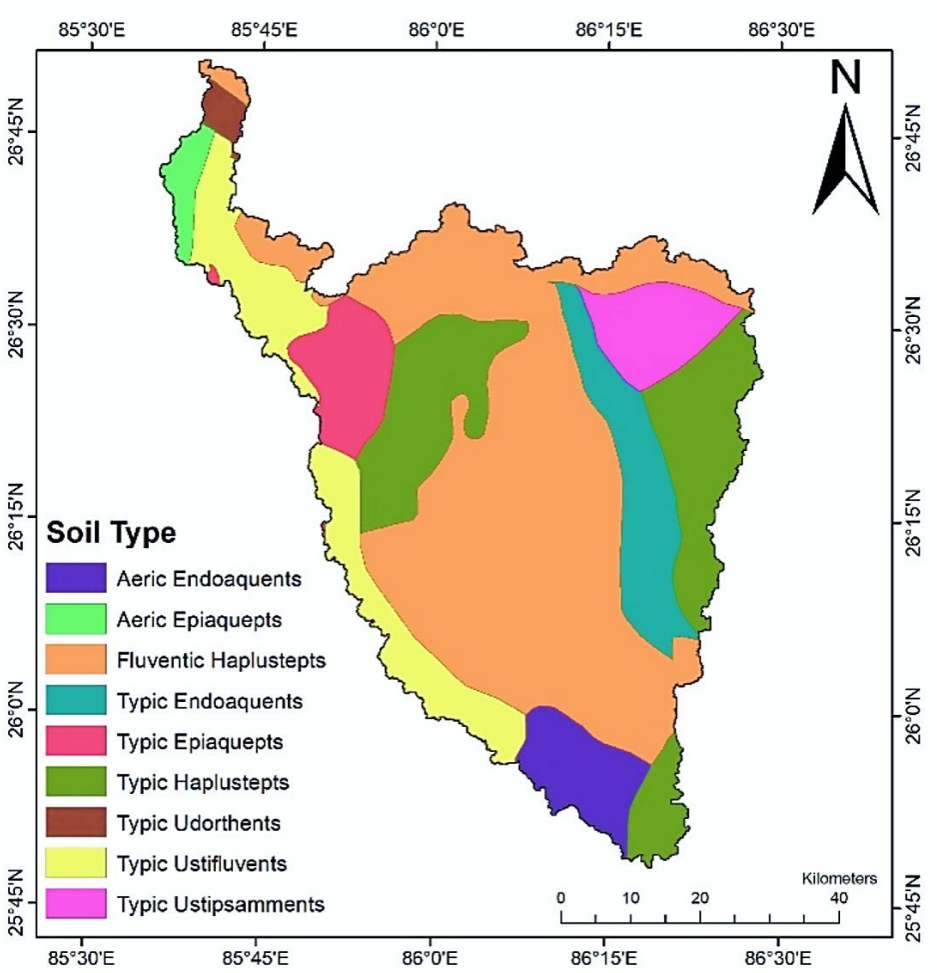

Figure 2.11 Soil Map of the Lower Kamla River Basin

Table 2.6 Soil classes in the Lower KRB (NBSS & LUP)

Soil Type	Soil	Area (km^2)	Area (%)
Aeric Endoaquents	Loam	342.32	7.59
Aeric Epiaquepts	Loam	111.85	2.48
Fluventic Haplustepts	Loam	460.48	10.21
Typic Endoaquents	Sandy loam	573.69	12.72
Typic Epiaquepts	Sandy loam	374.34	8.30
Typic Haplustepts	Loam	1370.17	30.38
Typic Udorthents	Clay	59.08	1.31
Typic Ustifluvents	Clay	859.18	19.05
Typic Ustipsamments	Sandy loam	359.00	7.96
Total		**4510.12**	**100.00**

2.3.2.4 Delivery Ratio (DR)

The delivery ratio is defined as the percentage of eroded material that finally finds entry into the river/stream (Khadse et al., 2015). It is generally governed by the type of material, soil erosion, relief length ratio, cover conditions, distance from the nearest stream, etc. It was calculated based on the kilometers closest to the stream-drainage density distance. Table 2.7 presents the values of the delivery ratio measured at various distances from the drainage networks (Wag and Manekar, 2022; Romshoo et al., 2017). This ratio was used to obtain the SYI values for each sub-watershed. The incorporation of SYI values of sub-watersheds is required to determine the sub-watershed quantitative priority value. Figure 2.12 demonstrates the spatial distribution of DR values in the study area. In the study area, the assigned delivery ratio ranges between 0.7 and 1.0.

Table 2.7 Values of delivery ratio used in the study.

Nearest Stream	Delivery Ratio
0 - 0.9 km	1.0
1.0 - 2.0 km	0.9
2.1 - 5.0 km	0.8
5.1 - 15.0 km	0.7
15.1 - 30.0 km	0.5

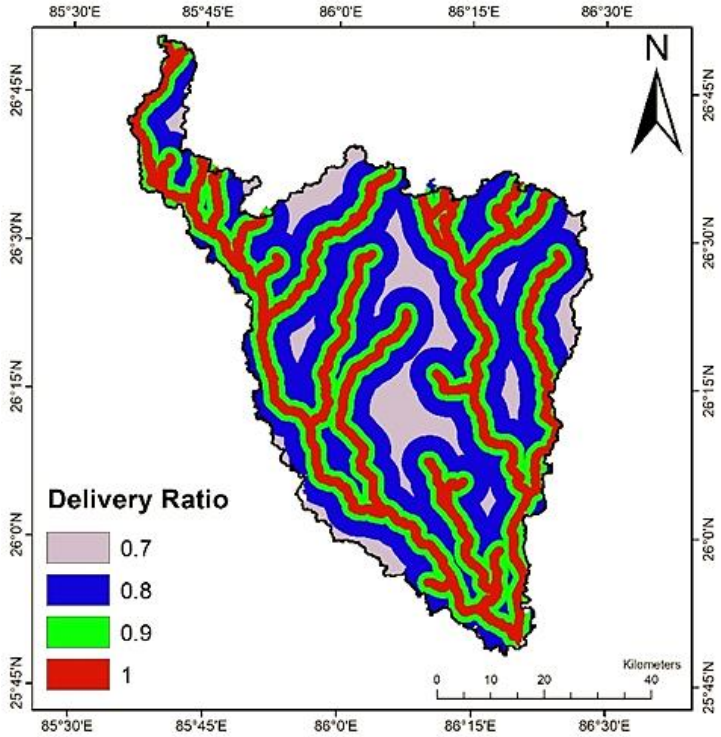

Figure 2.12 Spatial distribution of the delivery ratio

Chapter 3: Methodology

3.1 Soil Loss Estimation using RUSLE Model

Spatial and quantitative information on soil erosion at a sub-watershed scale is an essential requirement for proper planning of soil conservation, erosion control, and managing watershed health. In this view, the average annual soil loss in the project area was estimated using the Revised Universal Soil Loss Equation (RUSLE) model. The RUSLE is an empirical model for estimating long-term annual soil loss from a specified area under diverse land cover and management practices. This model is a simple multiplicative model and is widely reported in the literature (Angima et al., 2003; Pandey et al., 2008; Pandey et al., 2021). The average annual soil loss can be estimated using the following equation:

$$A = R \times K \times LS \times C \times P \quad (3.1)$$

where A = average soil loss **(**t ha^{-1} $year^{-1}$**);** R = rainfall erosivity factor (MJ mm ha^{-1} h^{-1} $year^{-1}$); K = soil erodibility factor (t ha h ha^{-1} MJ^{-1} mm^{-1}); LS = slope length factor (dimensionless); C = crop management factor (dimensionless); P = conservation practice factor (dimensionless). Analogous to the DEM, all USLE input layers, i.e., the R, K, C, and P factors, shall be prepared for assessing soil erosion. The schematic flow chart for soil loss estimation using USLE is presented in Figure 3.1.

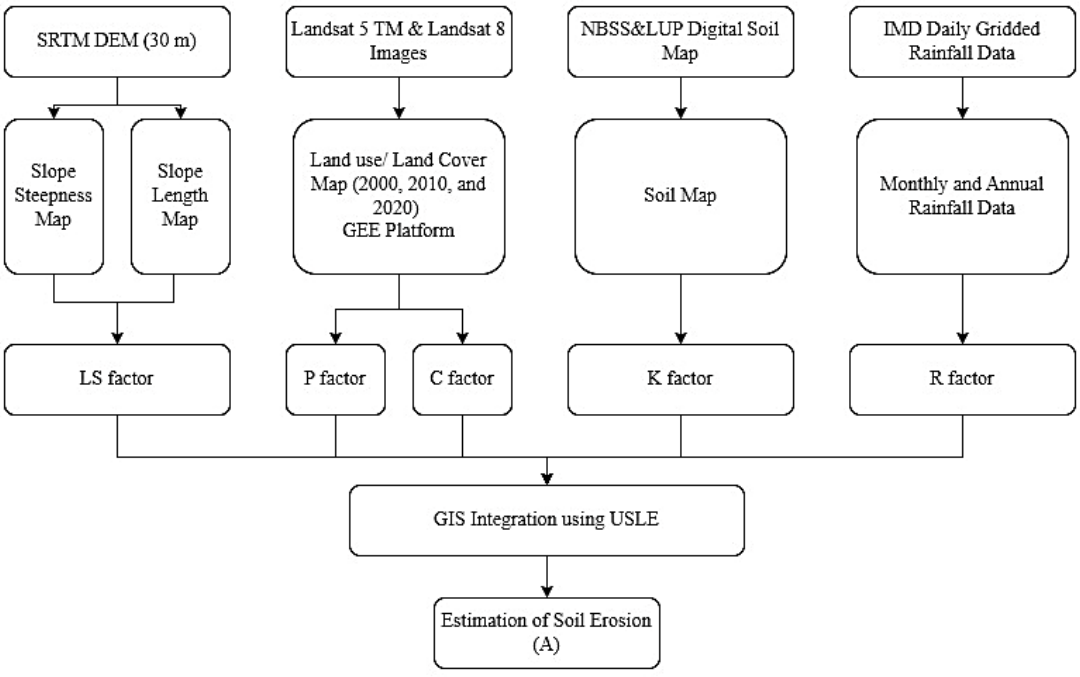

Figure 3.1 Methodology flowchart for RUSLE

3.1.1 Database Generated for Calculating Factors of RUSLE Model

An extensive database has been generated to calculate different factors of RUSLE (Eq. 3.1), compiled from various open sources, as described below:

Rainfall Erosivity (R)

The R-factor represents the erosivity from rainfall and runoff at a particular location (Renards et al., 1997). In estimating soil loss, it is considered a major contributing factor in the RUSLE model. It is computed as the average annual sum of the erosivity of the individual storms, which is the product of total storm energy and maximum 30-min intensity (Wischmeier and Smith, 1958). Based on data availability and precise estimation of soil loss at the sub-watershed and watershed levels, many researchers have developed a number of equations for the R-factor across various regions. However, in this study, a simple power-law formula has been used to calculate the R-factor developed by Raj et al. (2022) and is given as follows:

$$R = \propto \times MFI^{\beta} \quad (3.2)$$

Where R = rainfall erosivity (MJ mm ha^{-1} h^{-1} yr^{-1}; β is the law's exponent and α is a constant (for the East and Northeast India α = 0.041 and β = 1.785)

MFI is the Modified Fournier Index (mm) given as

$$MFI = \frac{1}{P}\sum_{i=1}^{12} p_i^2 \quad (3.3)$$

where P_i is the monthly precipitation (mm) in the month i and P is the annual precipitation.

In this study, there is no rainfall intensity data available for the KRB. Therefore, the daily gridded rainfall data was used to calculate the R-factor. The R-factor for the years 2000, 2010, and 2020 were calculated using daily gridded rainfall data from the India Meteorological Department (IMD) of $0.25° \times 0.25°$ spatial resolution using Equation 3.2.

Soil Erodibility (K)

Factor K indicates the potential erodibility of particular soil under specific conditions. It depends on the soil's inherent properties, e.g., soil texture, permeability, organic matter contents, and soil structure. Because a soil's resistance or vulnerability to water erosion is mainly dependent on its physical and compositional properties, the K-factor values vary with different soil types. The soil types of the project area are shown in Figure 2.5 in the previous

chapter. Based on this generated soil map, the K values of each soil were estimated using the following relationship developed by Williams (1995):

$$K = A \times B \times C \times D \quad (3.4)$$

$$A = 0.2 + 0.3\exp(-0.0256 \times S(1 - \frac{S_i}{100}) \quad (3.5)$$

$$B = \left[\frac{S_i}{C+S_i}\right]^{0.3} \quad (3.6)$$

$$C = \left[1 - \frac{0.25 \times OM}{OM \times exp[(3.72 - 2.95 \times C)]}\right] \quad (3.7)$$

$$D = \left[1 - \frac{0.70 \times SN1}{SN1 + \exp[(-5.41 + 22.9 \times SN1]}\right] \quad (3.8)$$

where S: % sand, S_i: % $silt$, C: % clay, and OM: organic matter SN1:$\left(1 - \frac{S}{100}\right)$

Topographic Factor (LS)

It combines slope length (L) and Steepness factors. It expresses the effect of the topographical configuration of an area on water-induced soil erosion. This factor portrays the effect of slope and slope length in the detachment, transportation, and deposition of soil particles during erosion. Studies have suggested that increasing slope length and angle directly and significantly influence soil erosion (Wischmeier and Smith 1978; Gashaw al. 2017; Koirala et al. 2019). Alternatively stated, steeper and longer slopes allow for higher soil erosion rates due to an increase in runoff accumulation (Gashaw et al. 2017). However, slope steepness plays a higher role than slope length (Koirala et al. 2019). In this study, the LS factor was derived using STRM DEM (30m × 30m) data. The topographic factor (LS) was calculated using the equation 3.9 (Moore and Wilson, 1992).

$$\text{LS} = \left[\frac{\text{A}_\text{S}}{22.13}\right]^{\text{n}} . \left[\frac{\sin\beta}{0.0896}\right]^{\text{m}} \quad (3.9)$$

where A_S = specific area; A/b = upslope contributing area for an overland cell (A)/width normal; β = Slope gradient in degree; n = 0.4 and m = 1.3

In ArcGIS interface it is calculated as follows

$$LS = (\text{Flow accumulation} \times \text{cell size}/22.13)^{0.4} \times (\sin((\text{Slope}) \times 0.01745)/0.0896)^{1.3}$$

where cell size is 30 m, and slope in degree

Crop Management Factor (C)

The C-factor is a ratio of soil loss from land cropped under specified conditions to soil loss from clean-tilled fallow on identical soil and slope and under similar rainfall. Alternatively, it depicts the effect of vegetation cover, cropping patterns, and other management practices (such as mulching and artificial covers) on the rate of erosion. Typically, more vegetation cover can significantly reduce soil erosion by minimizing the direct impact of rainfall on detaching soil particles (Igwe and Egbueri, 2018; Djoukbala et al., 2018). In the study, the land use/land cover map was derived from satellite images (Landsat 5 TM and Landsat 8 Collections) and served as a guiding tool in the allocation of C and P factors for different land use classes. The C factor values were the representative values for allocating the USLE land cover and management factors corresponding to each crop/vegetation condition. The Google Earth Engine (GEE) platform was used for the digital interpretation of satellite imagery. Supervised classification (after several ground truth verifications) with Random Forest algorithm was used for digital classification of satellite data. The study area has been classified into five land use classes namely, 1) barren land, 2) waterbodies, 3) built-up, 4) agricultural land (paddy), and 5) plantation. Crop management factors were assigned for different land use patterns (Table 3.1) (Pandey et al., (2007); USDA, (1972); Rao, (1981); Aslam et al., (2021)).

Table 3.1 Crop management factor for different land use/land cover classes

Land use/ land cover	C factor value
Barren land	0.35
Agricultural land	0.5
Built-up	0.1
Water	0.28
Plantation	0.008

Conservation Practice Factor (P)

It is a ratio of soil loss with a specific support practice to soil loss without conservation practices. It reflects the effects of conservation practices, e.g., contouring, terracing, strip cropping, check dam, and field bunding on reducing the volume and rate of soil loss. In the project site, no major conservation practices are followed except bunded agricultural lands. Specifically, these bunded fields are limited to paddy growing areas only. It may be observed that major agricultural land covered under paddy cultivation. Hence, the conservation practice

factors of 0.28 and 1 as suggested by Rao (1981) were assigned to bunded fields and non-paddy fields respectively.

3.2 InVEST Sediment Delivery Ratio (SDR) model description

The InVEST sediment delivery model aims to map and quantify the sediment delivery and retention services. The model is fully distributed and GIS-based, accepting inputs of raster of climate, soil, topography, and land use land cover (LULC) data. The outputs represent average annual sediment delivery and retention per sub-catchment, as well as maps representing the per-pixel contribution to sediment yield. For each pixel, the model first computes the amount of annual soil loss from that pixel, then computes the sediment delivery ratio (SDR), which is the proportion of soil loss actually reaching the stream. Once sediment reaches the stream, we assume that it will be delivered to the catchment outlet; thus, no in-stream processes that could increase or decrease sediment loads are modeled. This approach was proposed by Borselli et al. (2008).

3.2.1 Soil Loss Estimation

The average amount of annual soil loss on pixel i, $usle_i$ (ton·ha^{-1}·yr^{-1}), is given by the revised universal soil loss equation (RUSLE1 – Renard et al. 1997):

$$usle_i = (\mathrm{R} \times \mathrm{K} \times \mathrm{LS} \times \mathrm{C} \times \mathrm{P})_i \quad (3.10)$$

where: R is the rainfall erosivity (MJ·mm (ha.hr.yr)$^{-1}$), K is the soil erodibility (ton·ha·hr (MJ·ha·mm)$^{-1}$), LS is the slope length–gradient factor, C is the cover-management factor and P is the support practice factor (Renard et al., 1997). The LS factor is computed from the digital elevation model (DEM) based on the algorithm by Desmet and Govers (1996).

3.2.2 Sediment Delivery Ratio

The sediment delivery ratio (SDR) represents the proportion of fine sediment produced on a given area that will travel to the stream. It is computed as a function of the hydrologic connectivity of the area, following an approach first proposed by Vigiak et al. (2012). The algorithm first computes an index of connectivity IC (Figure 3.2), which determines the degree of hydrological connectivity of a pixel to the stream, based on its upslope contribution and flow path to the stream (Borselli et al., 2008):

$$IC = \log_{10} \frac{D_{up}}{D_{dn}} \quad (3.11)$$

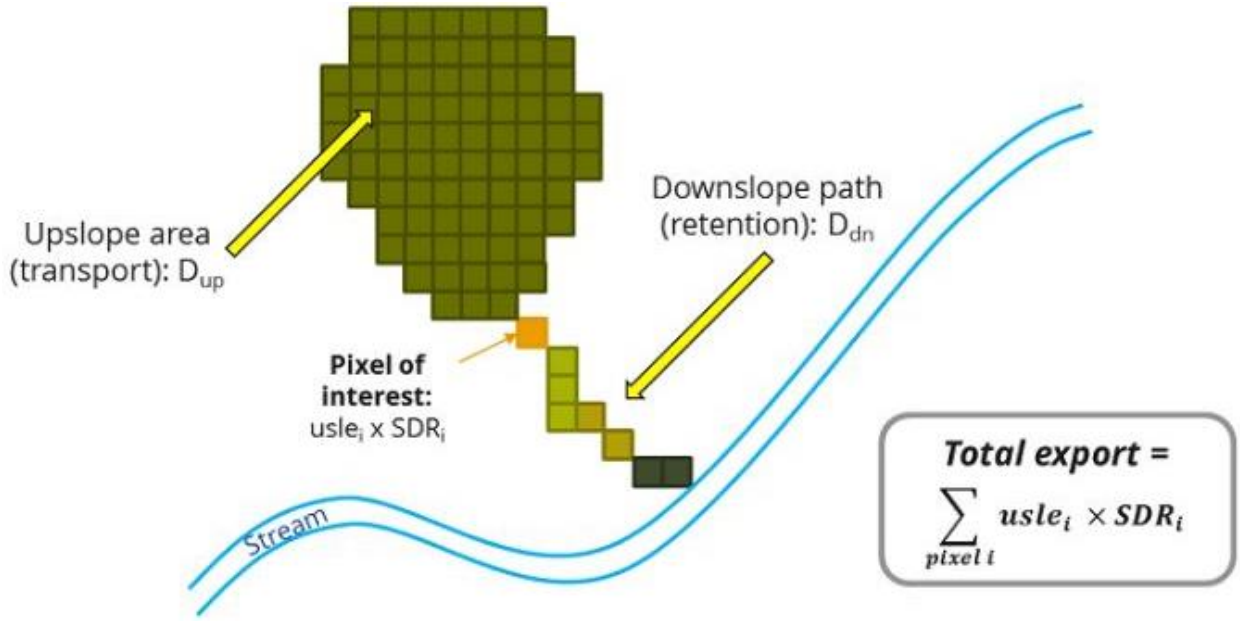

Figure 3.2. Conceptual representation of the index of connectivity, adapted from Borselli et al. (2008)

D_{up} is the upslope component defined as:

$$D_{up} = \bar{C}\bar{S}\sqrt{A} \tag{3.12}$$

where $\bar{C}$ is the average C factor of the upslope contributing area, S is the average slope gradient of the upslope contributing area (m/m) and A is the upslope contributing area (m^2). The upslope contributing area is delineated from the D-infinity flow algorithm (Tarboton, 1997).

The downslope component D_{dn} is given by:

$$D_{dn} = \sum_i \frac{d_i}{C_i S_i} \tag{3.13}$$

where d_i is the average length of the flow path in the downslope direction, from the ith pixel to the stream (m); C_i and S_i are the C factor and the slope gradient of the ith pixel, respectively. The downslope flow path is determined from the D-infinity flow routing algorithm (Tarboton, 1997). Streams are defined as the pixels with a contributing area exceeding a user-defined threshold, termed tfac.

The sediment delivery ratio for a pixel i is then directly derived from the conductivity index IC using a sigmoid function (Figure 3.3; Vigiak et al., 2012):

$$SDR_i = \frac{SDR_{Max}}{1+exp\frac{IC_0 - IC_i}{k_b}} \tag{3.14}$$

where SDR_{Max} is the maximum theoretical SDR, defined as the maximum proportion of fine sediment (< 1000 μm) which can travel to the stream; in the absence of detailed soil information, it has a default value of 0.8 (Vigiak et al., 2012). IC_0 and k_b are calibration parameters that define the shape of the sigmoid function SDR–IC relationship. Essentially, and intuitively, if the pixel connectivity is low (meaning there is a lower contribution of upslope area and/or higher downslope retention), the amount of sediment delivered from a given pixel to the stream approaches zero, and if the connectivity is high, the amount of sediment delivered from a given pixel approaches the total proportion of fine sediment on that pixel.

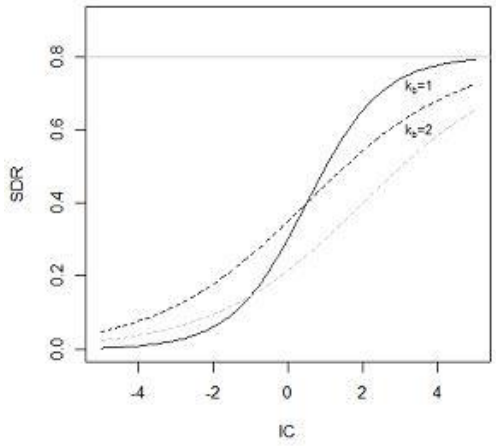

Figure 3.3 Sigmoid function used to convert the connectivity index IC to the SDR factor. The maximum value of SDR is set to $SDR_{max} = 0.8$. The effect of the calibration is illustrated by setting $k_b = 1$ and $k_b = 2$ (solid and dashed lines, respectively), and $IC_0 = 0.5$ and $IC_0 = 2$ (black and gray dashed lines, respectively).

3.2.3 Sediment yield

The sediment yield from a given pixel i, sed_export_i ($ton \cdot ha^{-1} \cdot yr^{-1}$) is a direct function of the soil loss and SDR factor:

$$sed\_export_i = usle_i \times SDR_i \quad (3.15)$$

Ultimately, total catchment sediment yield from sheetwash erosion, sed_export ($ton \cdot ha^{-1} \cdot yr^{-1}$), is calculated as the sum of the sediment yield from all pixels.

Two things should be noted about the use of the SDR concept for sediment retention modeling. First, both IC and SDR factors are functions of the DEM resolution, which introduces uncertainty in the absolute predictions. However, sensitivity to the DEM is expected to be low due to the fact that IC is a ratio, with pixel size both at the numerator and denominator (Vigiak et al., 2012). Second, it is possible that sediment transport is affected by man-made

infrastructure (e.g. roads), rather than natural flow paths only. The model allows representation of this process by enabling users to input a drainage layer. Any pixel from this layer is considered as a stream network pixel (i.e. the downslope routing considers these pixels as a sink, with the sediment load being added to the catchment sediment export).

3.2.4 InVEST-SDR Model Parameter Calculation

LULC: The European Space Agency (ESA) WorldCover 10 m 2020 product was used which provides a global land cover map for 2020 at 10 m resolution based on Sentinel-1 and Sentinel-2 data. The WorldCover product comes with 11 land cover classes, aligned with UN-FAO's Land Cover Classification System, and has been generated in the framework of the ESA WorldCover project, part of the 5th Earth Observation Envelope Programme (EOEP-5) of the European Space Agency.

Rainfall Erosivity: Rainfall erosivity was calculated for each year from 2007 to 2012 using Modified Fournier Index (MFI) approach. CHIRPS Satellite precipitation product was used as an input and a code was developed in Google Earth Engine to generate annual Erosivity raster.

Soil Erodibility: Soil erodibility map was generated for the entire basin using FAO global soil data.

Topographic Factor: In this study, the LS factor is calculated from the method developed by Desmet and Govers (1996) for two-dimension surface by the InVEST-SDR model. The detailed calculation method can be found in the users' guide of the InVEST model.

Biophysical Table: P and C Coefficients

The cover-management factor, C, accounts for the specified crop and management relative to tilled continuous fallow. The support practice factor, P, accounts for the effects of contour plowing, strip-cropping or terracing relative to straight row farming up and down the slope. These values were obtained from a literature search and are listed in the Table 3.2.

Table 3.2. Values of C and P factors used in the InVEST model

Landuse class	C factor	P factor
Tree cover	0.008	1
Shrubland	0.1	1
Grassland	0.1	1
Cropland	0.33	0.5
Built-up	1	1
Bare/sparse vegetation	0.18	1
Permanent water bodies	0.28	1
Herbaceous wetland	0.05	1

Model Calibration

IC_0 and k_b are calibration parameters that define the relationship between the index of connectivity and the sediment delivery ratio (SDR). Vigiak et al. (2012) suggest that IC_0 is landscape independent and that the model is more sensitive to k_b. Advances in sediment modeling science should refine our understanding of hydrologic connectivity and help improve this guidance. In the meantime, following other authors (Jamshidi et al., 2013), we recommend setting these parameters to their default values (IC_0 =0.5 and k_b =2), and using k_b only for calibration (Vigiak et al., 2012).

In the InVEST (Integrated Valuation of Ecosystem Services and Tradeoffs) Sediment Delivery Ratio (SDR) model, the calibration parameter 'k' is typically not expected to change on an annual basis within a given area. The 'k' parameter represents a coefficient that relates land cover and land use to the amount of soil erosion and sediment delivery in a specific location. It is often considered as a constant for a given land cover and land use type within a specific region.

The purpose of calibrating the 'k' parameter is to establish a relationship between land cover and land use types and the sediment delivery ratio in the specific study area, and this relationship is assumed to remain relatively stable over time, at least for the duration of the study or analysis.

3.3 Modified Universal Soil Loss Equation (MUSLE)

The empirical model has been adopted to estimate the event base sediment yield from the catchment. The MUSLE model considers the runoff effects on soil detachment through the product between the peak discharge and the runoff volume for a single heavy storm. Therefore, the rainfall factor (R) previously used in the RUSLE can be replaced by a runoff factor. Other factors viz., soil erodibility factor (K), topographic factor (LS), cover management factor (C_m), and support practice factor (P_s) were adopted to reflect the effects of geomorphologic characteristics of soil properties, topography (such as slope length and steepness), land use and land cover, and support practice regarding sediment yield. The general form of the MUSLE model is expressed as follows:

$$Y = \frac{a(Q \times q_p)^b \times K \times LS \times C_m \times P_S}{100A} \quad (3.16)$$

where Y is the sediment yield (t ha^{-1}), Q is the volume of runoff (m^3), q_p is the peak discharge (m^3 s^{-1}), A is the drainage area (km^2), K is the soil erodibility factor (t h MJ^{-1} mm^{-1}), LS is the

topographic factor (dimensionless), C_m is the cover management factor (dimensionless), P_s is the support practice factor (dimensionless), and a and b are the empirical coefficients (dimensionless).

Runoff Volume (Q) Estimation

The most widely used rainfall-runoff model, the Natural Resources Conservation Service (formerly known as the Soil Conservation Service) Curve Number (SCS-CN) method (SCS, 1972) has been used to generate the surface runoff volume from the basin. During the past four decades, many modified versions of the original SCS-CN model have been developed for various applications (Mishra et al. 2008; Sahu et al. 2010; Babu and Mishra 2012; Singh et al. 2015). The basic hypothesis and principle of the SCS-CN method are expressed as follows:

$$R = \begin{cases} 0 & (P \leq 0.3S) \\ \frac{(P-0.3S)^2}{(P+07S)} & (P > 0.3S) \end{cases} \quad (3.17)$$

Where R is the depth of surface runoff (mm), P is the rainfall depth (mm), S is the potential maximum retention (mm), which can be calculated by:

$$S = \frac{25400}{CN} - 254 \quad (3.18)$$

Where CN ranged from 0 to 100 (dimensionless), where CN = 0 represents an infinitely abstracting catchment with $S = \infty$ and a CN value of 100 represents a condition of zero potential (i.e., impervious catchment), in practical CN values ranges between 40 and 98. The curve number CN depends upon soil types, antecedent moisture condition, and land use/cover. In this study, Global Hydrologic Curve Number used to calculate maximum potential retention in the basin. The weighted CN of the basin is 88.404 (As per the Global Hydrologic Curve Number Data).

In the absence of peak discharge data, daily gauge discharge information is considered as the peak flow as provided by the Central Water Commission (CWC) at Jhanjhapur gauging site.

For the soil erodibility factor (K), the average weighted value for the basin is 0.2423. The Cm and Ps factors were calculated by extracting land cover attributes, assigning values according to the look-up tables, and weighting the Cm and Ps factor values for each land cover category with the total area. Similarly, LS factor value was extracted from the catchment topographic information using STRM DEM.

Table 3.3 Summary of MUSLE model inputs for the catchment

Data Type	Resolution	Sources/Description
Runoff Volume (Q)	-	SCS-CN Method
CN	250 m	Global Hydrologic Curve Number Data
Peak Discharge (Qp)	Event-based	CWC Daily Gauge Data at Jhanjharpur Station
Soil Erodibility (K) Factor	1:5 000 000 scale	Food and Agricultural Organization (FAO)
Ps and Cs	10 m	Average of assigned weightage values for the different LULCs (Table 2.1)

Model Parameters Optimization

In the application of the Modified Universal Soil Loss Equation (MUSLE) for estimating sediment yield, the accurate calibration of the model parameters is crucial for ensuring the reliability of the predictions. The MUSLE model incorporates parameters 'a' and 'b', which modulate the relationship between runoff and sediment yield, and are not universally fixed; they must be tailored to the specific conditions of the study area.

In this context, the Dynamically Dimensioned Search (DDS) optimization algorithm emerges as an effective tool for fine-tuning these parameters. DDS, an adaptive and stochastic search method, excels in exploring the vast and complex parameter space by dynamically adjusting its strategy. It focuses on the most promising areas, enabling efficient and accurate identification of the optimal parameter combination. This flexibility is particularly advantageous for complex and nonlinear models like MUSLE, which often exhibit multiple local optima in their response surfaces. In this study, we analyzed 104 sediment yield events using the MUSLE Model. We optimized parameters ‘a’ and ‘b’ for 72 of these events, employing the Nash–Sutcliffe efficiency (NSE) as the objective function. The optimized values were then applied to predict sediment yield in MUSLE for model verification purposes.

Model Performance Evaluation

The Nash–Sutcliffe efficiency (NSE) (Nash and Sutcliffe, 1970; Risse et al., 1994) and root mean square error (RMSE) values were used to evaluate the goodness of fit between the measured and estimated data in this study. The Percent bias (PBIAS) measures the average tendency of the simulated values to be larger or smaller than their observed ones. The calculation formulas can be expressed as follows:

$$NSE = \left[1 - \frac{\sum_{j=1}^{N}\left(Y_j - Y_j^*\right)^2}{\sum_{j=1}^{N}\left(Y_j - \bar{Y}\right)^2}\right] \quad (3.19)$$

$$RMSE = \sqrt{\frac{1}{N}\sum_{j=1}^{N}\left(Y_j - Y_j^*\right)^2} \quad (3.20)$$

$$PBIAS = \frac{\sum_{j=1}^{N}\left(Y_j - Y_j^*\right)}{\sum_{j=1}^{N} Y_j} \times 100 \quad (3.21)$$

Where $\boldsymbol{Y_j}$ and $\boldsymbol{Y_j^*}$ are the observed and estimated sediment of the events at the Jhanjharpur gauging site, $\boldsymbol{\bar{Y}}$ is the mean value of the observed events, and N is the total number of events. The value of NSE ranges from − ∞ to 100 %, wherein the high NSE and low RMSE values indicate good consistency between the predicted and observed values.

3.4 Silt Yield Index (SYI) and Sub-watershed Prioritization

The SYI considering sedimentation as the product of erosivity, erodibility, and aerial extent was conceptualized in the All India Soil and Land Use Survey (AISLUS) in 1972. The methodology has been progressively refined over time and tested for validity. The sediment detachment process predominates in the upland phase whereas sediment transport and deposition are the main processes in the low land phase. The most basic sediment yield model that could be conceived should involve precipitation, runoff, infiltration, soil characteristics, and transport components. The Erosivity determinants are the climatic factors and soil and land attributes that have a direct or reciprocal bearing on the unit of the detached soil material. The relationship can be expressed as:

Soil Erosivity = f (Climate, Physiography, slope, soil parameters, land use, soil management)

Sediment delivery from a hydrologic unit to a reservoir is a multiplicative function of the potential soil detachment representing the erosive factor, transportability of the detached material (delivery ratio), and area of the hydrologic entity. This can be expressed as

Sediment Yield = f × Delivery Ratio (DR) × Area (3.22)

So, the Erosivity is simulated whereas the DR is adjusted with the sediment yield weightage value, by the likely delivery of the eroded material. The SYI is defined as the yield per unit area and the SYI value for the hydrologic unit is obtained by taking the weighted arithmetic mean over the entire area of the hydrologic unit by using a suitable empirical equation.

In this study, the soil loss rate is estimated for each of the 12 sub-watersheds. The sub-watersheds are ranked into five priority classes (very high, high, medium, low, and very low)

based on the SYI values. The sediment yield index (SYI) in t km^{-2} yr^{-1} for individual sub-watersheds is calculated by using Eq. (2.1) as shown below.

$$\text{Sediment yield index (SYI)} = \sum (A_i \times W_i \times D_i) \times 100 / A_W \quad (3.23)$$

where A_i = area of the i^{th} unit (Erosion Intensity Mapping Unit), W_i = weighted value of the i^{th} mapping unit; D_i = delivery ratio; A_w = total area of the watershed. The determination of the erosion intensity mapping unit (EIMU) of each sub-watershed is based on the integrated information concerning the factors affecting erosion intensity considered as soil texture, slope, and land use land cover. Different sub-watersheds have different area classes (A_i) of each factor affecting erosion intensity differently. Hence, each area class of all factors needs proper consideration in determining the sediment yield index by assigning an appropriate weightage value (W_i). The weightage value has been assigned to each of the themes depending on the importance of the features in the watershed. The weighted value represents the collective effect of different factors of sediment detachment in terms of sediment yield.

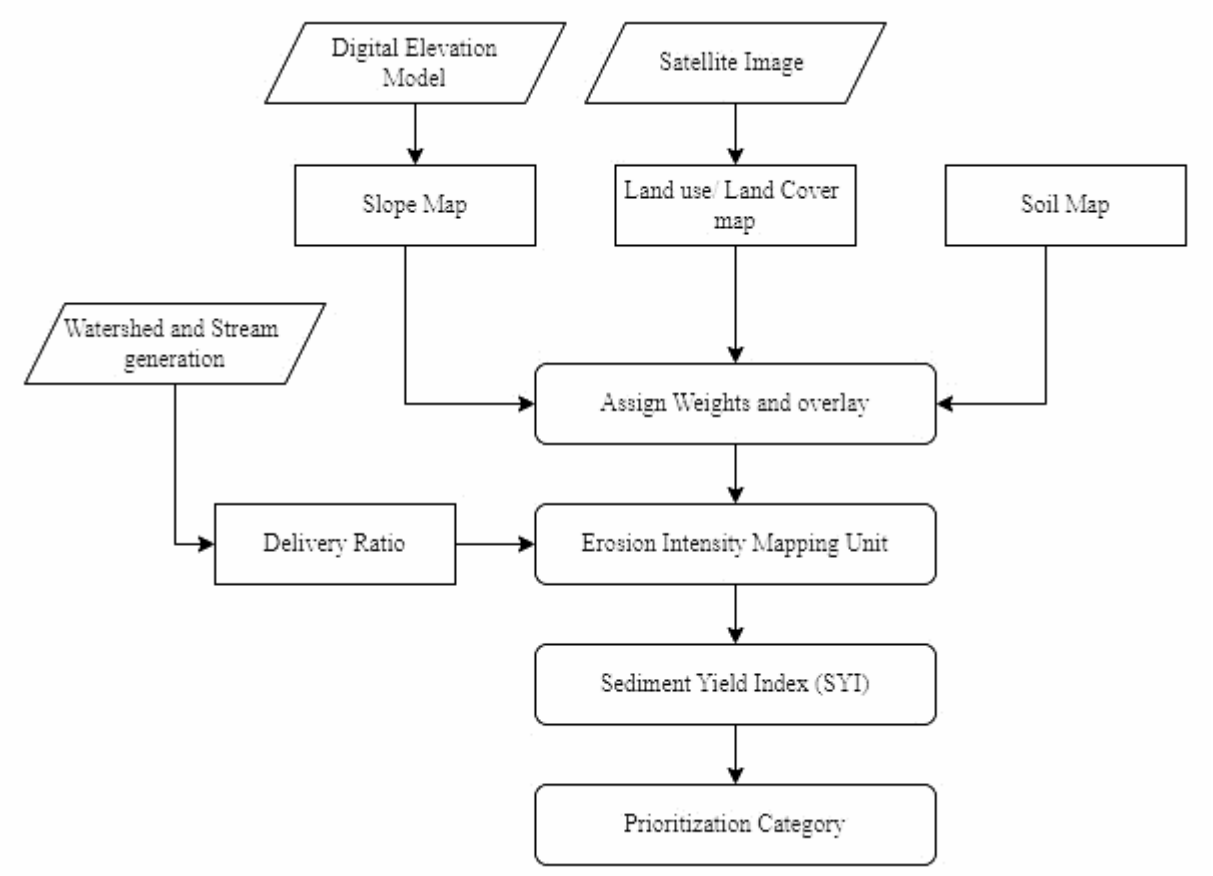

Figure 3.4 Schematic flow chart for micro-watershed prioritization using SYI

In this study, map layers are prepared in ArcGIS for each of the parameters, and the area of each EIMU is computed for individual sub-watersheds. The methodology adopted in the present study is described in Figure 3.4.

Prioritization of Sub-watersheds

The watershed prioritization and formulation of proper watershed management programs for sustainable development require information on watershed sediment yield. In general, implementation of management programmes in the sub-watersheds may not be taken up simultaneously, due to financial or technical constraints. In such a situation, it is always better to start management measures from the most critical sub-watersheds, which makes it mandatory to prioritize the sub-watersheds available. Thus, watershed prioritization is the ranking of different critical sub-watersheds according to the order in which they have to be taken up for the treatment and soil and water conservation measures. A particular sub-watershed may get top priority due to various reasons but often the intensity of land degradation is taken as the basis.

The prioritization of smaller hydrologic units within the vast catchments is based on the Silt Yield Index (SYI) of the smaller units. The watershed or sub-watersheds are subsequently rated into various categories corresponding to their respective SYI values. The application of the SYI model for prioritization of sub-watersheds in the catchment area involved the evaluation of:

a) Geomorphic factors comprising landforms, physiography, slope, and drainage characteristics.
b) Surface cover factors governing the flow of hydraulics and
c) Management factors

The various steps involved in the application of the model are:

- Systematic delineation of the sub-watersheds of KRB.
- Generation of a map indicating erosion intensity mapping units.
- Assignment of weightage values to various mapping units based on relative silt yield potential.
- Computing SYI for individual watershed / sub-watersheds.
- Grading of watersheds / sub-watersheds into very high, high, medium, low, and very low priority categories.

The SYI values obtained thus are further adjusted by multiplication with a suitable factor to account for the erosion and deposition of the material at the site. The gradation and the

assignment of priority ratings to the sub-watershed are based on the descending values of the sediment yield index.

3.5 Catchment Area Treatment Planning

Soil erosion poses a significant threat to the ecological balance and sustainability of landscapes, particularly in catchment areas where the intricate interplay of soil, water, and vegetation influences the overall health of the environment. The deleterious effects of erosion extend beyond the loss of fertile topsoil; they encompass degraded water quality, diminished agricultural productivity, and increased vulnerability to natural disasters. Recognizing the urgency of mitigating soil erosion and safeguarding the catchment's vital ecosystems, an integrated and proactive Catchment Area Treatment (CAT) Plan needs to be devised.

The CAT plan pertains to preparation of a management plan for treatment of erosion prone areas of the catchment through biological and engineering measures. However, a comprehensive CAT plan should also include the social dimensions associated directly or indirectly with the catchment. This comprehensive plan aims to address the multifaceted challenges posed by soil erosion within the lower KRB in India. By strategically combining preventive measures, conservation practices, and restoration efforts, immediate impact of erosion can be curtailed and can lead to a long-term resilience and sustainability.

Chapter 4: Results and Discussion

4.1 Soil Loss Estimated using RUSLE Model

4.1.1 Thematic Maps of USLE Factors

R factor

The R-factor values observed in the years 2000, 2010, and 2020 ranged between 312 and 1168, 345 and 779, and 1142 and 3710 MJ mm/ ha^{-1} h^{-1}, respectively. Figure 4.1(a, b, and c) shows the spatial distribution of the rainfall erosivity factor for 2000, 2010, and 2020. The spatial and temporal variability of rainfall in the basin causes a variable rainfall erosivity factor (R), highly correlated with the mean annual rainfall distribution.

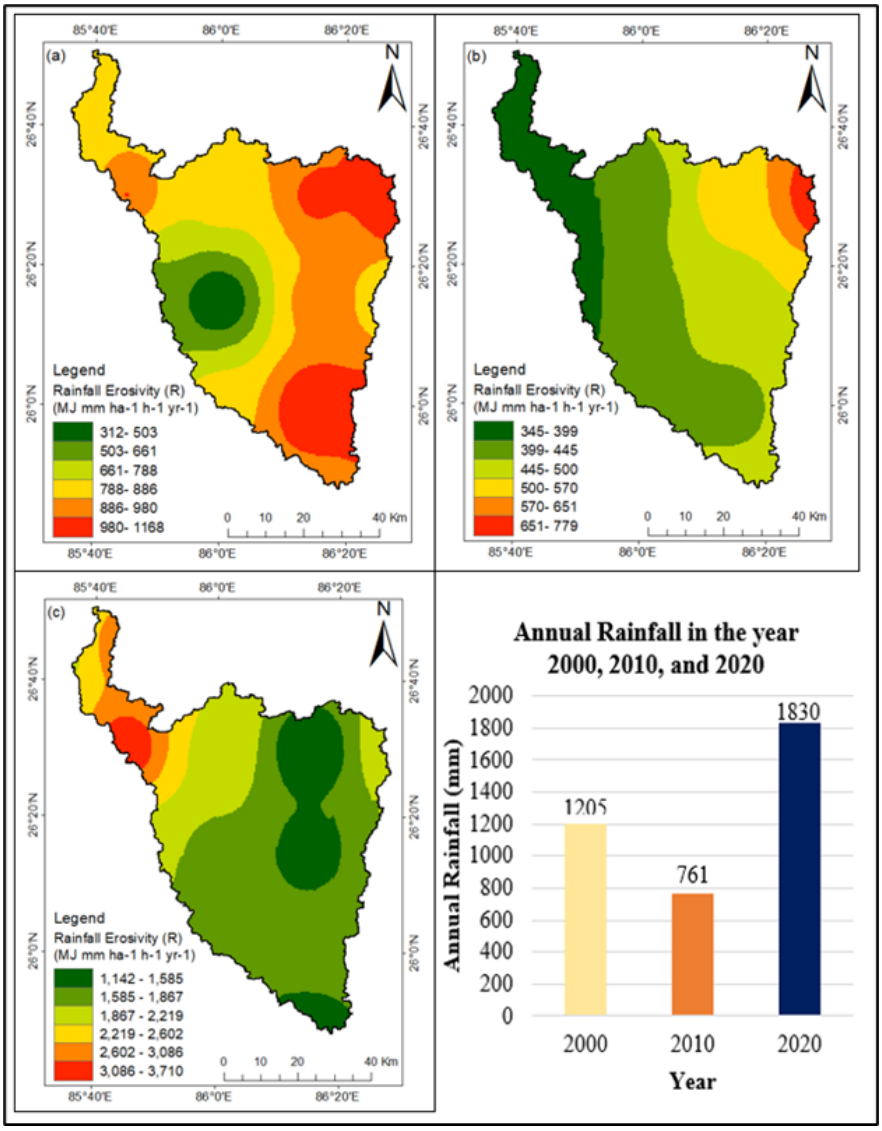

Figure 4.1 (a, b, and c): Spatial distribution of R-factor for the years 2000, 2010 and 2020, respectively

The R-factor in 2010 was low due to shorter rainfall events, whereas in 2020, the basin exhibited a higher R-factor due to high annual rainfall. The decrease in rainfall has significantly reduced the soil losses over the basin.

K-factor

The soil erodibility factor (K-factor) depicts the contributions of different soil types to water erosion. The spatial distribution of the K factor indicates dissimilarity in soil erosion from different types of soil under the same identical conditions. Similar to R factors, the K factor was estimated using the results obtained from soil samples analysis (Figure 4.2). The computed values of K factor were ranged between 0.10 and 0.15 $\mathrm{t\,ha^{-1}MJ^{-1}mm^{-1}}$. The high K value indicates the soil particles are easily detachable, high rate of infiltration but severely prone to runoff and sedimentation. The lower K value shows less detachable and is highly resistant to raindrop energy (Fu et al., 2011; Pal and Debanshi, 2018; Kayet et al.,2018). In the basin, most of the agricultural land falls under the loam soils, exhibiting a K value of 0.15, whereas clay soil shows a lower K value of 0.1. The sandy loam soil found along the riverbanks has a K-factor of 0.13, rendering it very erodible due to the steep topography.

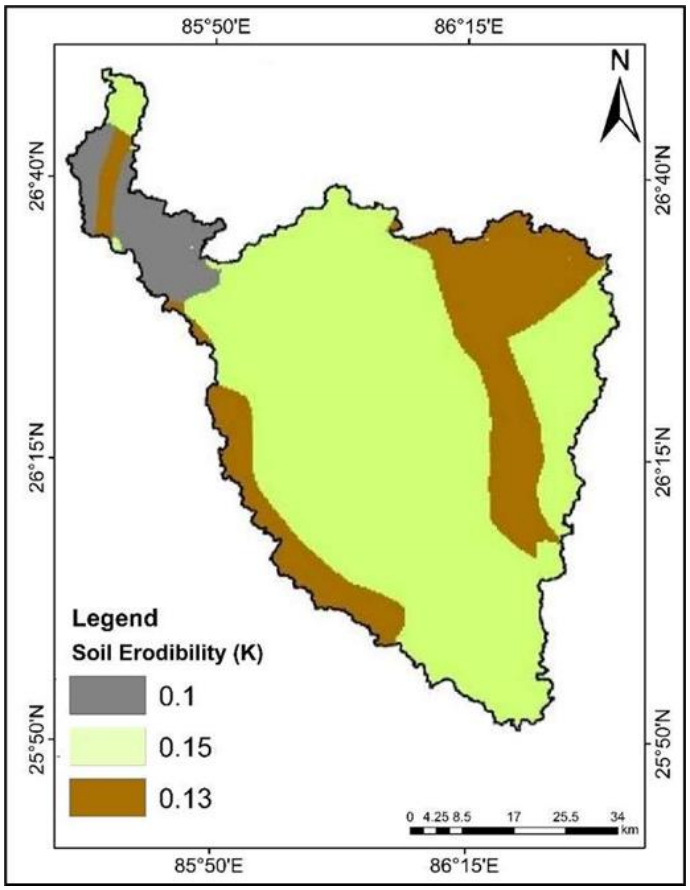

Figure 4.2 Spatial distribution of Soil erodibility factor (K factor)

LS Factor

The basin slope varies from 0- 32 degrees with a maximum elevation of 99 m. The calculated topographic factor (LS) of the basin ranges between 0 and 222. The areas with steep slopes near the river networks exhibited the highest LS factor and maximum annual soil erosion. The annual soil loss is strongly correlated with the LS factor, as the velocity of overland flow increases with an increment in slope length and steepness, leading to higher soil erosion (Haan et al., 1994).

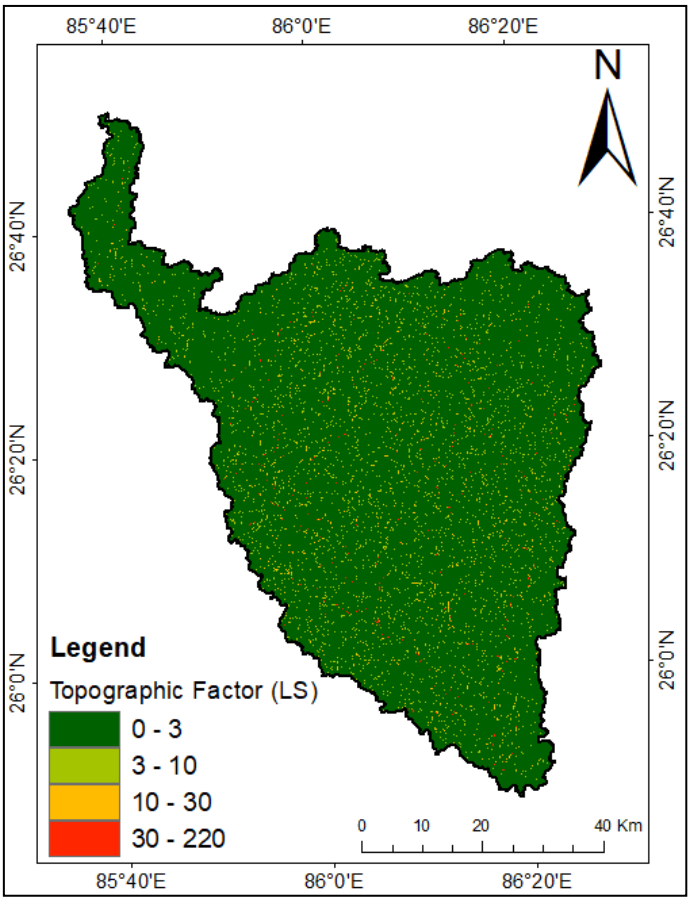

Figure 4.3 Topographic factor of the basin

C factor

The C factor indicates how far soils are exposed to the direct impact of rainfall and runoff significantly determines the tendency to erode. Hence, the more barren land in a region shows a higher rate of soil loss. In contrast, higher vegetation cover slows down erosion by plants canopy structures and litter covers. In general, the C-factor values range between 0 and 1, where values tend to 1 indicate more prone to erosion due to lack of proper vegetation cover and vice-

versa. The spatial distribution of the C factor for decadal land use/land cover maps is shown in Figure 4.4.

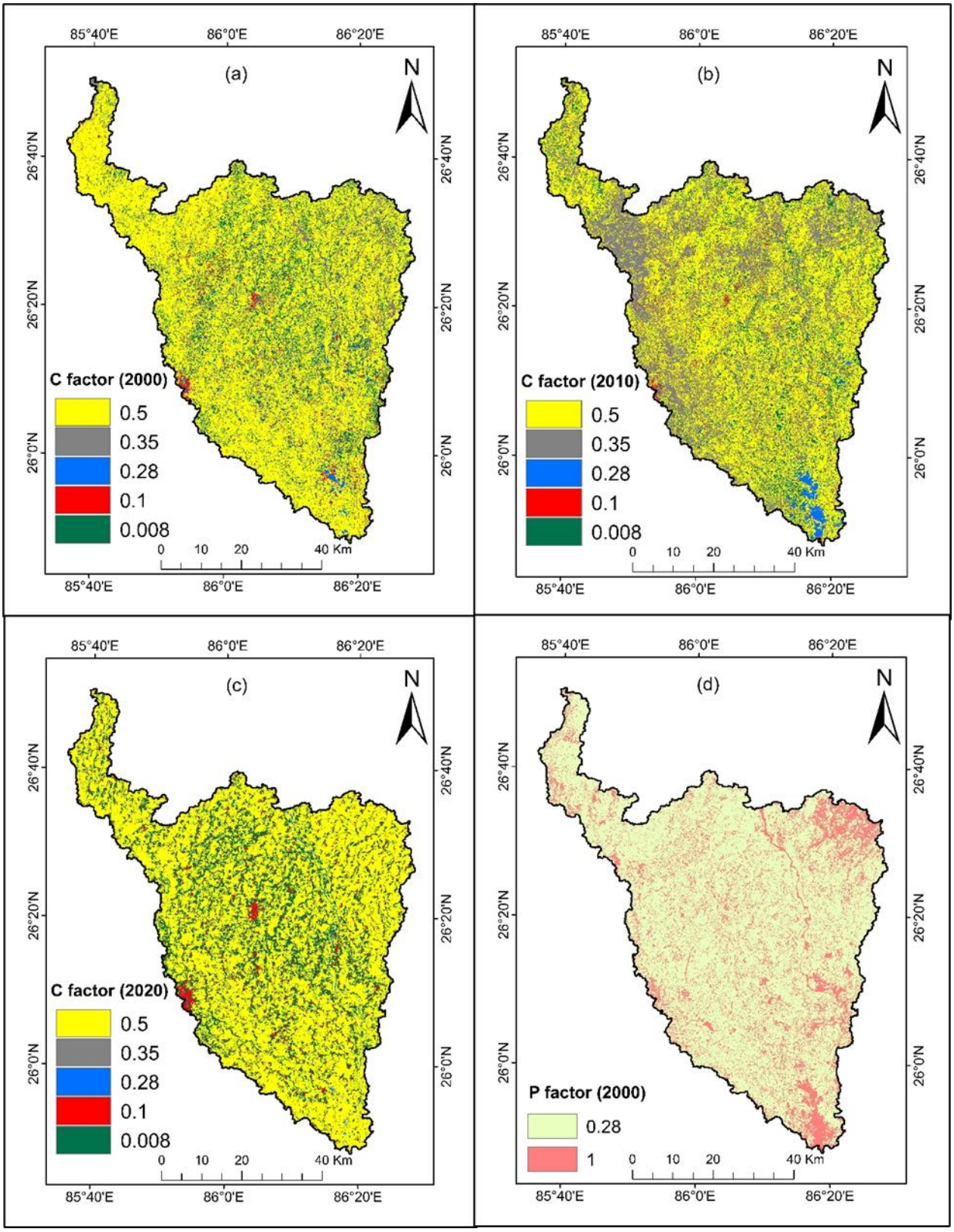

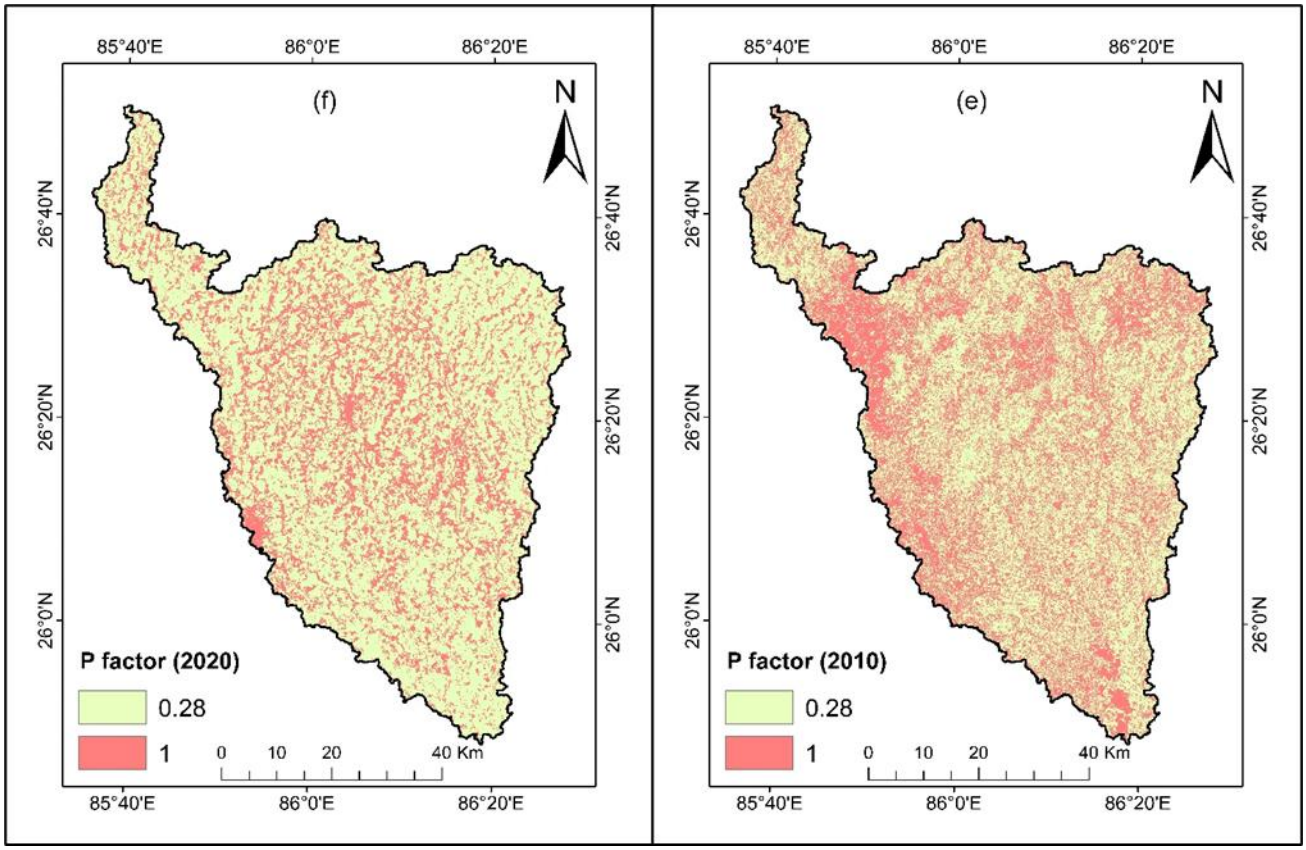

Figure 4.4 Spatial distribution of C and P factors for the years 2000, 2010, and 2020

P factor

The P-factor reveals the effectiveness of soil conservation measures in an erosion-prone area. Generally, P values vary between 0 and 1. Areas well-protected from erosion forces usually have lower P-factor values while, areas that are not well-protected from erosion (i.e., lacking effective soil conservation practices) are assigned higher P-factor values. Figure 4.4 shows the magnitude and spatial distribution of conservation practice factors for 2000, 2010, and 2020. The P-factor values indicate that agricultural land with paddy fields is less susceptible to erosion as compared to other land use classes.

4.1.2 Spatial Distribution of Soil Erosion

The spatial distribution of the annual soil loss map was developed for the lower Kamla River basin using RUSLE in ArcGIS framework using climatic and geospatial data. For better visual interpretation and easy understanding, the annual soil loss ranges are divided into six erosion risk classes based on the previous literature class intervals (Babu et al., (1984); Pandey et al., (2009); Prasannakumar et al., (2011)). The assigned soil erosion class intervals are slight (<5 t/h/yr), moderate (5–10 t/h/yr), high (10–20 t/h/yr), very high (20–40 t/h/yr), severe (40–80

t/h/yr), and very severe (>80 t/h/yr). The results of decadal soil erosion maps are shown in Figure 4.5 (a, b, and c) and a comprehensive summary has been provided in Table 4.1.

Table 4.1 reveals that nearly 58% of the area of the lower Kamla basin falls under the slight erosion risk category of less than 5 t/ha/yr. The estimated average annual soil loss in the years 2000, 2010, and 2020 was 19.94, 12.11, and 31.81 t/ha/yr. Nearly, 58.34% area of the basin exhibited slight erosion in 2000, 62.76% in 2010, and 52.56% in 2020, respectively. It indicates that agricultural land areas with low slopes are dominant in these regions. Moderate soil loss (5-10 t/ha/yr) occurred in 11.17% area of the basin in 2000, 13.76% in 2010, and 6.68% in 2020.

Table 4.1 Percentage of the area under different soil erosion classes

Soil erosion rate intervals (tonnes/ha/yr)	**Erosion class**	**Annual soil loss (percentage of Area)**					
		Year 2000		**Year 2010**		**Year 2020**	
		Area (%)	**Area (km^2)**	**Area (%)**	**Area (km^2)**	**Area (%)**	**Area (km^2)**
<5	Slight	58.34	2592.41	62.76	2788.82	52.56	2335.57
5-10	Moderate	11.17	496.35	13.76	611.44	6.68	296.83
10-20	High	12.55	557.67	11.68	519.01	11.55	513.24
20-40	Very High	8.87	394.15	6.71	198.17	13.56	602.55
40-80	Severe	4.99	221.74	2.97	131.98	8.77	389.70
>80	Very Severe	4.08	181.30	2.12	94.20	6.88	305.72

Consequently, a significant percentage of the land area exhibits high to very severe erosion (>80 t/ha/yr), i.e., 30.49% in 2000, 23.48% in 2010, and 40.76% in the year 2020 of the total basin area. The decadal soil erosion map shows that in 2010, more areas fell into the "slight erosion" category. This was because a lower R factor led to less rainfall, which directly affected soil erosion.

The spatial distribution pattern of soil loss in the basin shows that the mostly agricultural and plantation areas fall under the category of slight erosion (0–5 t/ha/yr), whereas severe (40–80 t/ha/yr) to very severe (>80 t/ha/yr) erosion occurs mostly along the rivers and their networks. Riverbanks that are unprotected from bank erosion and are mostly composed of sandy loam soil are the most vulnerable to erosion in the basin. Also, the soil loss varies with high rainfall erosivity, land use, and land cover changes over the decades in the basin.

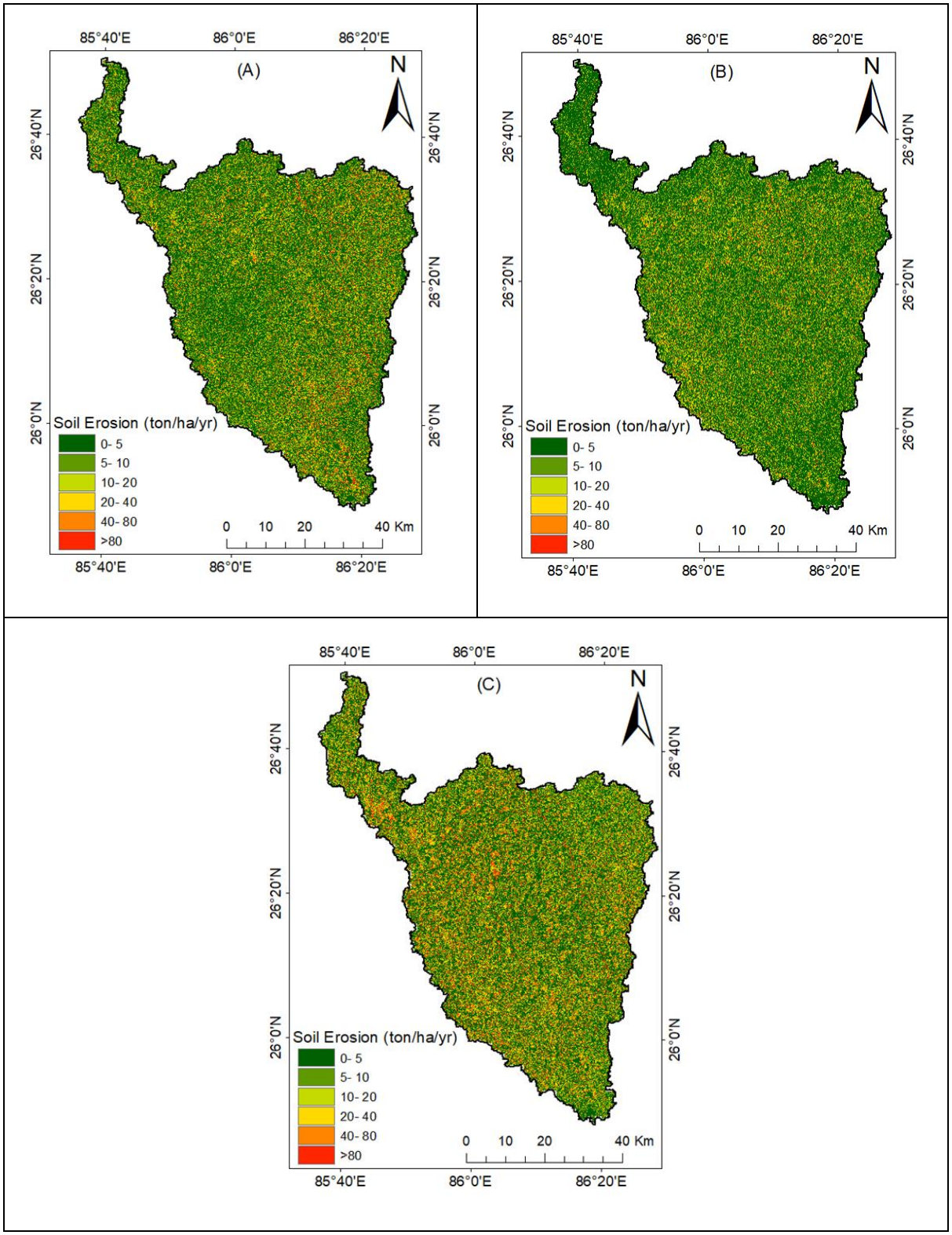

Figure 4.5 Soil erosion risk map of lower Kamla basin (A) 2000 (B) 2010 and (C) 2020

Furthermore, the RUSLE model was employed for quantitative assessment of sub-watershed-wise annual soil erosion in tonnes/ha/year for each year from 2010 to 2020. The results obtained are presented in Table 4.2.

Table 4.2 Yearly sub-basin-wise soil erosion estimated by RUSLE during 2000-2020

Year	SW1	SW2	SW3	SW4	SW5	SW6	SW7	SW8	SW9	SW10	SW11	SW12
2000	14.39	14.53	11.84	18.11	25.06	21.66	14.31	15.00	26.64	27.16	22.95	35.90
2001	17.46	18.22	13.27	28.15	21.03	18.43	15.67	14.86	20.57	22.22	13.34	31.89
2002	24.52	34.16	26.16	57.80	43.65	46.40	32.16	26.14	34.16	30.92	18.71	33.72
2003	9.35	12.50	11.59	23.17	24.60	21.86	16.65	24.04	20.98	29.07	13.29	27.62
2004	8.89	15.70	15.82	41.39	79.05	86.66	31.94	20.44	58.07	57.66	43.08	72.57
2005	27.76	26.53	19.70	40.53	35.12	24.09	22.27	20.28	24.89	27.16	15.63	43.03
2006	14.82	14.25	10.39	21.02	14.48	12.13	11.24	11.02	14.40	17.50	10.41	33.85
2007	41.89	37.73	56.07	58.15	45.26	30.38	42.21	50.25	41.68	41.42	17.41	29.10
2008	13.57	16.25	23.55	25.00	15.88	12.30	17.83	24.32	21.77	24.10	10.69	18.01
2009	17.74	19.76	37.80	34.36	36.10	19.99	27.22	25.94	26.84	26.50	12.46	28.20
2010	7.92	9.61	13.87	16.13	12.79	11.48	12.20	14.26	15.90	15.52	7.60	13.28
2011	12.67	14.38	23.76	25.53	25.60	19.98	21.05	26.23	29.06	27.48	13.16	20.86
2012	4.34	5.07	11.30	10.58	10.48	9.00	10.37	21.20	17.61	22.15	8.98	16.56
2013	4.58	6.35	9.51	11.44	9.13	9.09	8.90	10.85	11.29	11.81	5.95	11.48
2014	7.93	11.95	13.66	20.75	16.40	16.23	15.38	14.75	23.67	26.11	13.11	18.43
2015	5.17	6.16	7.65	10.45	7.61	7.91	7.78	8.07	11.28	13.68	6.42	11.85
2016	11.45	12.20	12.82	18.49	13.51	16.85	13.46	14.72	24.22	28.59	14.91	17.70
2017	21.07	24.84	32.96	44.73	21.33	21.98	30.74	29.33	30.77	35.47	15.00	19.24
2018	8.93	11.52	16.23	21.83	10.00	9.50	15.10	14.08	13.91	16.28	6.74	9.39
2019	17.42	20.92	22.85	34.85	25.41	27.08	25.13	25.10	37.10	41.45	20.58	27.22
2020	11.63	13.45	13.64	17.96	11.60	11.98	13.94	12.93	12.57	14.16	9.44	6.40

4.1.3 Inferences- RUSLE

This study demonstrates the spatial distribution of the annual soil loss in the lower Kamla River basin using the RUSLE model. It is more important to assess and identify the soil erosion-prone areas for conservation to support decision-making for soil and water conservation over the entire basin. It is also necessary to understand the spatial pattern of soil erosion processes at the basin level for the effective application of erosion control measures to minimize the

negative impact of erosion downstream. In this study, decadal soil loss was estimated under changing land use cover and uncertain climatic conditions. The erosion risk map of the basin indicates that on an average 58 % area of the basin falls under slight erosion category, mostly agricultural and plantation areas. It is due to flatter topography, where the slope varies between 27 to 99 m above MSL and agricultural dominant (nearly 75%) land use land cover. As earlier mentioned, paddy is the major monsoonal crop in the basin, which is further protected with earthen bund of 1-4 ft to reduce water losses during irrigation. These structures have efficiently conserved the soil and runoff losses from agricultural lands (Annexure B (Figure B.10)). Narayana and Babu (1983) have found that Indian soils face the annual soil loss of 16.4 t/ha. It was reported that 56% of soil loss occurs due to rainwater erosion, and 29% of losses are carried away by rivers (Biswas and Pani, 2015; Narayana and Babu, 1983). In this study, severe (40-80 t/ha/yr) to very severe (>80 t/ha/yr) erosion occurred along the major rivers and their networks. It is because of a lack of bank stabilization, higher water forces, high steep slopes, most minor vegetation, and sandy loam soils, which are more susceptible to erosion. Although we don't have the observed sediment data at gauge sites, we compared our results with Google Earth Pro images (Figure 4.6). It provides robust evidence and better visualization of soil erosion along the river bank in the basin.

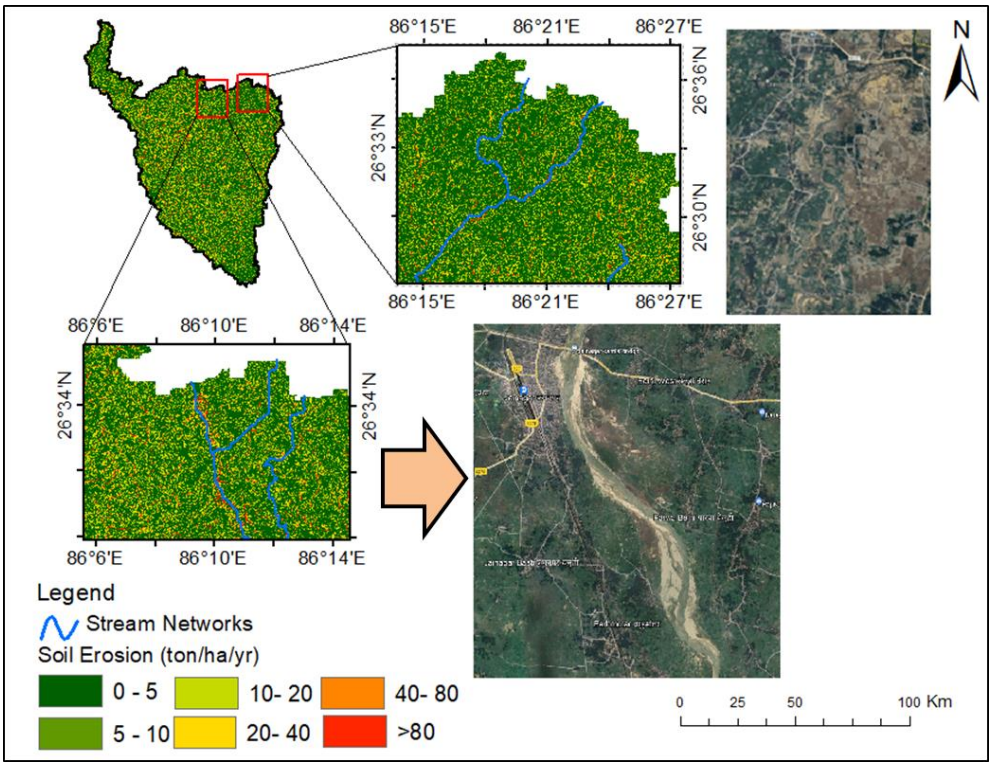

Figure 4.6 Verification of soil erosion with Google Earth Pro image

A major part of the basin is approx. 62% (4,510 km^2 out of a total area 7,232 km^2) falls in India while, the rest is in southeast Nepal. As the Kamla River basin has experienced a high sediment issue over the years downstream of the basin. In this study, only Indian parts (62%) of the basin were considered, which shows that a significant percentage of the basin area falls under the high to very severe erosion category. It is due to high annual rainfall, unprotected cultivation practices near the river bank areas, and lack of bank stabilization.

Additionally, a significant contribution of sediments comes from the upper parts of Nepal, mostly from the upper KRB and erosion processes in the upstream mountainous regions and transitional sub-basins (Uddin et al., 2016). It is due to higher topographic steepness, rainfall erosivity, and transitional land use practices i.e., unprotected agricultural practices at the higher elevated areas. The rest comes from the floodplains and the river channels due to the reworking of sediments and agricultural activities. Our findings indicated that a significant erosion occurred from the basin, mostly stream bank erosion, which is a major issue in the lower KRB, which may be exacerbated by high-intensity rainfall and frequent floods, resulting in a significant contribution of sediments at the lower parts.

4.2 Soil Erosion Simulated using InVEST-SDR Model

The InVEST-SDR model combines RUSLE with a sediment delivery ratio (SDR) to estimate sediment export. In this study, the model was employed to quantify the spatial distribution of soil loss and sediment delivery within the Kamla River Basin at the Jhanjharpur outlet. It accounts for spatial heterogeneity in land cover, topography, soil properties, and rainfall erosivity. Finally, maps of soil loss, sediment delivery, and sediment retention have been produced.

4.2.1 Calibration Results

The observed sediment yield at Jhanjharpur outlet was provided from 2005 to 2012 (continuous daily sediment concentration data). The model was calibrated using these data to obtain the values for k_b and IC_0 and consequently simulate the sediment export. The calibration of k_b was started from 2 with an increment of 0.2. In this case, k_b value of 5 and IC_0 of -15 were obtained, which provided good agreement with the measured values. The observed and simulated values for the sediment yield at the above-mentioned values of calibration coefficients are presented in Table 4.3 Additionally, the observed and simulated values show R^2 of 0.72, as shown in Figure 4.7.

Table 4.3 Observed and simulated sediment at Jhanjharpur for k_b=5, IC_0=-15

Year	Observed Sediment (tonnes/year)	Simulated Sediment (tonnes/ Year)
2005	1053031	2027901.012
2006	1058077	2280359.804
2007	7682950.87	3761279.073
2008	7393222.13	4119859.858
2009	3116236.65	3785362.989
2010	2117325.42	2539445.226
2011	4228337.06	2683779.098
2012	920191.501	2369155.675

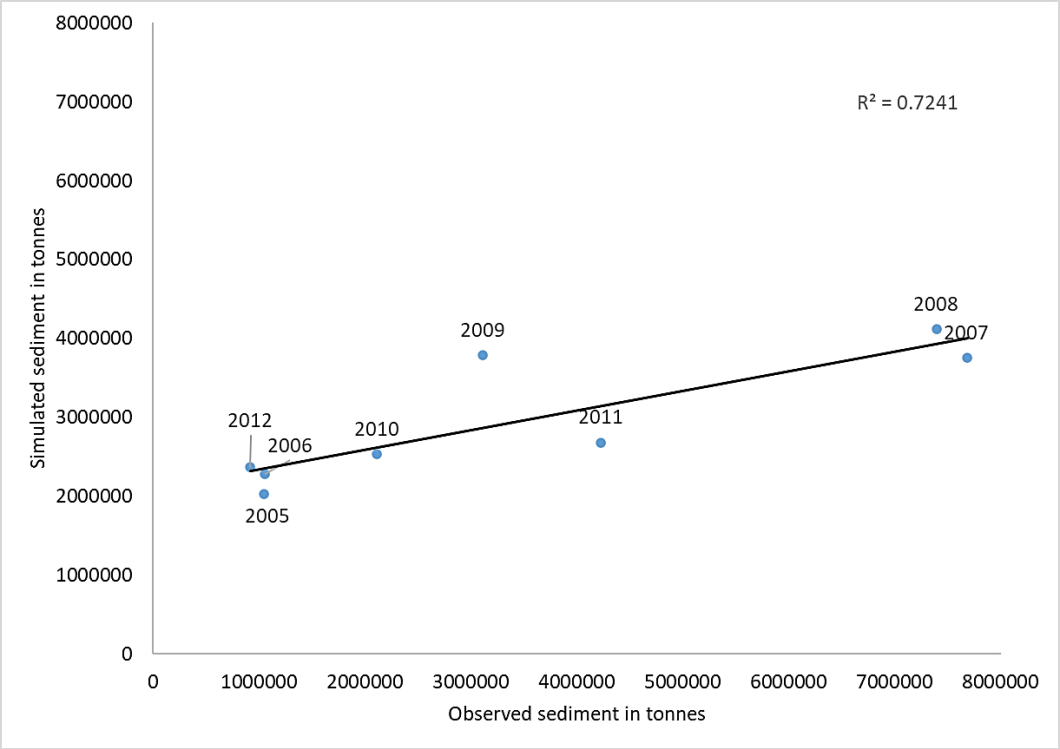

Figure: 4.7 Correlation between observed sediment and simulated sediment

These calibration coefficients are obtained for the watershed at Jhanjharpur outlet, which constitutes the majority of the region in Nepal. Since there is no data available at the outlet of Lower Kamla River Basin, which happens to be the area of interest it is assumed that same calibration coefficients will be applicable here. Using this set of calibration parameters, sediment export and critical soil erosion-prone areas are identified.

4.2.2 Soil Loss and Sediment Export

InVEST SDR model runs using the calibrated parameters generated spatial soil loss and exported sediment outputs. Figures 4.8 (a, b, c, d, e, f) show the total potential soil loss per pixel of the original land cover calculated from the USLE equation for 2007, 2008, 2009, 2010, 2011, and 2012, respectively.

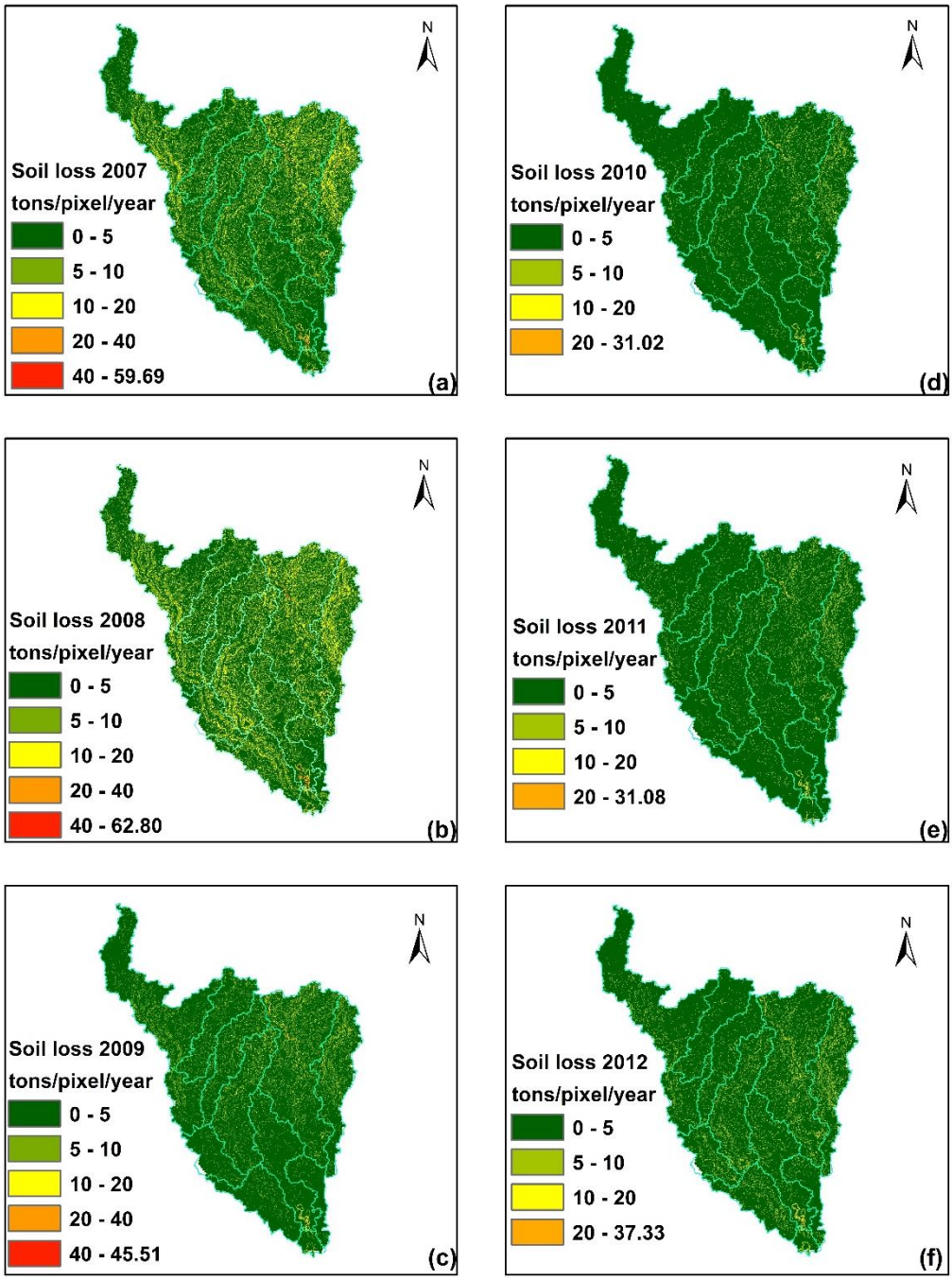

Figure 4.8 Expected Annual Soil Loss in tons/pixel/year for 2007, 2008, 2009, 2010, 2011, and 2012

Table 4.4 presents the biophysical values for each watershed derived after successful model runs from 2007 to 2012. The details included are as follows: TSE: Total amount of sediment exported to the stream per watershed. TPSL: Total amount of potential soil loss in each watershed calculated by the USLE equation. SAExp: The sum of avoided exports in the watershed. SAEr: The sum of avoided local erosion in the watershed. TSD: Total amount of sediment deposited on the landscape in each watershed, which does not enter the stream.

The table provides an assessment of sediment exported, deposited, and retained in each sub-watershed for the Indian part of the Kamla River Basin.

Table 4.4 Simulated results using calibrated parameters k_b=5, IC_0=-15 for LKRB

Year	Sub-watershed	TPSL	TSE	TSD	SAExp	SAEr
2007	SW1	326171.14	222017.49	12975.22	882025.51	1533071.80
	SW2	147733.13	101924.87	9330.23	559009.52	861015.78
	SW3	100750.08	70124.06	19482.99	366544.44	560285.23
	SW4	141807.72	98526.57	17997.98	558142.97	828605.22
	SW5	527947.16	359691.45	80832.09	1865550.67	2780785.63
	SW6	286092.77	184378.07	18188.48	745514.88	1277740.41
	SW7	241368.26	167382.23	73937.72	971201.90	1334589.17
	SW8	84075.56	58815.32	13583.72	286335.68	418302.69
	SW9	174833.30	121897.07	55058.72	636946.80	876277.08
	SW10	116620.23	82017.04	9935.68	345954.95	529823.04
	SW11	57624.29	39073.81	3140.24	164804.99	264766.28
	SW12	21644.41	15474.47	491.98	39335.79	72215.31
	Total	2226668.05	1521322.45	314955.05	7421368.1	11337477.64
2008	SW1	341130.44	231366.43	13268.25	917025.00	1602399.77
	SW2	150249.46	103676.43	9517.80	569628.64	877114.38
	SW3	114565.75	79768.14	22150.66	416183.09	636260.12
	SW4	153875.89	106987.24	19192.87	604107.98	896033.85
	SW5	567299.56	386920.98	87027.60	2014985.20	2999767.38
	SW6	291782.11	185649.44	18945.40	752132.93	1309959.44
	SW7	294235.95	204254.65	89883.78	1172423.91	1607697.74
	SW8	108249.89	75745.35	17557.30	368113.87	535635.90
	SW9	221061.71	154093.16	69329.39	804543.22	1106549.18
	SW10	160460.48	112858.62	13820.80	475605.40	726275.48
	SW11	70397.01	47729.54	3832.80	200036.93	322032.36
	SW12	26858.38	19203.30	612.48	48876.10	89452.59
	Total	2500166.64	1708253.29	365139.15	8343662.26	12709178.18
2009	SW1	206004.84	139660.38	8075.66	554834.44	968941.54
	SW2	100317.02	69157.55	6408.36	377622.50	582815.00
	SW3	60560.76	42137.53	12102.16	221369.05	336233.76
	SW4	101638.31	70549.80	12751.82	399538.85	594770.90
	SW5	353355.89	240115.69	52115.64	1232738.63	1850637.38

Year	Sub-watershed	TPSL	TSE	TSD	SAExp	SAEr
	SW6	172776.48	111504.54	10660.31	449332.35	771337.24
	SW7	160080.07	110834.38	49254.22	653654.06	901280.27
	SW8	42189.42	29521.13	6696.92	143194.98	209319.91
	SW9	103647.96	72251.42	32385.81	377741.69	521095.58
	SW10	72532.26	51031.57	6363.07	215050.73	328159.08
	SW11	34961.26	23704.76	1853.60	98094.97	158946.01
	SW12	14410.37	10301.09	326.35	26185.99	48291.00
	Total	1422474.64	970769.84	198993.91	4749358.22	7271827.67
2010	SW1	133108.65	89979.15	5202.51	358473.56	628767.72
	SW2	65576.06	45229.59	4155.73	247932.06	382552.93
	SW3	45095.24	31385.82	8842.81	164057.19	250717.74
	SW4	66474.60	46187.28	8299.48	261031.05	388264.81
	SW5	269646.17	183866.27	40970.12	954773.43	1423156.05
	SW6	150530.88	95923.15	9495.35	386777.75	674983.95
	SW7	115712.66	80238.15	35445.65	466284.34	641610.05
	SW8	36338.75	25427.56	5802.39	123358.14	180589.44
	SW9	88829.43	61993.65	27593.59	320719.66	442063.89
	SW10	61017.72	42946.65	5346.35	180608.32	276069.25
	SW11	30135.12	20441.09	1590.01	84678.03	137170.76
	SW12	12891.10	9215.28	291.92	23367.32	43257.38
	Total	1075356.39	732833.64	153035.90	3572060.85	5469203.97
2011	SW1	157574.99	106607.04	5961.91	421895.81	740910.54
	SW2	71163.98	49060.19	4416.64	266223.34	411752.64
	SW3	47685.91	33192.32	9324.08	173755.61	265319.52
	SW4	68284.82	47450.49	8652.45	268603.58	399165.83
	SW5	269345.01	183694.88	40543.70	947972.95	1415105.55
	SW6	146090.25	93232.59	9438.96	377318.40	654856.16
	SW7	119851.57	83094.96	36724.91	484128.40	666403.70
	SW8	39569.40	27690.94	6411.88	134539.93	196478.66
	SW9	94602.04	65941.15	29716.02	344877.90	475196.16
	SW10	63912.03	44959.06	5562.72	189687.59	290267.96
	SW11	31313.60	21234.61	1683.93	88929.69	143405.06
	SW12	12059.54	8621.01	273.42	21876.28	40503.92
	Total	1121453.14	764779.23	158710.63	3719809.48	5699365.71
2012	SW1	163841.91	111451.03	6317.24	440107.82	768739.48
	SW2	68770.39	47482.08	4317.01	261246.52	402037.39
	SW3	55051.88	38319.93	10641.43	201086.20	308012.88
	SW4	71866.03	50011.20	8750.09	282104.15	419021.47
	SW5	291897.48	199220.27	47376.15	1055963.42	1562960.60
	SW6	162227.29	102720.44	10624.29	416670.85	730823.69
	SW7	146302.37	101567.23	44659.50	583308.64	800558.24
	SW8	56703.52	39677.36	9142.64	192820.82	281753.30
	SW9	119386.72	83371.70	36970.35	428809.25	590046.76
	SW10	88681.52	62395.57	7674.38	262561.06	401583.29
	SW11	39804.14	26987.11	2114.71	111937.63	181170.32

Year	Sub-watershed	TPSL	TSE	TSD	SAExp	SAEr
	SW12	16866.54	12058.74	383.75	30530.59	56389.16
	Total	1281399.80	875262.66	188971.55	4267146.95	6503096.59

TPSL: Total potential soil loss (tons/watershed/year)
TSE: Total sediment exported (tons/watershed/year)
TSD: Total sediment deposited (tons/watershed/year)
SAExp: Sum of avoided export (tons/watershed/year)
SAEr: Sum of avoided erosion (tons/watershed/year)

Similarly, using the values of calibrated parameters, the model was run for the year 2020 to estimate the total amount of expected annual soil loss from each pixel (Figure 4.9). This gives a clear scenario that has been generated using the observed data of the past and gauge into the future.

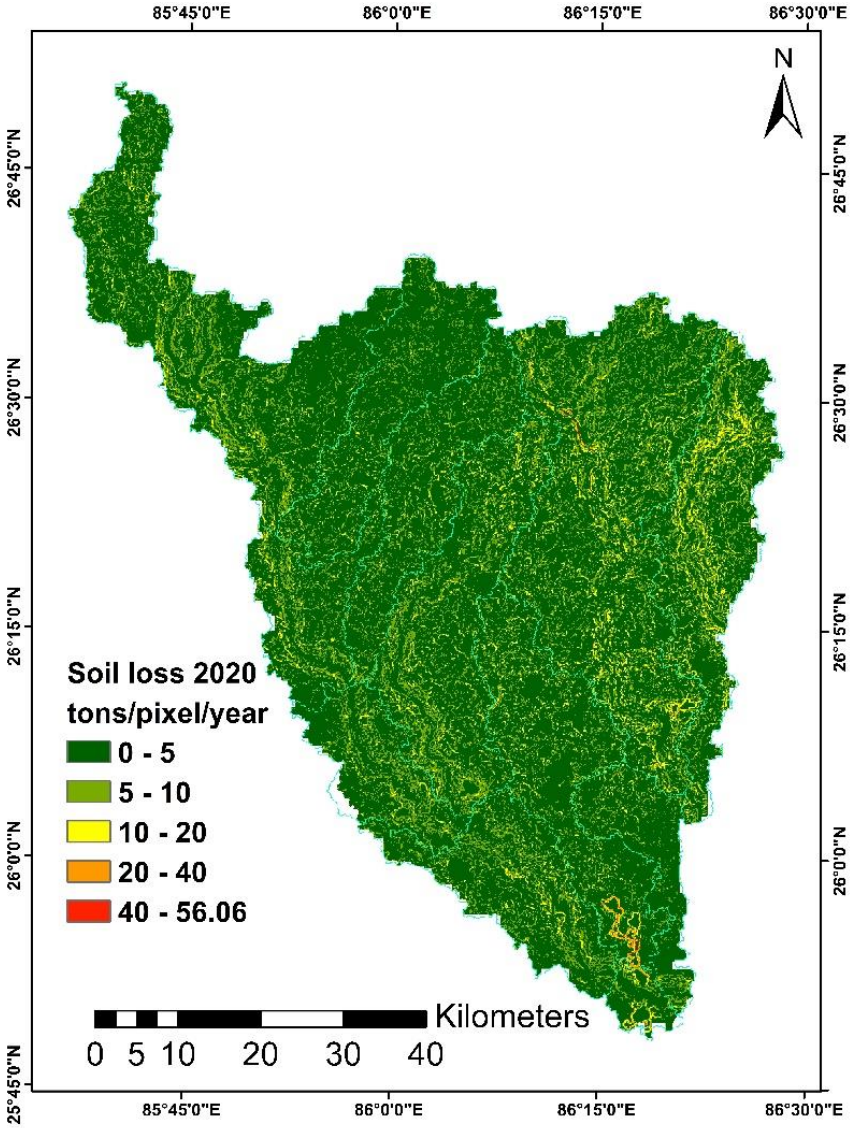

Figure 4.9 Expected Annual Soil Loss in tons/pixel/year for 2020

Since the InVEST model was calibrated for the KRB (India and Nepal region) it was required to use global satellite rainfall data to generate Rainfall Erosivity layers. CHIRPS rainfall data was used for this purpose. The CHIRPS data is available upto year 2020, and therefore, this study proposed CAT plan based on the critical soil erosion prone areas identified for the year 2020. Table 4.5 shows the detailed assessment of exported, deposited, and retained sediment in each sub-watershed.

Table 4.5: Simulated results using calibrated parameters k_b=5, IC_0=-15 for LKRB for 2020

Sub-watershed	TPSL	TSE	TSD	SAExp	SAEr
SW1	274272.31	184357.40	9975.44	724595.52	1283544.48
SW2	102123.08	70521.67	6533.67	390261.69	600113.83
SW3	81666.32	56871.28	15689.74	296106.38	453293.13
SW4	106928.94	74368.32	13570.62	421749.49	624996.64
SW5	421551.43	288704.84	68036.68	1525790.14	2250788.72
SW6	234959.66	147870.89	14581.75	598841.13	1058838.39
SW7	205439.13	142522.59	62864.47	823109.43	1130386.18
SW8	71675.28	50149.97	11568.65	242964.72	354784.39
SW9	177815.32	124172.67	54461.19	636781.19	877986.10
SW10	122923.46	86513.03	10658.22	362704.53	554146.64
SW11	59202.62	40083.82	3046.47	164768.76	268798.95
SW12	24169.10	17282.18	553.36	43911.00	80525.30
Total	1882726.65	1283418.65	271540.25	6231583.99	9538202.74

Finally, the results of total potential soil loss expressed in tons/watershed/year from Table 4.4 and 4.5 were converted into tons/hectare by dividing the values by respective sub-watershed areas. Consequently, the quantitative assessment of sub-watershed-wise annual expected soil erosion in tonnes/ha/year for each year from 2010 to 2012 and 2020 was conducted. The results obtained are presented in Table 4.6.

Table 4.6 Yearly sub-basin-wise soil erosion estimated by InVEST-SDR during 2000-2012 and 2020

Year	SW1	SW2	SW3	SW4	SW5	SW6	SW7	SW8	SW9	SW10	SW11	SW12
2007	4.76	4.39	4.72	4.54	5.75	6.48	4.99	4.29	4.21	3.91	3.46	4.41
2008	4.98	4.47	5.37	4.93	6.18	6.61	6.08	5.53	5.33	5.39	4.23	5.47
2009	3.01	2.98	2.84	3.26	3.85	3.91	3.31	2.15	2.50	2.43	2.10	2.94
2010	1.94	1.95	2.11	2.13	2.94	3.41	2.39	1.86	2.14	2.05	1.81	2.63
2011	2.30	2.12	2.23	2.19	2.94	3.31	2.48	2.02	2.28	2.15	1.88	2.46
2012	2.39	2.04	2.58	2.30	3.18	3.68	3.03	2.90	2.88	2.98	2.39	3.44
2020	4.00	3.04	3.83	3.43	4.59	5.32	4.25	3.66	4.29	4.13	3.56	4.92

4.2.3 Inferences-InVEST-SDR Model

The main motive behind employing InVEST-SDR model in this study was to make use of observed sediment data and develop an accurate model to simulate and estimate soil loss for LKRB. However, there is a major limitation with this model particularly in context of this study. In this study, the observed sediment data was provided at Jhanjharpur station, using which the model was calibrated for the catchment area at Jhanjharpur outlet encompassing a total area of 3436.43 km^2. Interestingly, of the total area, only 733.19 km^2 falls in India which accounts for only 21.3 % area, and the remaining area lies in Nepal. The calibration parameters obtained for the model were assumed to be valid and applicable for the Lower KRB which may produce uncertainty in the results. Due to the paucity of data at the outlet of Lower KRB, the InVEST-SDR was run for the LKRB to model the sediment dynamics, and the results obtained are considered to be a representation of critical erosion-prone areas.

The outputs produced by RUSLE (Table 4.2) and InVEST-SDR (Table 4.6) indicate soil loss in various sub-watersheds of LKRB. It is difficult to compare or comment on the accuracy of results because no data is available at the outlet. However, Table 4.7 shows sediment estimates from both approaches for each sub-watershed. Interestingly, there is a striking difference between the results of both models. For each year, the RUSLE model shows very high annual soil loss (tons/ha/year) in comparison to the InVEST model. The reason for very low soil erosion simulated by InVEST can be attributed to the terrain of LKRB, which has comparatively lower elevation range in contrast to the high elevation terrain of the KRB which encompasses more than 78% area in Nepal.

The InVEST model results in this study cannot be validated due to a lack of observed data at the outlet.

Table 4.7 Comparison of annual soil loss (tons/ha/year) estimated by RUSLE and InVEST

Year	SW1		SW2		SW3		SW4	
	RUSLE	**InVEST**	**RUSLE**	**InVEST**	**RUSLE**	**InVEST**	**RUSLE**	**InVEST**
2007 (t/ha)	41.89	4.76	37.73	4.39	56.07	4.72	58.15	4.54
2008 (t/ha)	13.57	4.98	16.25	4.47	23.55	5.37	25.00	4.93
2009 (t/ha)	17.74	3.01	19.76	2.98	37.80	2.84	34.36	3.26
2010 (t/ha)	7.92	1.94	9.61	1.95	13.87	2.11	16.13	2.13
2011 (t/ha)	12.67	2.30	14.38	2.12	23.76	2.23	25.53	2.19
2012 (t/ha)	4.34	2.39	5.07	2.04	11.30	2.58	10.58	2.30
2015 (t/ha)	5.17	2.94	6.16	2.64	7.65	2.78	10.45	2.76
2020 (t/ha)	11.63	4.00	13.45	3.04	13.64	3.83	17.96	3.43

Year	SW5		SW6		SW7		SW8	
	RUSLE	**InVEST**	**RUSLE**	**InVEST**	**RUSLE**	**InVEST**	**RUSLE**	**InVEST**
2007 (t/ha)	45.26	5.75	30.38	6.48	42.21	4.99	50.25	4.29
2008 (t/ha)	15.88	6.18	12.30	6.61	17.83	6.08	24.32	5.53
2009 (t/ha)	36.10	3.85	19.99	3.91	27.22	3.31	25.94	2.15
2010 (t/ha)	12.79	2.94	11.48	3.41	12.20	2.39	14.26	1.86
2011 (t/ha)	25.60	2.94	19.98	3.31	21.05	2.48	26.23	2.02
2012 (t/ha)	10.48	3.18	9.00	3.68	10.37	3.03	21.20	2.90
2015 (t/ha)	7.61	3.37	7.91	3.83	7.78	3.08	8.07	2.39
2020 (t/ha)	11.60	4.59	11.98	5.32	13.94	4.25	12.93	3.66

Year	SW9		SW10		SW11		SW12	
	RUSLE	**InVEST**	**RUSLE**	**InVEST**	**RUSLE**	**InVEST**	**RUSLE**	**InVEST**
2007 (t/ha)	41.68	4.21	41.42	3.91	17.41	3.46	29.10	4.41
2008 (t/ha)	21.77	5.33	24.10	5.39	10.69	4.23	18.01	5.47
2009 (t/ha)	26.84	2.50	26.50	2.43	12.46	2.10	28.20	2.94
2010 (t/ha)	15.90	2.14	15.52	2.05	7.60	1.81	13.28	2.63
2011 (t/ha)	29.06	2.28	27.48	2.15	13.16	1.88	20.86	2.46
2012 (t/ha)	17.61	2.88	22.15	2.98	8.98	2.39	16.56	3.44
2015 (t/ha)	11.28	2.86	13.68	2.71	6.42	2.22	11.85	3.02
2020 (t/ha)	12.57	4.29	14.16	4.13	9.44	3.56	6.40	4.92

Nonetheless, the modeling results obtained from InVEST-SDR model highlighted the process of soil loss dynamics (soil erosion, sediment export, and SDR), to distinguish sediment source and sediment delivery rates for the Lower KRB. The model focused only on overland erosion; it does not model gully, bank, or mass erosion. Outputs from the model included the sediment load delivered to the stream at an annual time scale, as well as the amount of sediment eroded in the catchment and retained by vegetation and topographic features. Note that SDR only

created biophysical results. For the valuation of the sediment retention service, appropriate valuation approaches will be highly dependent on the particular application, context, and beneficiaries, and need to be implemented independently of InVEST.

InVEST-SDR model can be the preferred choice for identifying critical soil erosion-prone areas and consequent CAT planning only if data is available at the desired catchment outlet. This is a distributed model which after calibration, is capable of estimating potential soil loss from each pixel and computing the delivery of sediment from each pixel to the stream. Considering the above-highlighted limitation of data availability, RUSLE model output is used to identify critical soil erosion-prone areas.

4.3 Sediment Yield Estimation using MUSLE

4.3.1 Data Processing for MUSLE

In this study, the application of the Modified Universal Soil Loss Equation (MUSLE) for the period 2001 to 2012 necessitates the careful pre-processing of sediment concentration data, specifically the removal of outliers. The MUSLE model, a widely recognized tool for predicting sediment yield, relies on accurate and representative input data to yield reliable estimates. Outliers in sediment data can arise from a variety of sources, such as extreme weather events, data recording errors, or unusual watershed conditions, and can significantly skew the model's predictions. These outliers should be removed to ensure that the MUSLE model's inputs reflect typical soil loss conditions rather than atypical events or errors. This improves the model's robustness and validity, allowing for more accurate and reliable predictions of soil erosion. It is crucial, however, to approach outlier removal with caution, ensuring that significant environmental phenomena that could legitimately influence soil erosion are not inadvertently excluded. The goal is to strike a balance between removing data points that represent anomalies and retaining those that could indicate meaningful variations in soil loss conditions. The box and whisker plot provide a comprehensive visual representation of sediment concentration at the Jhanjharpur Gauging Site from 2001 to 2012 (Figure 4.10). This graph shows year-wise sediment concentration fluctuation and distribution, including median values, quartiles, and potential outliers. Table 4.8 quantifies the basic statistical metrics, including mean, standard deviation, and range (minimum to maximum) for each year. Notably, years like 2007 and 2008 show exceptionally high mean sediment concentrations, potentially indicative of anomalous hydrological events or data outliers.

The identification and removal of outliers is a critical step in data pre-processing, particularly for environmental data like sediment concentrations, which can be influenced by extreme weather events or measurement errors. Outliers can be detected using various statistical techniques, with one common method being the Interquartile Range (IQR) rule. This approach involves calculating the IQR (the difference between the 75th and 25th percentiles) and identifying data points that fall below the 25th percentile minus 1.5 times the IQR or above the 75th percentile plus 1.5 times the IQR as outliers. Removing these outliers can help in obtaining a more accurate and representative statistical analysis. However, it is essential to carefully consider the context and potential reasons for these outliers before removal, as they may represent significant environmental phenomena or data collection issues. Figure 4.11 shows the number of outliers in each year from 2001 to 2012.

Table 4.8 Statistical metrics for the observed sediment data at Jhanjharpur gauging station

Year	Mean	Stdv.	Min. Value	25%	50%	75%	Max. Value
2001	5177.387	17217.44	44.064	226.9002	867.5493	4465.498	149976.5
2002	4596.196	7083.55	24.51013	251.1959	2080.598	5621.797	53054.35
2003	6413.036	22144.29	38.14636	124.4104	711.7503	3532.717	225697
2004	6557.012	27529.9	13.2503	96.42326	383.8666	4891.705	365870.8
2005	2885.017	6221.785	2.892672	6.197472	208.5696	2971.469	49054.12
2006	2898.841	8156.74	20.93472	162.2246	504.6624	1352.557	81373.25
2007	21049.18	51227.53	18.144	196.2576	1279.757	14788.4	480003.8
2008	20200.06	36467.67	5.30064	28.66277	689.2249	20800.84	312069.9
2009	8537.635	22512.67	0.850522	11.67782	283.2399	5362.157	157414.2
2010	5800.892	17684.4	1.750378	9.452851	166.9041	5624.571	194842.6
2011	11584.49	29015	3.073594	15.79046	283.5233	10772.78	327514.6
2012	3683.121	5775.754	1.312576	21.44016	801.0006	5129.957	36320.61

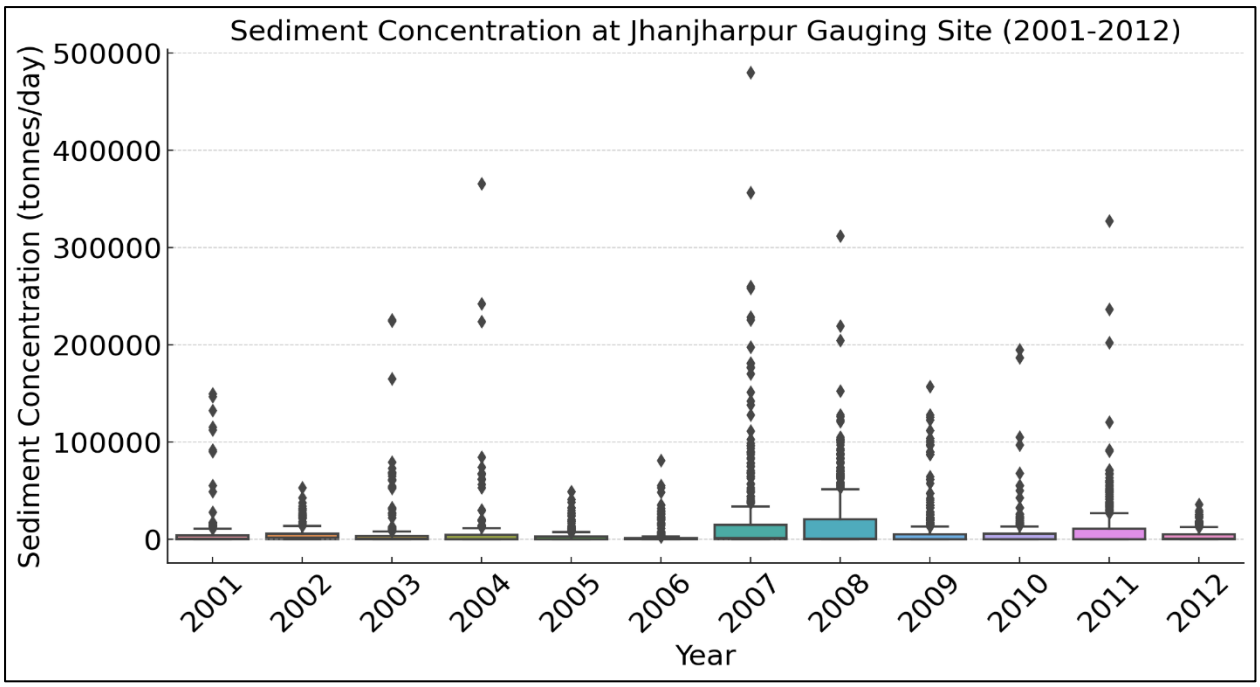

Figure 4.10 Box and whisker plot for the sediment data at Jhanjharpur gauging station

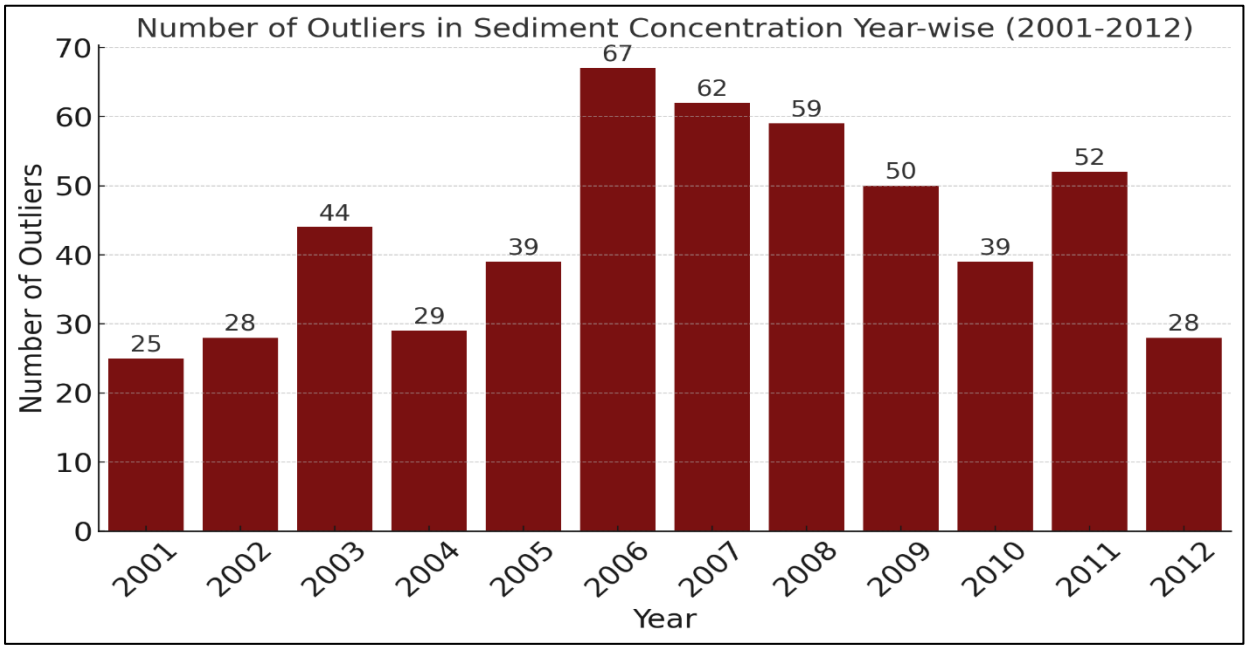

Figure 4.11 Outlier count among the daily sediment concentration observed values

4.3.2 Model Calibration and Verification

As previously mentioned, 72 events were used for the optimization of model parameters, whereas 32 events were used for model verification. Figure 4.12 shows the scatter plot between the observed and simulated sediment yield values during calibration. The 1:1 line represents

the perfect agreement benchmark for the calibration model. The observed values approximately match the simulated values. The key performance indicators NSE, coefficient of determination (R^2), Root Mean Square Error (RMSE), PBIAS were 0.74, 0.74, 8305.63 tonnes/year, and 2.18%, respectively for the calibration. The calibrated results show a slight under-estimation of sediment yield. The optimization algorithm (DDS) calibrated parameters 'a' and 'b' shows values of 10.7 and 0.429.

Model verification was performed using the calibrated parameters. Figure 4.13 shows the scatter plot between the simulated and observed sediment yield data during the verification events. During model verification, the NSE, R^2, RMSE, and PBIAS values were 0.69, 0.69, 10579, and 0.24% respectively. The verification results show a slight overestimation of sediment yield as compared to the observed sediment yield. Table 4.9 indicates the summary of the calibration and verification statistics of the model.

Table 4.9 Summary of calibration and verification of the model at Jhanjharpur gauging site

Model Calibration				Model Verification			
NSE	**R^2**	**RMSE**	**PBIAS (%)**	**NSE**	**R^2**	**RMSE**	**PBIAS (%)**
0.74	0.74	8305.63	2.18	0.69	0.69	10579	0.24

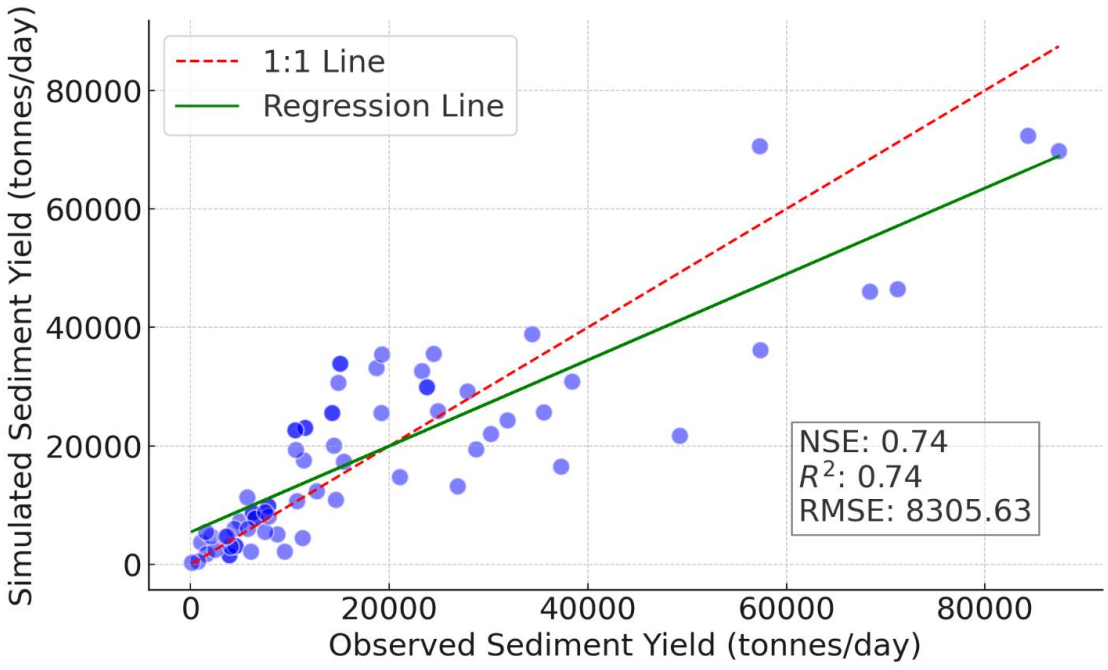

Figure 4.12 Observed versus simulated sediment yield for the model calibration

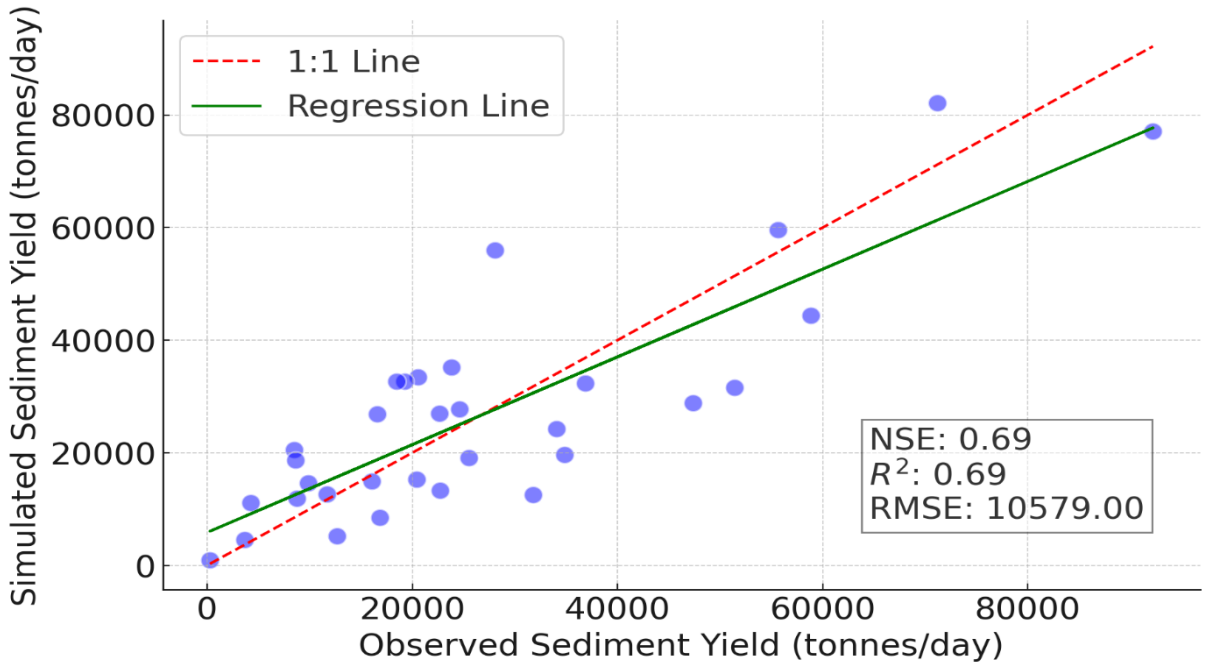

Figure 4.13 Observed versus simulated sediment yield for the model verification

4.3.3 MUSLE model for the Catchment (Janjharpur Outlet)

After the successful completion of model calibration and verification, we have determined the coefficient values 'a' and 'b' for the catchment area. The resulting model for the catchment is expressed as follows:

$$Y = \frac{10.7(Q \times q_p)^{0.429} \times K \times LS \times C_m \times P_s}{100A} \quad (4.1)$$

where Y is the sediment yield (t ha^{-1}), Q is the volume of runoff (m^3), q_p is the peak discharge (m^3 s^{-1}), A is the drainage area (km^2), K is the soil erodibility factor (t h MJ^{-1} mm^{-1}), LS is the topographic factor (dimensionless), C_m is the cover management factor (dimensionless), and P_s is the support practice factor (dimensionless).

The developed model is designed for the estimation of sediment yield at the Jhanjharpur gauging station. It allows for the calculation of sediment yield using inputs of rainfall volume and peak runoff at the outlet for each event. This model provides a valuable tool for understanding and predicting sediment transport in the catchment area, contributing to more informed watershed management and planning.

4.3.4 Inferences-MUSLE

The development of a Modified Universal Soil Loss Equation (MUSLE)-based model for the catchment area has proven to be highly effective in watershed management. This model excels as a predictive tool, accurately estimating sediment yield from specific storm events. Such precise predictions are vital for implementing efficient soil and water conservation strategies, identifying high erosion zones, and mitigating soil loss while preserving soil fertility. The model's adaptability to local conditions enhances its accuracy and versatility across diverse geographic and climatic scenarios.

In this study, our primary focus was on the region-specific variable coefficients of the MUSLE model for the Kamla River basin, utilizing data from the Jhanjharpur gauging station. The comparative analysis of the study demonstrates a strong correlation between the observed and the modeled sediment yield data. Consequently, the MUSLE model, with its optimized, calibrated, and validated parameters (a and b), offers an accurate estimation of sediment yield at the Jhanjharpur outlet. Moreover, this model can be extensively applied to estimate and predict sediment yield for various rainfall events under similar hydrological conditions.

4.4 SYI Model

4.4.1 Composite Erosion Intensity Mapping

The composite erosion intensity mapping unit (CEIU) was assigned relative erosivity values adjudged as indicative of the combined effect of the dynamic interrelationship of the factors in terms of the active erosivity of the units. Table 4.10 shows the weights assigned to different land use classes, slope categories, and soil classes.

Table 4.10 Key factors used for evaluation of composite erosion intensity mapping

S. No.	Land use/ Weightage	Soil Types/ Weightage	Slope/ Weightage
1	Cultivation / 4	Sandy loam / 3	0-3 /1
2	Bare / Sparse Vegetation / 5	Loam / 2	3-5 / 2
3	Grassland / 3	Clay / 1	5-8 / 3
4	Plantation, Settlement /2		8-11 / 4
5	Shrubland, Herbaceous wetland / 1		>11 / 5
6	Waterbodies / 0		

After assigning these weights, all the maps were superimposed to obtain a composite erosion intensity mapping unit. The erosion intensity mapping unit was divided into five distinct classes, as listed in Table 4.11.

Table 4.11 Output key for erosion intensity mapping

S. No.	Sum of Weightages	Erosion Intensity class
1	12-13	Very Severe
2	9-11	Severe
3	6-8	Moderate
4	4-5	Slight
5	0-3	Negligible

The weightages assigned to each class of soil, slope, and land use land cover maps were added to obtain a Composite Erosion Intensity Unit (CEIU) map. Table 4.12 shows the areas under the different categories of soil erosion. Figure 4.14 depicts the spatial variation of the erosion intensity classes.

Table 4.12 Erosion intensity classification for the study area

Erosion Class	Area (Km^2)	Area (%)
Negligible	5.92	0.13
Slight	360.15	7.99
Moderate	3169.81	70.28
Severe	968.23	21.47
Very Severe	6.01	0.13
Total	**4510.12**	**100**

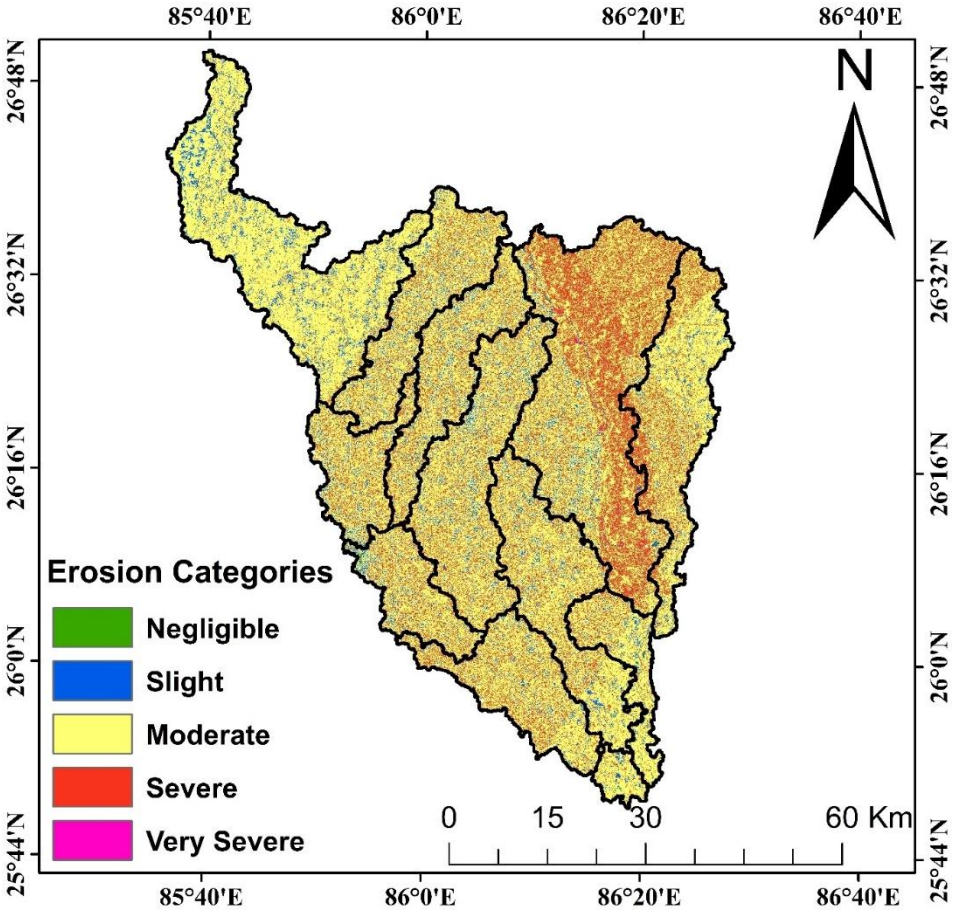

Figure 4.14 Composite Erosion Intensity Mapping Unit (CEIU) of lower KRB

4.4.2 Computation of Sediment Yield Index (SYI)

The SYI provides the comparative erodibility criteria of watersheds in terms of Very High, High, and Medium. Low and Very Low but does not provide an absolute silt yield. The sediment yield index was calculated using the methodology developed by the All India Soil and Land Use Survey (AISLUS). Each erosion intensity unit is assigned a weight. When considered collectively, the weighting value approximately represents the relative comparative erosion intensity. A basic value of K=10 was used to determine the weights. A value of 10 indicates a static condition of equilibrium between erosion and deposition. The range of weightage values assigned for CEIU in this study ranged from 12 to 20, depending on the variables within the CULL. The catchment area of the lower KRB was divided into 12 sub-watersheds for prioritization.

The sub-watersheds were prioritized based on SYI values. The catchment was divided into six priority zones based on SYI values, as shown in Table 4.13. Table 4.14 illustrates the priority ranking of lower KRB sub-watersheds based on calculated SYI values.

Table 4.13 Prioritized SYI value of erosion intensity rates

S. No.	SYI Value	Priority rating
1	>1300	Very High
2	1200-1299	High
3	1100-1199	Medium
4	1000-1099	Low
5	<1000	Very low

Table 4.14 Priority rating of sub-watersheds of lower KRB as per calculated SYI

Sub-Watershed	Erosion Intensity	Area(ha)	Weightage	Delivery Ratio	SYI	Priority
SW-1	Negligible	146.4096	10	0.85	1.85	Very Low
	Slight	7851.3195	12	0.85	118.91	Low
	Moderate	55988.5353	14	0.85	989.29	Medium
	Severe	4465.5708	16	0.85	90.18	High
	Very Severe	1.1648	18	0.85	0.03	Very High
	Total	68453.00			1200.25	**High**
SW-2	Negligible	19.52	10	0.7	0.41	Very Low
	Slight	3270.60	12	0.7	81.99	Low
	Moderate	23903.56	14	0.7	699.07	Medium
	Severe	6415.10	16	0.7	214.41	High
	Very Severe	1.21	18	0.7	0.05	Very High
	Total	33610			995.92	**Very Low**
SW-3	Negligible	39.96	10	0.5	0.95	Very Low
	Slight	2108.46	12	0.5	59.92	Low
	Moderate	14764.38	14	0.5	489.54	Medium
	Severe	4414.56	16	0.5	167.28	High
	Very Severe	4.65	18	0.5	0.20	Very High

	Total	21332.00			717.89	**Very Low**
SW-4	Negligible	24.63	10	0.5	0.40	Very Low
	Slight	3032.02	12	0.5	58.37	Low
	Moderate	21675.36	14	0.5	486.83	Medium
	Severe	6442.43	16	0.5	165.37	High
	Very Severe	3.55	18	0.5	0.10	Very High
	Total	31178.00			711.06	**Very Low**
SW-5	Negligible	103.92	10	0.9	1.03	Very Low
	Slight	3743.72	12	0.9	44.47	Low
	Moderate	54004.42	14	0.9	748.49	Medium
	Severe	33327.05	16	0.9	527.89	High
	Very Severe	509.88	18	0.9	9.09	Very High
	Total	91689.00			1330.97	**Very High**
SW-6	Negligible	31.55	10	0.7	0.51	Very Low
	Slight	2364.94	12	0.7	45.53	Low
	Moderate	31157.13	14	0.7	699.80	Medium
	Severe	10482.93	16	0.7	269.09	High
	Very Severe	566.22	18	0.7	16.35	Very High
	Total	44602.77			1031.27	**Low**
SW-7	Negligible	26.40	10	0.8	0.44	Very Low
	Slight	4662.32	12	0.8	92.54	Low
	Moderate	34039.76	14	0.8	788.20	Medium
	Severe	9588.21	16	0.8	253.74	High
	Very Severe	7.30	18	0.8	0.22	Very High
	Total	48324.00			1135.13	**Medium**
SW-8	Negligible	42.69	10	0.87	1.90	Very Low

	Slight	1761.70	12	0.87	94.20	Low
	Moderate	13469.57	14	0.87	840.27	Medium
	Severe	4290.22	16	0.87	305.87	High
	Very Severe	2.83	18	0.87	0.23	Very High
	Total	19567.00			1242.46	**High**
SW-9	Negligible	47.57	10	0.7	0.80	Very Low
	Slight	3434.74	12	0.7	69.56	Low
	Moderate	30190.51	14	0.7	713.34	Medium
	Severe	7778.72	16	0.7	210.05	High
	Very Severe	4.46	18	0.7	0.14	Very High
	Total	41456.00			993.90	**Very Low**
SW-10	Negligible	10.43	10	0.85	0.30	Very Low
	Slight	2046.26	12	0.85	70.32	Low
	Moderate	21163.43	14	0.85	848.51	Medium
	Severe	6546.94	16	0.85	299.99	High
	Very Severe	2.95	18	0.85	0.15	Very High
	Total	29770.00			1219.27	**High**
SW-11	Negligible	79.88	10	0.85	4.12	Very Low
	Slight	1375.42	12	0.85	85.12	Low
	Moderate	12637.38	14	0.85	912.47	Medium
	Severe	2536.41	16	0.85	209.30	High
	Very Severe	2.90	18	0.85	0.27	Very High
	Total	16632.00			1211.28	**High**
SW-12	Negligible	19.51	10	0.9	3.61	Very Low
	Slight	363.44	12	0.9	80.72	Low
	Moderate	3987.03	14	0.9	1033.16	Medium

Severe	534.87	16	0.9	158.40	High
Very Severe	0.16	18	0.9	0.05	Very High
Total	4905.00			1275.94	**High**

4.4.3 Prioritization of sub-watersheds in lower KRB based on SYI

The priority category of sub-watersheds of lower KRB, as per the calculated Silt Yield Index (SYI), is presented in Table 4.15. The table contains five priority categories: Very High, High, Medium, Low, and Very Low. These categories were determined by the SYI values, which measure the sediment yield from the sub-watersheds. Sub-watersheds with SYI values of more than 1300 were classified as a very high-priority category. This indicates that these sub-watersheds have a very high potential for soil erosion and sediment generation. This category includes the sub-watershed SW5, which covers 20.33% of the total area. The high-priority category included sub-watersheds with SYI values ranging from 1200 to 1299. These sub-watersheds have high sediment yield potential, although they are slightly lower than those in the very high category. The sub-watersheds listed under this category are SW1, SW8, SW10, SW11, and SW12, covering 30.89% of the total area. Sub-watersheds with SYI values ranging from 1100 to 1199 are included in the medium category. These sub-watersheds have a moderate sediment yield potential. The specific sub-watershed falling under this category is SW7, covering 10.71% of the total area. Sub-watersheds with SYI values ranging from 1000 to 1099 are listed in the low-priority category. These sub-watersheds have a relatively lower sediment yield potential compared to the previous categories. The sub-watershed included in this category is SW6, covering 9.78% of the total area. Lastly, the very low priority category includes sub-watersheds with SYI values below 1000. These sub-watersheds have the lowest sediment yield potential. This category includes the sub-watersheds SW2, SW3, SW4, and SW9, which cover 28.29 percent of the total area.

In this study, the prioritization of sub-watersheds was carried out into twelve sub-watersheds based on the SYI approach documented by the All-India Soil and Land Use Survey (AISLUS) (Figure 4.16). In the SYI method, the composite erosion intensity mapping unit (CEIU) was derived from the spatially varied soil texture, land use/land cover, and topography of the study area. Different sub-watersheds with different area classes (Ai) for each factor affect the erosion intensity differently. Thus, all factors must be properly weighted while computing the sediment yield index. The weightage value has been assigned to each theme depending on the importance of the features in the watershed. The weighted value represents the collective effect of different

sediment detachment factors regarding sediment yield. For each sub-watershed, the delivery ratio (Di) (Table 4.14) and weightage value (Wi) (Table 4.10) were assigned to calculate the Silt Yield Index (SYI). In the case of land use/land cover, bare/ sparse vegetation areas are given the highest rank in terms of soil erosion, followed by cropland, grasslands, plantation/settlement, and shrubland, whereas zero values were assigned for waterbodies. Sandy loam soil is ranked first owing to its high susceptibility to erosion, followed by loam and clay soil (Quansah, 1981). The topography of the area was divided into five slope classes, as suggested by the AISLUS. The highest weight was assigned to the sloppiest areas because of the soil particle instability (Fox and Bryan, 2000). The CEIU map generated from the dynamic inter-related factors was classified into five distinct classes: negligible, slight, moderate, severe, and very severe. The results showed that moderate and severe erosion accounted for 70.28% and 21.47% of the total area, respectively (Table 4.12). The SYI values for different sub-watersheds were obtained by multiplying CEIU by the delivery ratio and the corresponding area of the sub-watershed (Table 4.14). The delivery ratio values were assigned according to the distance from the stream (Table 4.13). Sub-watersheds were prioritized based on SYI values with five priority classes (very low, low, medium, high, and very high) (Wagh and Manaker, 2022). Table 4.13 gives detailed information about the input values and sediment yield index values of all the sub-watersheds of the study area. The calculated SYI values indicate that one sub-watershed (SW5) fall under a very high (SYI>1300) priority class, which accounts for 20.33% of the area of the lower KRB, five (SW1, SW8, SW10, SW11, and SW12) fall under the high (1200<SYI<1299) priority zone, one (SW7) in the medium (1100<SYI<1199) priority zone, one (SW6) fall under the low (1000<SYI<1099) priority zone, and four (SW2, SW3, SW4, and SW9) fall under the very low (SYI<1000) priority zone (Table 4.15). The advantage of determining the SYI of each watershed is that it enables us to understand the amount of sediment produced by each watershed. Therefore, prioritization enables efficient management of the watershed.

The priority category of the sub-watersheds of the Lower Kamla River Basin is presented in Figure 4.16. Prioritization of sub-watersheds depicts SW5 as the major source of water-induced soil loss in the lower KRB, followed by sub-watersheds SW1, SW8, SW10, SW11, and SW12 fall under high-priority zones. Furthermore, in these sub-watersheds, improper agricultural activity and the mono-cropping system make it more vulnerable to erosion under extreme climatic conditions. Hence, these sub-watersheds require immediate implementation of conservation practices.

Figure 4.17 shows photographs of the most priority sub-watersheds with latitude and longitude captured in the first and second field visits. Figures 4.17 (a) and (b) illustrate agricultural fallow lands in the study area. Most of the farmers follow the mono-cropping pattern in the study area. Similarly, Figure 4.17(c) illustrates the formation of small gullies and aggravated gully heads toward the agricultural lands due to poor agricultural practices, which result in aggravated soil loss and minimized crop yields. Figure 4.17(d) shows the up-protected riverbanks, which further contribute to increasing soil erosion in the adjacent areas.

Table 4.15 Sub-watersheds under different priority zones

Priority Category	SYI Values	Sub-watersheds	Area (%)
Very High	>1300	SW5	20.33
High	1200-1299	SW1, SW8, SW10 SW11, SW12	30.89
Medium	1100-1199	SW7	10.71
Low	1000-1099	SW6	9.78
Very Low	<1000	SW2, SW3, SW4, SW9	28.29

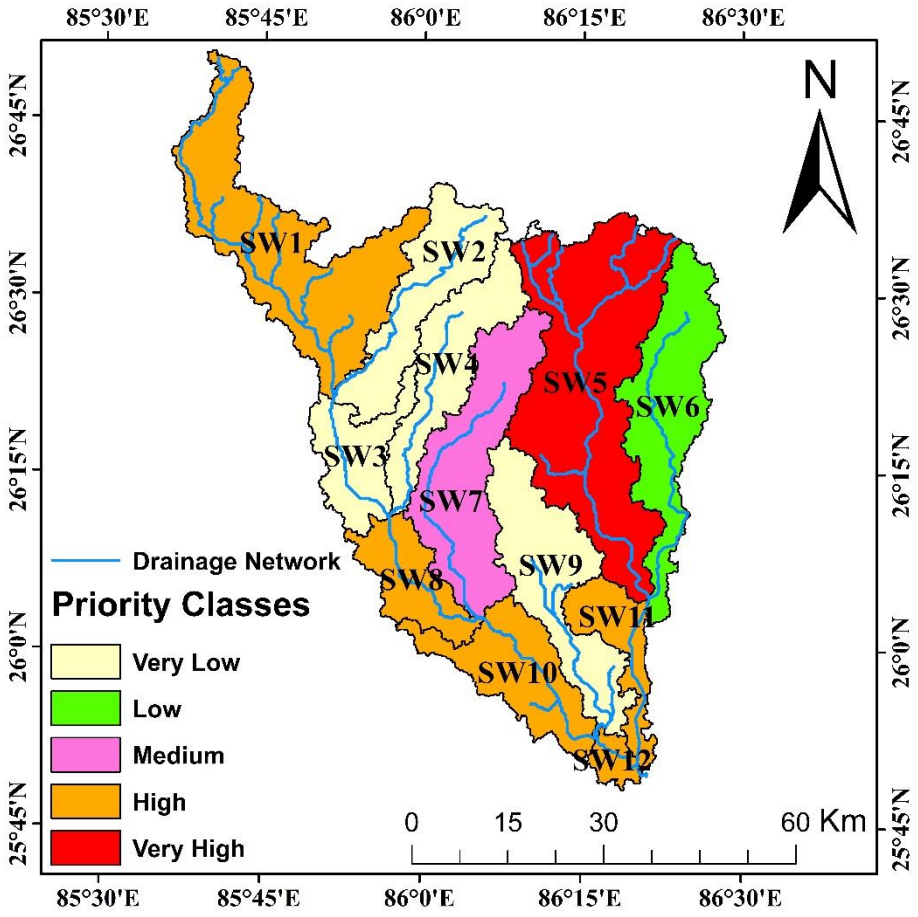

Figure 4.16 Treatment priority for the catchment of the Lower Kamla River basin

Figure 4.17 (a) and (b) Agricultural fallow lands (mono-cropping pattern), (c) Gully formation, and (d) Unprotected riverbank

Chapter 5: Catchment Area Treatment Plan

5.1 Catchment Area Treatment

Soil erosion poses a significant threat to the ecological balance and sustainability of landscapes, particularly in catchment areas where the intricate interplay of soil, water, and vegetation influences the overall health of the environment. To control the rate of soil erosion in the catchment, a sub-watershed-wise Catchment Area Treatment (CAT) plan has been prepared.

This comprehensive plan addresses the multifaceted challenges posed by soil erosion within the lower KRB in India. By strategically combining preventive measures, conservation practices, and restoration efforts, the immediate impact of erosion can be curtailed and can lead to long-term resilience and sustainability.

The management plan for the treatment of erosion-prone areas of the catchment includes both biological and engineering measures besides the incorporation of social dimensions associated directly or indirectly with the catchment. The proposed CAT plan will not only control sedimentation in the proposed barrage but also will provide a life support system to the local population through its involvement. This is a key factor to make the water resources project eco-friendly and sustainable. Thus, the CAT plan encompasses (a) understanding of the erosion characteristics of the terrain and (b) suggesting remedial measures to reduce erosion rate.

In the present study, the 'Silt Yield Index' (SYI) method, developed by All India Soil and Land Use Surveys (AISLUS) and widely used for water resources projects, has been applied. To this end, the terrain is subdivided into various sub-watersheds, and relative erodibility is determined. SYI method provides comparative erodibility values to assess the catchment vulnerability to erosion as Very High, High, Medium, Low, and Very Low. It, however, does not provide the value of absolute silt yield.

In general, it is common experience that environmental problems are created by science and technology and, therefore, can be controlled by science and technology only. For a sustainable action plan, the watershed development concept has been applied in this study. The approach is a holistic, multi-disciplinary, and practicable approximation of systems planning. The treatment measures are suggested for land use classes based on Erosion Severity Classes. As per the

treatment required under varied land use classes, suitable treatment models have been proposed, and these are discussed in this chapter.

5.2 BIOLOGICAL MEASURES

Besides the "mechanical" or "engineering" techniques, another way of treating soil conservation has been extensively used. This is usually referred to as "Vegetative" or "Biological" conservation. The underlying principle here is that the soil only becomes subject to erosion if it is bare and exposed to the erosive forces of wind and water. If the soil can be kept under a permanent or near-permanent cover of vegetation, little or no erosion will occur.

5.2.1 Restoration of Degraded Areas

In critically degraded areas, plantation of locally useful and indigenous plant species such as timber species, fodder species, fuel wood species, grasses, shrubs and legumes, and medicinal and aromatic plants shall be used. Nurseries shall be developed in the catchment to raise plantations.

5.2.2 Afforestation

This will include the raising of multi-tier mixed vegetation of suitable local species in steep and sensitive catchment areas of rivers/streams with the objective of keeping such area under permanent vegetative cover by way of plantation of suitable species.

5.2.3 Fodder Plantation

To overcome the problem of scarcity of fodder, it is proposed that a substantial area under fodder plantation be created with suitable fast-growing fodder species.

5.2.4 Plantation of Horticulture Crops

Under the treatment plan, suitable horticultural crop species like Chilli (Cedrus deodar), Anar (Punica granatum), and citrus shall be distributed to families residing in villages within the catchment with the objective of supplementing their income.

5.2.5 Pasture Development

As there are degraded patches of pastures in the area, this measure shall be adopted to encourage developing new and healthy pastures for cattle in the area. Under this treatment, suitable grasses,

fodder trees, and leguminous plant species should be planted in the land area earmarked for the purpose.

5.2.6 Non-Timber Forest Product (NTFP) Cultivation

To increase the areas of rich medicinal plants in natural habitats, participatory management shall be encouraged by enhancing adaptability. Moreover, cultivation of high-priority medicinal plant species can also be practiced. Priority shall be given to the organic cultivation of medicinal plants. Effective fencing would also be provided for the protection of saplings. Before any new area is taken up, eradication of weeds and unpalatable grass species is important. Therefore, it is recommended that some parts of the pasture should be closed for seeding purposes only.

5.2.7 Measures for Cropped Areas

A number of measures can be adopted for soil erosion conservation in agricultural areas. **Cover Cropping** can be adopted, wherein planting cover crops during the off-season will help maintain soil cover and structure, reducing erosion. Cover crops also have extensive root systems that anchor the soil and improve water-holding capacity. **Contour Farming** is another measure that involves plowing along the contour lines of the land to help slow down water runoff and reduce soil erosion. Planting crops in rows along the contour lines can further enhance this effect. **Agroforestry Systems** can be employed to integrate trees or shrubs within the agricultural landscape to provide additional soil stabilization. Agroforestry systems can enhance biodiversity and reduce erosion by combining crops with trees. **Conservation Tillage** can be opted to minimize soil disturbance through reduced tillage or no-till practices to maintain soil structure. This will help preserve organic matter and reduce erosion risk. **Mulching** is another effective measure that involves the application of organic or plastic mulch on the soil surface to protect against water and wind erosion. Mulching helps retain soil moisture and stabilize the soil structure.

5.2.8 Measures for Areas with Tree Cover

A number of measures can be adopted for soil erosion conservation in areas having tree cover. **Understory Planting** can be adopted, wherein understory vegetation is introduced beneath existing tree cover to enhance ground cover and reduce soil erosion. This can be done by selecting native plants that complement the existing tree species. **Soil Microbial Inoculation** can be

adopted, which involves beneficial soil microorganisms that enhance soil structure and stability. Mycorrhizal fungi, for example, can form symbiotic relationships with plant roots, improving nutrient uptake and soil aggregation. **Riparian Buffer Zones** can be created to establish vegetative buffer zones along water bodies within or adjacent to forested areas. These buffer zones will help filter sediment, nutrients, and pollutants before reaching the water. **Regeneration Practices** can be adopted to promote the natural regeneration of trees and vegetation in degraded areas within the forest. It involves controlling invasive species that may hinder the growth of native vegetation.

5.3 ENGINEERING MEASURES

Engineering measures are implemented over severe and very severe erosion intensity areas to control the sediment yield and further degradation of the free-draining catchment areas. The following engineering measures are suggested for the catchment area.

5.3.1 Field Bunding

Farm bunds are constructed on agricultural lands with the aim of arresting soil erosion and improving the soil moisture profile. Ideally, bunds on farms should be constructed on the contour line along the boundary of the field.

a) Contour Bunds

This is an engineering soil conservation measure used for retaining water by creating an obstruction to control erosion. Bunds are simply embankment-like structures constructed across the land slope.

b) Vegetative Contour Trenches

Contour staggered trenches are mainly provided to trap the silt and runoff. This is also done to prepare a fertile base for the plantation.

c) Gully Plugs (earthen, loose boulder, or check dam)

Gully plugs/check dams are proposed in first-order streams to check for initial erosion in the catchment. These are proposed at an interval of 100m in severe and very severe erosion intensity classes. Gully plugs/check dams are quite feasible where vegetative material for construction is abundantly available. Gully plugs/check dams can only be constructed in small gullies, not deeper than 1m depth. As the material required for the construction of these types of dams is available

locally, these can be constructed faster and in a very short span of time, thereby effectively reducing erosion in the early phase of the project.

5.4 TREATMENT OF INDIVIDUAL SUB-WATERSHEDS

The watershed prioritization and formulation of a proper watershed management program for sustainable development require information on watershed sediment yield. In general, implementation of management programmes in the sub-watersheds may not be taken up simultaneously due to financial or technical constraints. In such a situation, it is always better to start management measures from the most critical sub-watershed, which makes it mandatory to prioritize the sub-watersheds available. Thus, watershed prioritization is the ranking of different critical sub-watersheds according to the order in which they have to be taken up for treatment for soil and water conservation. A particular sub-watershed may get top priority for various reasons, but often, the intensity of land degradation is taken as the basis. In this study, the SYI method is used for the prioritization of sub-watersheds.

The area and type of treatment to be undertaken are based on the stream drainage pattern, extent of forest cover, accessibility of the area, land use, soil profile, and slope. The sub-watersheds under different priority categories are shown in Table 5.1. The sub-watershed-wise area (ha) and percentage under different Composite Erosion Intensity Units (CEIU) in the Lower Kamla River basin are presented in Table 5.2a and 5.2b, respectively. SW5 received very high priority, and SW1, SW8, SW10, SW11, and SW12 received high priority and were selected for detailed catchment treatment planning. The details of sub-watershed-wise treatment measures are described below.

Table 5.1 Priority category of sub watersheds using Sediment Yield Index (SYI) for different erosion intensities

S. No.	SW Number	Priority rating	Area (km^2)	Area (%)
1.	SW5	Very High [1 Nos.]	916.89	20.33
2.	SW1, SW8, SW10, SW11, SW12	High [5 Nos.]	1393.27	30.89
3.	SW7	Medium [1 Nos.]	483.24	10.71
4.	SW6	Low [1 Nos.]	440.96	9.78
5.	SW2, SW3, SW4, SW9	Very Low [4 Nos.]	1275.76	28.29
	Total Area (km^2)		**4510.12**	**100**

Table 5.2a Sub-watershed wise Area (ha) Composite Erosion Intensity Unit (CEIU) in the Lower Kamla River basin

Erosion Class	Negligible	Slight	Moderate	Severe	Very Severe	Total area
Sub-watershed	(0-3)	(4-5)	(6-8)	(9-11)	(11-14)	
SW1	146.4096	7851.32	55988.54	4465.571	1.1648	68453
SW2	19.5202	3270.604	23903.56	6415.104	1.2081	33610
SW3	39.9625	2108.456	14764.38	4414.558	4.6455	21332
SW4	24.6344	3032.023	21675.36	6442.431	3.5516	31178
SW5	103.9236	3743.719	54004.42	33327.05	509.8827	91689
SW6	31.5535	2364.941	31157.13	10482.93	59.4487	44096
SW7	26.4023	4662.323	34039.76	9588.207	7.3043	48324
SW8	42.6871	1761.696	13469.57	4290.216	2.8337	19567
SW9	47.5658	3434.741	30190.51	7778.717	4.4633	41456
SW10	10.4271	2046.258	21163.43	6546.938	2.9519	29770
SW11	79.8802	1375.425	12637.38	2536.414	2.9041	16632
SW12	19.5114	363.4371	3987.026	534.8708	0.1551	4905
Total Area (ha)	**592.4777**	**36014.94**	**316981.1**	**96823**	**600.5138**	**451012**

Table 5.2b Sub-watershed wise (%) Composite Erosion Intensity Unit (CEIU) in the Lower Kamla River basin

Erosion Class	Negligible	Slight	Moderate	Severe	Very Severe
Sub-watershed	(0-3)	(4-5)	(6-8)	(9-11)	(11-14)
SW1	0.21	11.47	81.79	6.52	0.00
SW2	0.06	9.73	71.12	19.09	0.00
SW3	0.19	9.88	69.21	20.69	0.02
SW4	0.08	9.72	69.52	20.66	0.01
SW5	0.11	4.08	58.90	36.35	0.56
SW6	0.07	5.36	70.66	23.77	0.13
SW7	0.05	9.65	70.44	19.84	0.02
SW8	0.22	9.00	68.84	21.93	0.01
SW9	0.11	8.29	72.83	18.76	0.01
SW10	0.04	6.87	71.09	21.99	0.01
SW11	0.48	8.27	75.98	15.25	0.02
SW12	0.40	7.41	81.28	10.90	0.00

5.4.1 Sub-Watershed-5

The total catchment area of Sub-watershed 5 is 91689 ha. The land use map of the SW-5 is presented in Figure 5.1 (a). In this sub-watershed, predominant land use / land cover is agriculture (60623.81 ha) followed by tree cover (21978.59 ha), built-up (4148.08 ha), grassland (3143.70 ha), water bodies (1066.65 ha) and Bare/sparse vegetation (606.94 ha). The area under different Composite Erosion Intensity Units (CEIU) in the Sub-watershed 5 is presented in Table 5.2a. In SW-5, 63.1 % of the area falls under moderate, slight, and negligible class. The area requiring treatment under severe and very severe erosion class in SW-5 is 33836.9 ha (36.9 %). Area is mostly concentrated in areas under agriculture and tree cover (Figure 5.1 (b)).

A.	**Biological Measures**	**Area (ha)**
1.	Cover Cropping	3000
2.	Agroforestry systems	3000
3.	Conservation tillage	3500
4.	Mulching	2500
5.	NTFP Cultivation	3000
6.	Understory planting	2500
7.	Soil Microbial Inoculation	2500
8.	Riparian Buffer Zones	3500
9.	Regeneration Practices	3500
	Subtotal	**29000**
B.	**Engineering Measures**	**Area (ha)**
1.	Field bunding	2000
2.	Contour bunding	1500
3.	Veg. Contour Trench	1336.9
	Subtotal	**4836.9**
	Grand Total (A+B)	**33836.9**

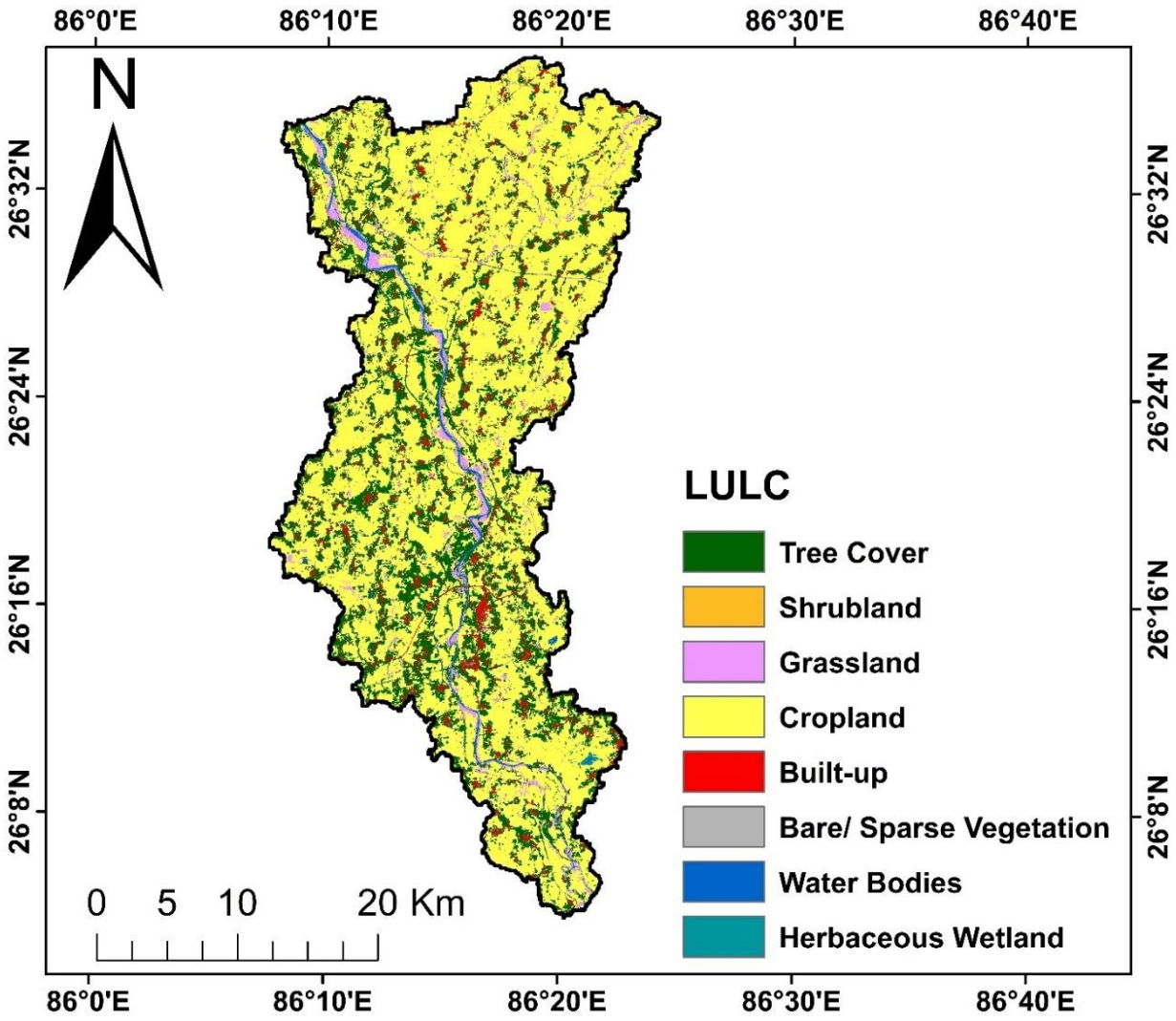

Figure 5.1 (a) Land Use/ Land Cover map of SW-5

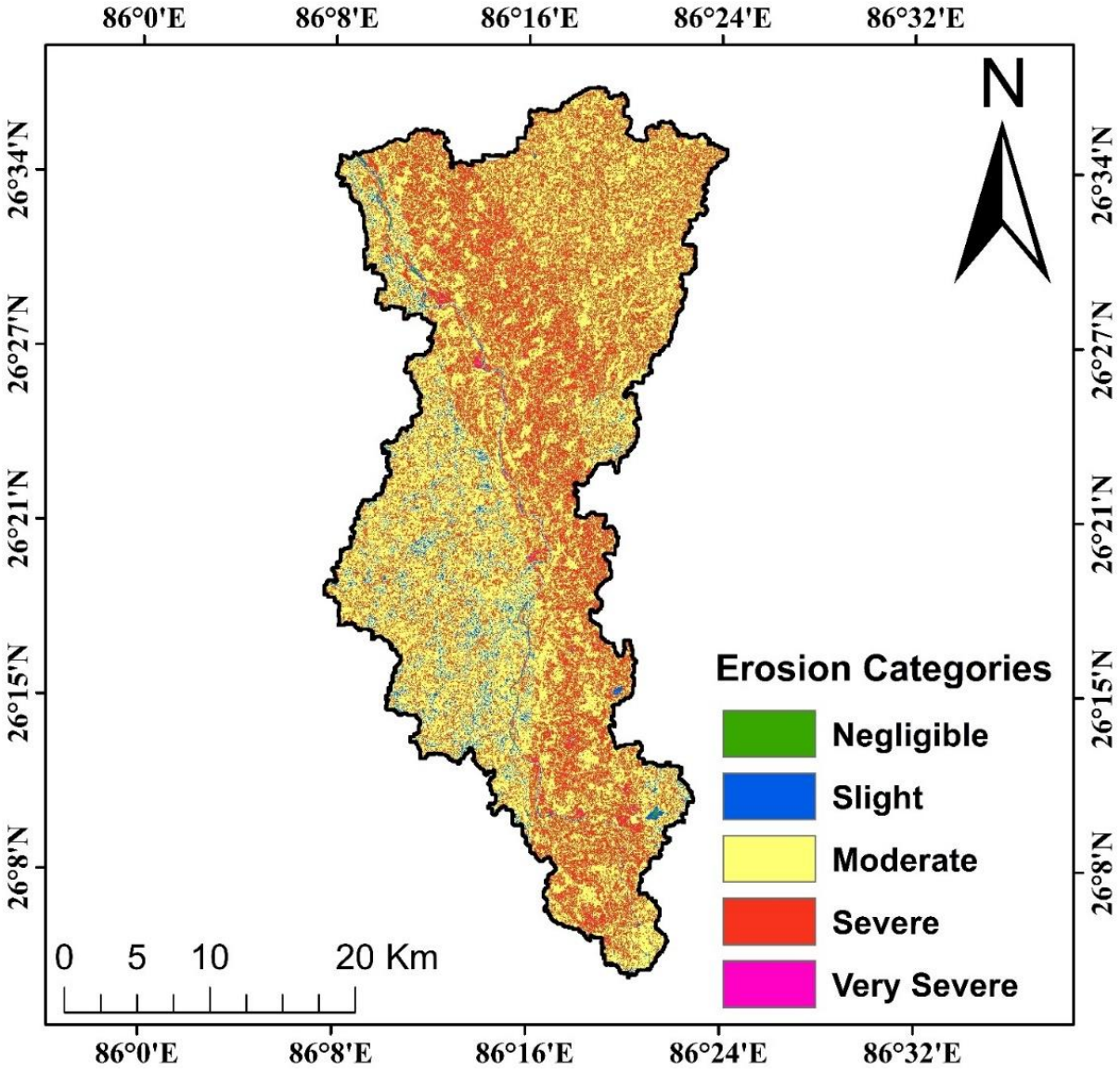

Figure 5.1 (b) Composite Erosion Intensity Unit (CEIU) map of SW-5

5.4.2 Sub-Watershed-1

The total catchment area of Sub-watershed 1 is 68453 ha. The land use map of the SW-2 is presented in Figure 5.2 (a). In this sub-watershed, predominant land use / land cover is agriculture (49634.20 ha) followed by tree cover (14613.97 ha), built-up (3013.39 ha), grassland (719.43 ha), settlement (315.42 ha), water bodies (315.01 ha), bare and sparse vegetation (143.26 ha), shrubland (4.05 ha) and herbaceous wetland (9.69 ha). The area under different Composite Erosion Intensity Unit (CEIU) in the Sub-watershed 1 is presented in Table 5.2. In SW-1, 93.47% of the area falls under moderate, slight, and negligible class. Erosion problem is not predominant in the SW-1. The area requiring treatment under severe and very severe erosion class in SW-1 is 4466.57 ha (6.52 %)**.** This area is mostly concentrated in areas under agriculture and tree cover (Figure 5.2 (b)).

A.	**Biological Measures**	**Area (ha)**
1.	Cover Cropping	500
2.	Conservation tillage	500
3.	Mulching	500
4.	NTFP Cultivation	500
5.	Soil Microbial Inoculation	500
6.	Regeneration Practices	400
7.	Afforestation	100
	Subtotal	**3000**
B.	**Engineering Measures**	**Area (ha)**
1.	Field bunding	500
2.	Contour bunding	500
3.	Veg. Contour Trench	466.57
	Subtotal	**1466.57**
	Grand Total (A+B)	**4466.57**

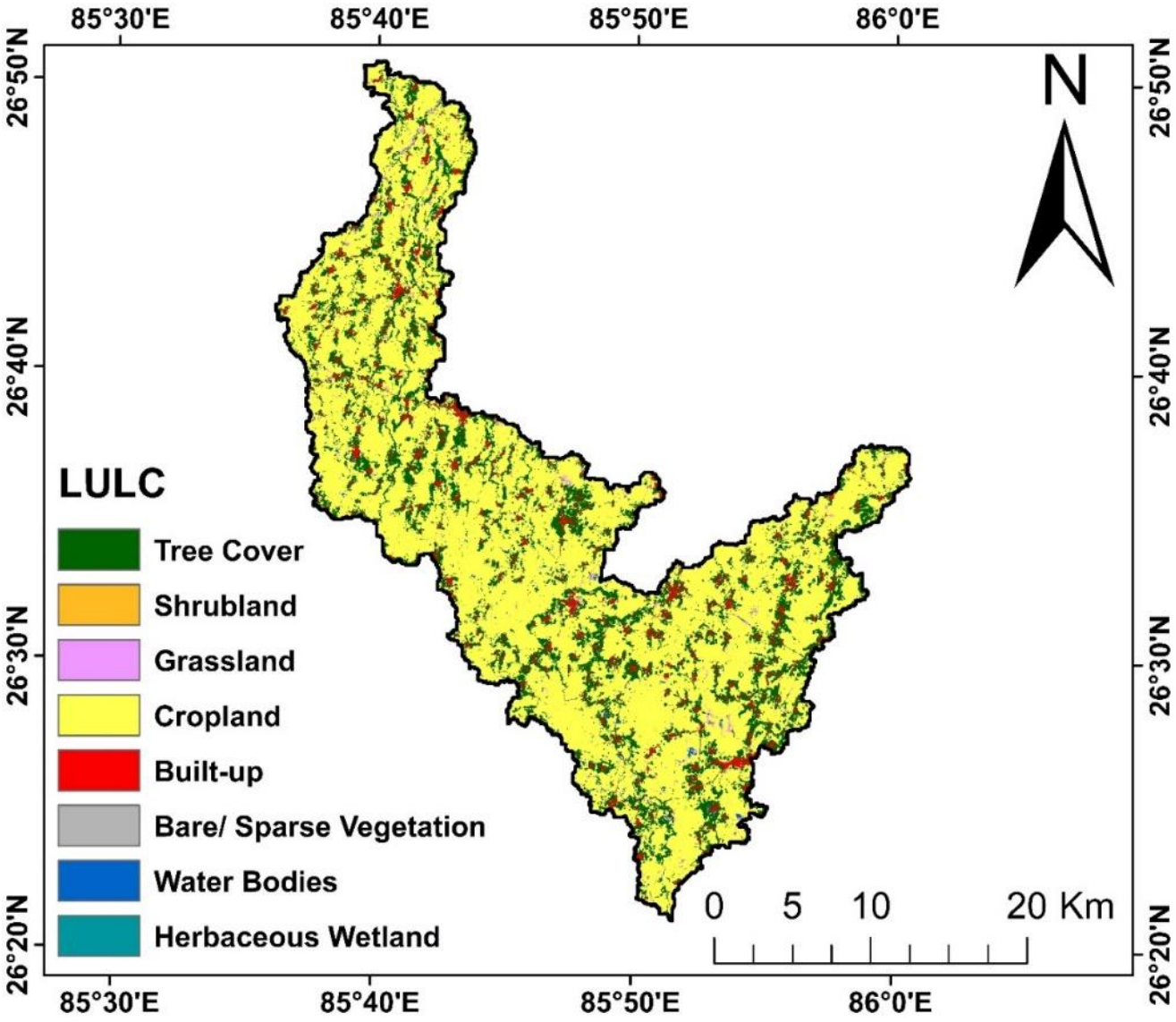

Figure 5.2 (a) Land Use/ Land Cover map of SW-1

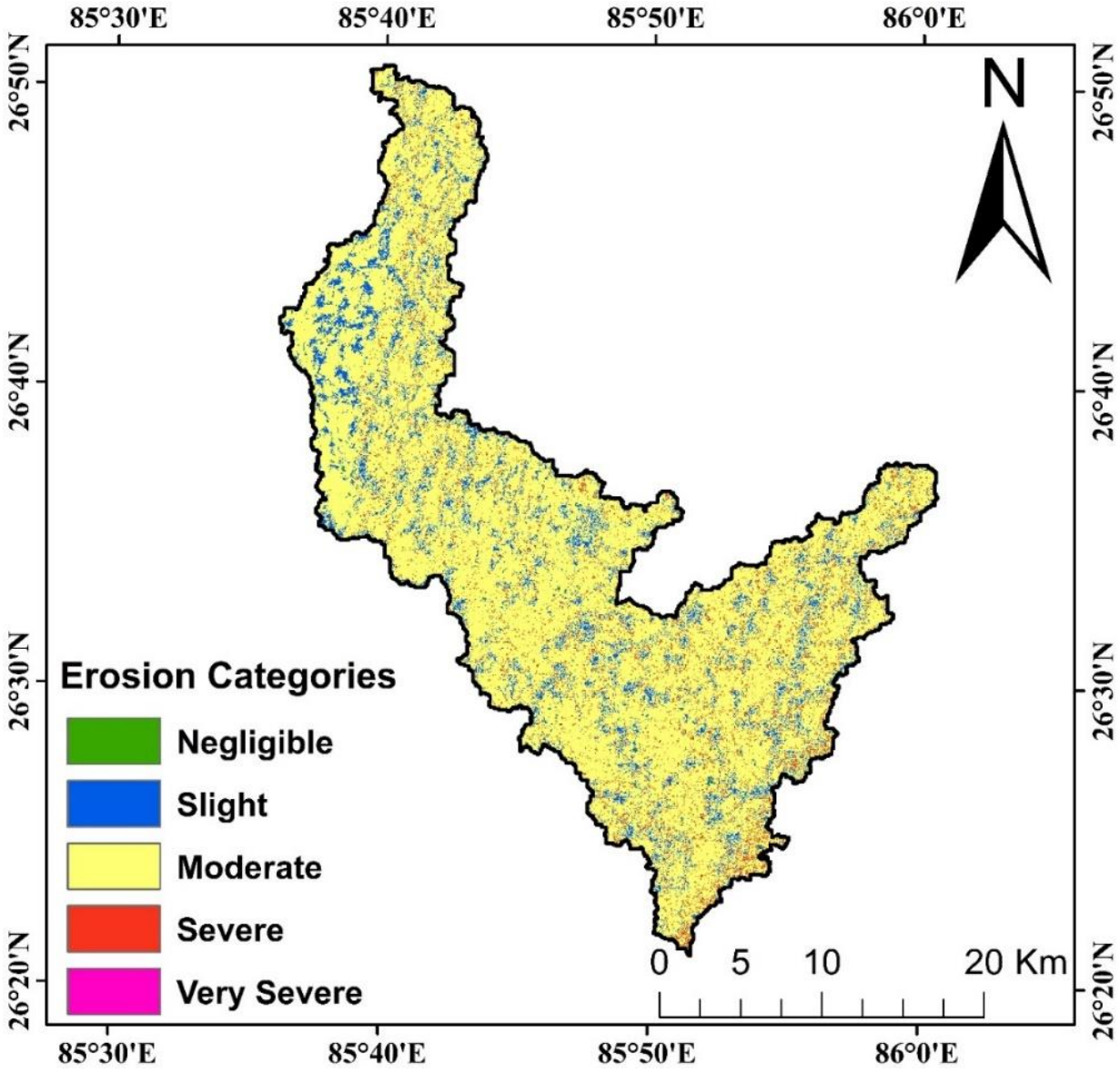

Figure 5.2 (b) Composite Erosion Intensity Unit (CEIU) map of SW-5

5.4.3 Sub-Watershed-8

The total catchment area of Sub-watershed 8 is 19567 ha. Land use map of the SW-8 is presented in Figure 5.3 (a). The predominant land use is agriculture (12671.36 ha) followed by tree cover (4686.31 ha), built-up (1768.10 ha), grassland (221.30 ha), water body (79.22 ha), herbaceous wetland (92.60 ha), and bare/sparse vegetation (57.68 ha). The area requiring treatment under the severe erosion class is about 4293.05 ha (21.94%). The erosion areas are mostly concentrated in areas under cropland and tree cover (Figure 5.3 (b)).

A.	**Biological Measures**	**Area (ha)**
1.	Cover Cropping	500
2.	Conservation tillage	500
3.	Mulching	500
4.	NTFP Cultivation	250
5.	Soil Microbial Inoculation	250
6.	Regeneration Practices	400
	Subtotal	**2400**
B.	**Engineering Measures**	**Area (ha)**
1.	Field bunding	600
2.	Contour bunding	500
3.	Veg. Contour Trench	793.05
	Subtotal	**1893.05**
	Grand Total (A+B)	**4293.05**

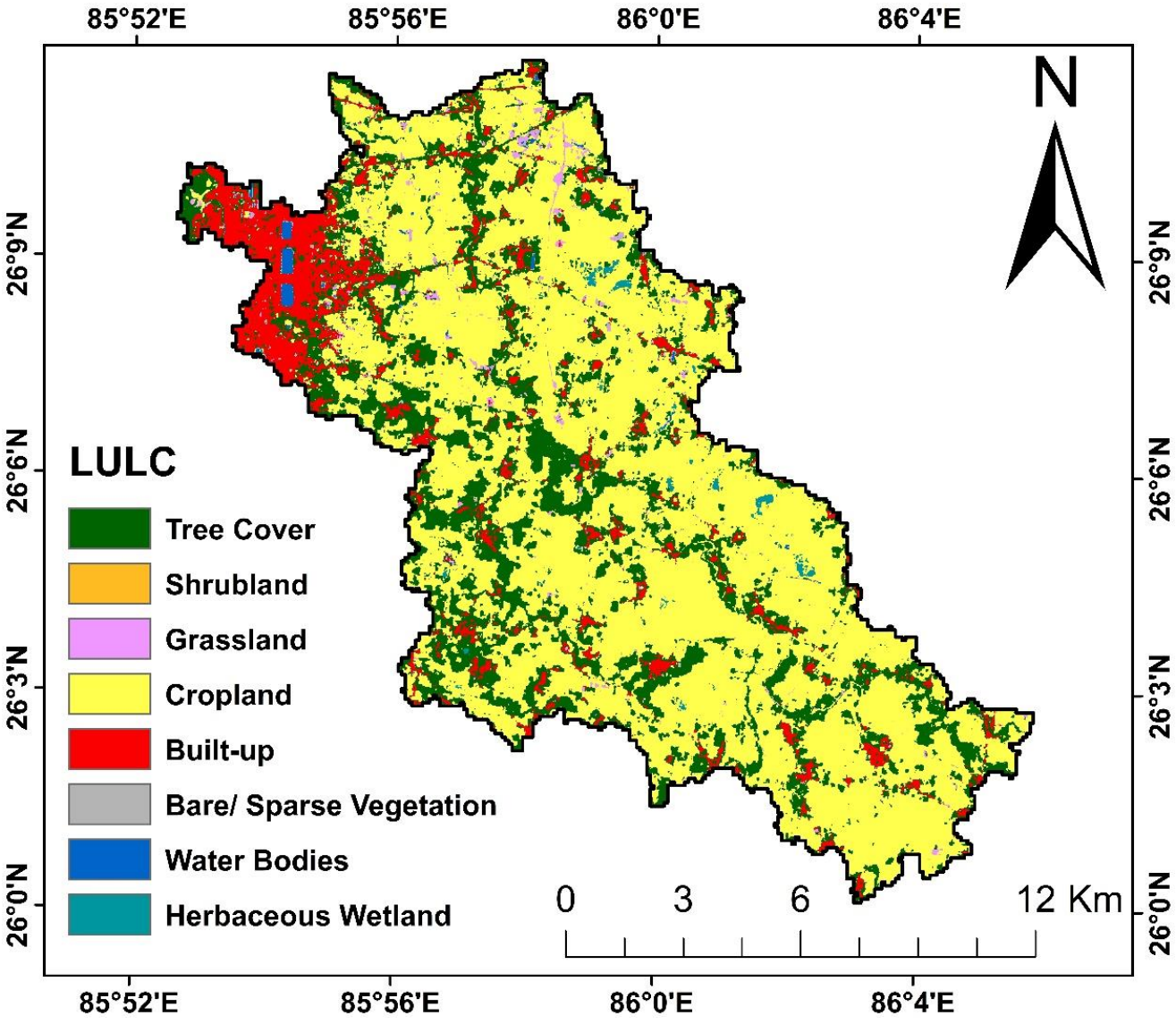

Figure 5.3 (a) Land Use/ Land Cover map of SW-8

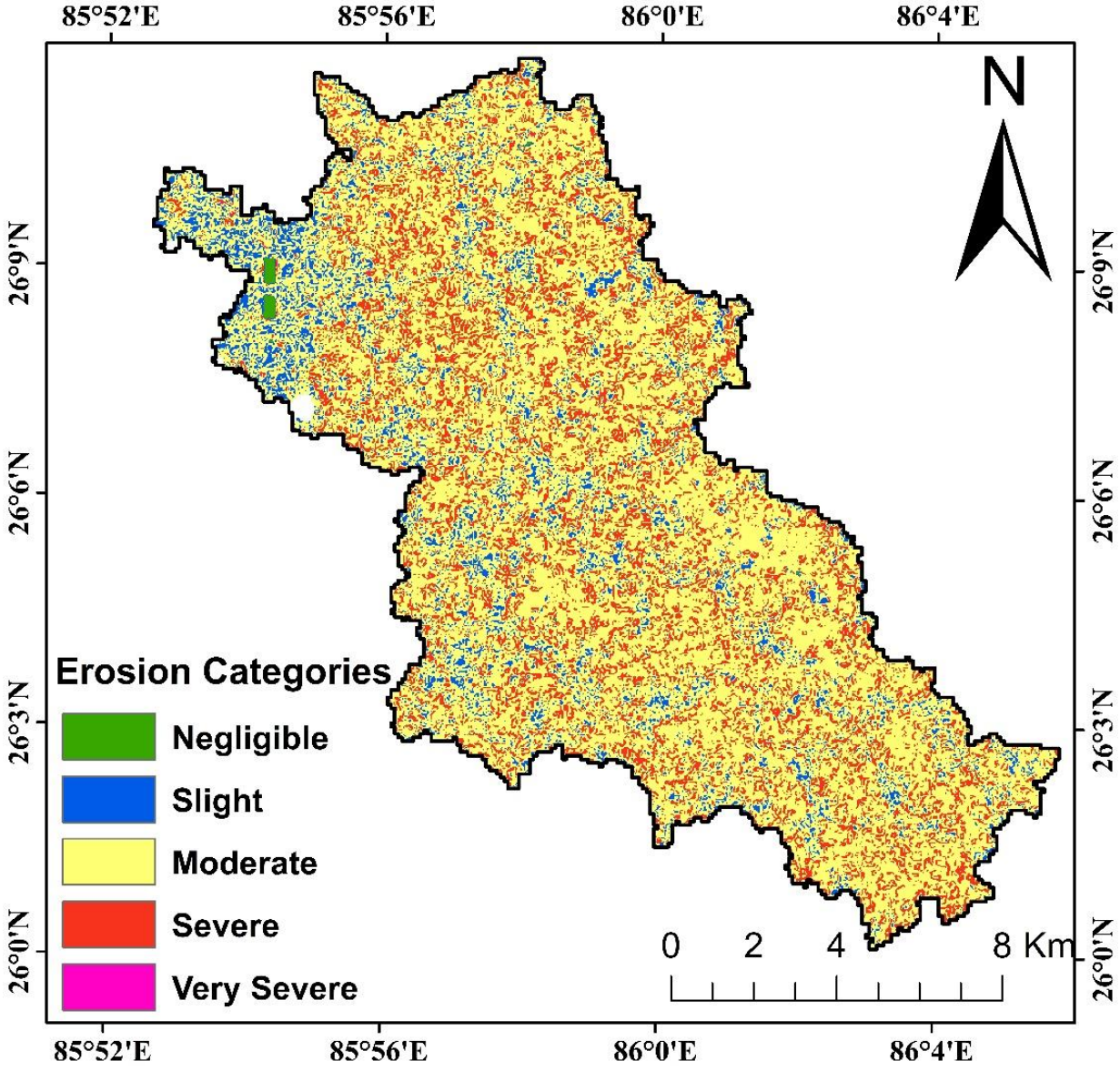

Figure 5.3 (b) Composite Erosion Intensity Unit (CEIU) map of SW-8

5.4.4 Sub-Watershed-10

This sub-watershed has a total catchment area of 29770 ha. The land use map of the sub-watershed is shown in Figure 5.4 (a). The predominant land use is agriculture (22327.56 ha) followed by tree cover (5622.43 ha), built-up (1465.46 ha), bare/sparse vegetation (64.24 ha), water body (29.83 ha) and herbaceous wetland (21.80 ha). The area requiring treatment under severe and very severe erosion class is about 6549.89 ha (22%) (Figure 5.4 (b)).

A. Biological Measures	**Area (ha)**
1. Cover Cropping	500
2. Agroforestry systems	500
3. Conservation tillage	500
4. Mulching	500
5. NTFP Cultivation	500
6. Understory planting	500
7. Soil Microbial Inoculation	500
8. Riparian Buffer Zones	500
9. Regeneration Practices	500
Subtotal	**5000**
B. Engineering Measures	**Area (ha)**
1. Field bunding	500
2. Contour bunding	500
3. Veg. Contour Trench	549.89
Subtotal	**1549.89**
Grand Total (A+B)	**6549.89**

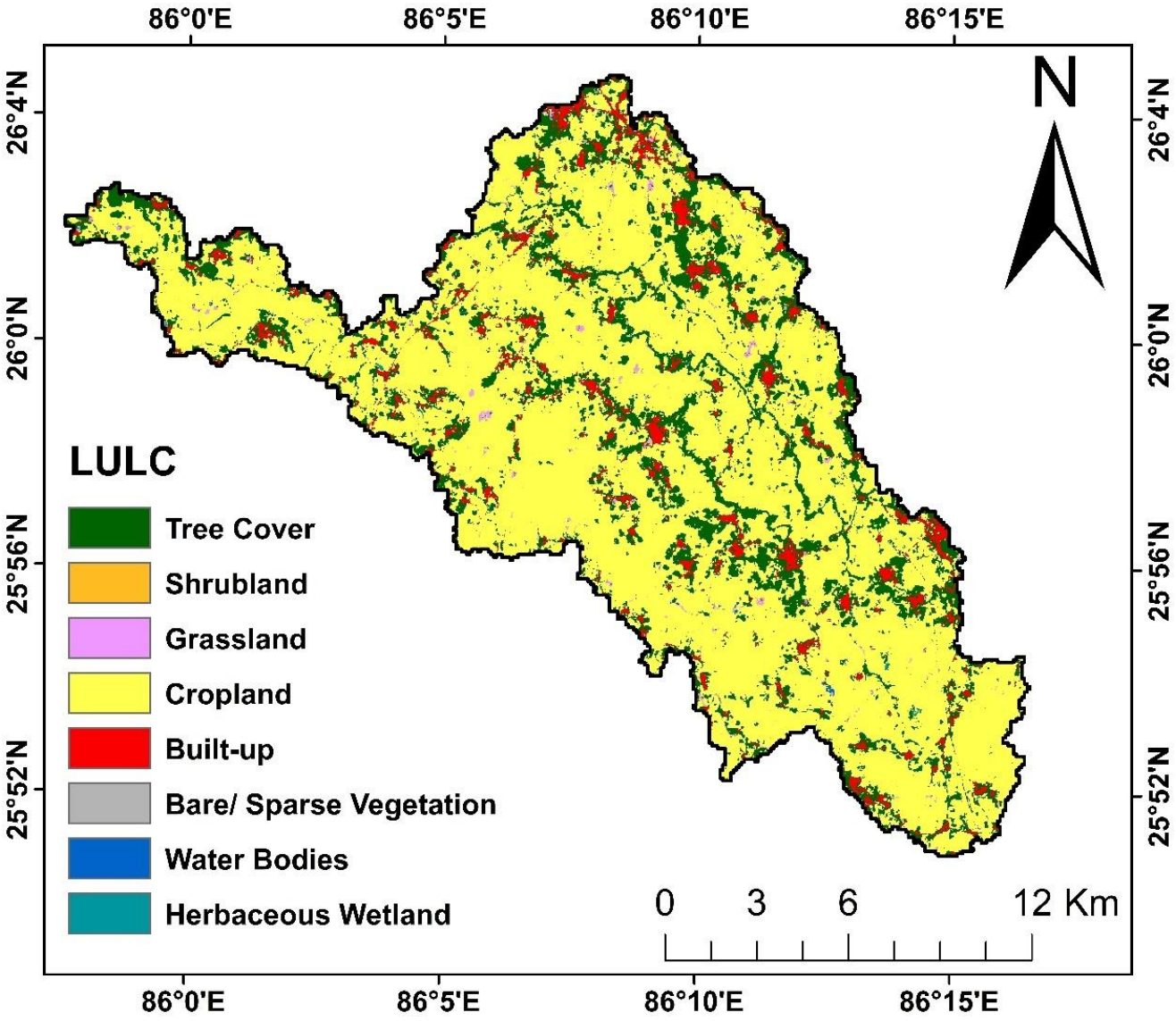

Figure 5.4 (a) Land Use/ Land Cover map of SW-10

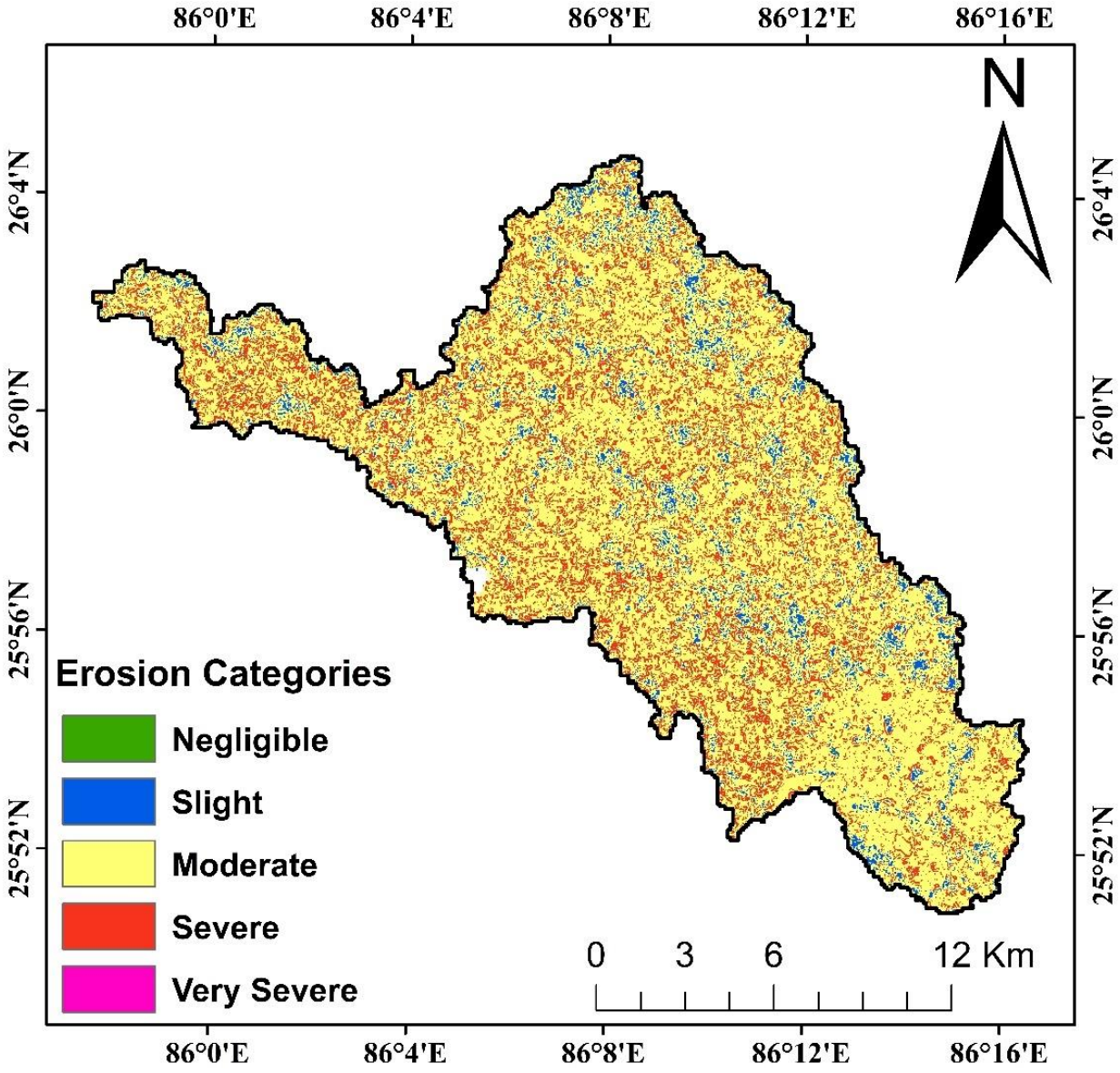

Figure 5.4 (b) Composite Erosion Intensity Unit (CEIU) map of SW-10

5.4.5 Sub-Watershed-11

SW-11 has a catchment area of 16632 ha. Land use map of SW-11 is presented in Figure 5.5 (a). The predominant land use is agriculture (12165.18 ha) followed by tree cover (2934.40 ha), built-up (709.05 ha), scrub (516.47 ha), grassland (457.03 ha), water body (191.35 ha) and bare/sparse vegetation (160.08 ha). The area requiring treatment under very severe and severe erosion class is about 2539.32 ha (15.27%). The erosion areas are mostly concentrated in areas under agriculture (Figure 5.5 (b)).

A.	**Biological Measures**	**Area (ha)**
1.	Cover Cropping	200
2.	Conservation tillage	200
3.	Mulching	200
4.	NTFP Cultivation	300
5.	Soil Microbial Inoculation	200
6.	Regeneration Practices	300
	Subtotal	1**400**
B.	**Engineering Measures**	**Area (ha)**
1.	Field bunding	500
2.	Contour bunding	500
3.	Veg. Contour Trench	139.32
	Subtotal	**1139.32**
	Grand Total (A+B)	**2539.32**

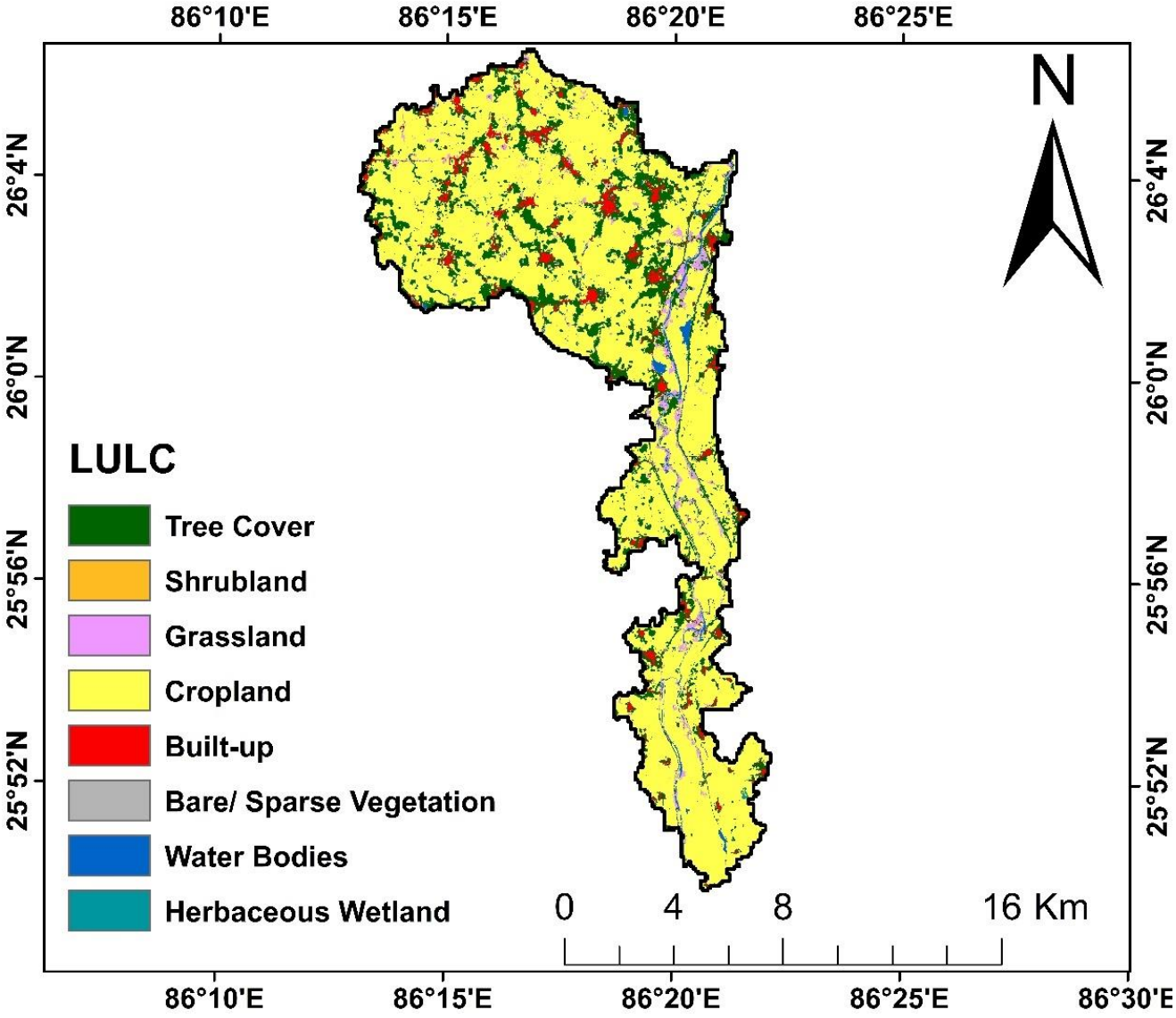

Figure 5.5 (a) Land Use/ Land Cover map of SW-11

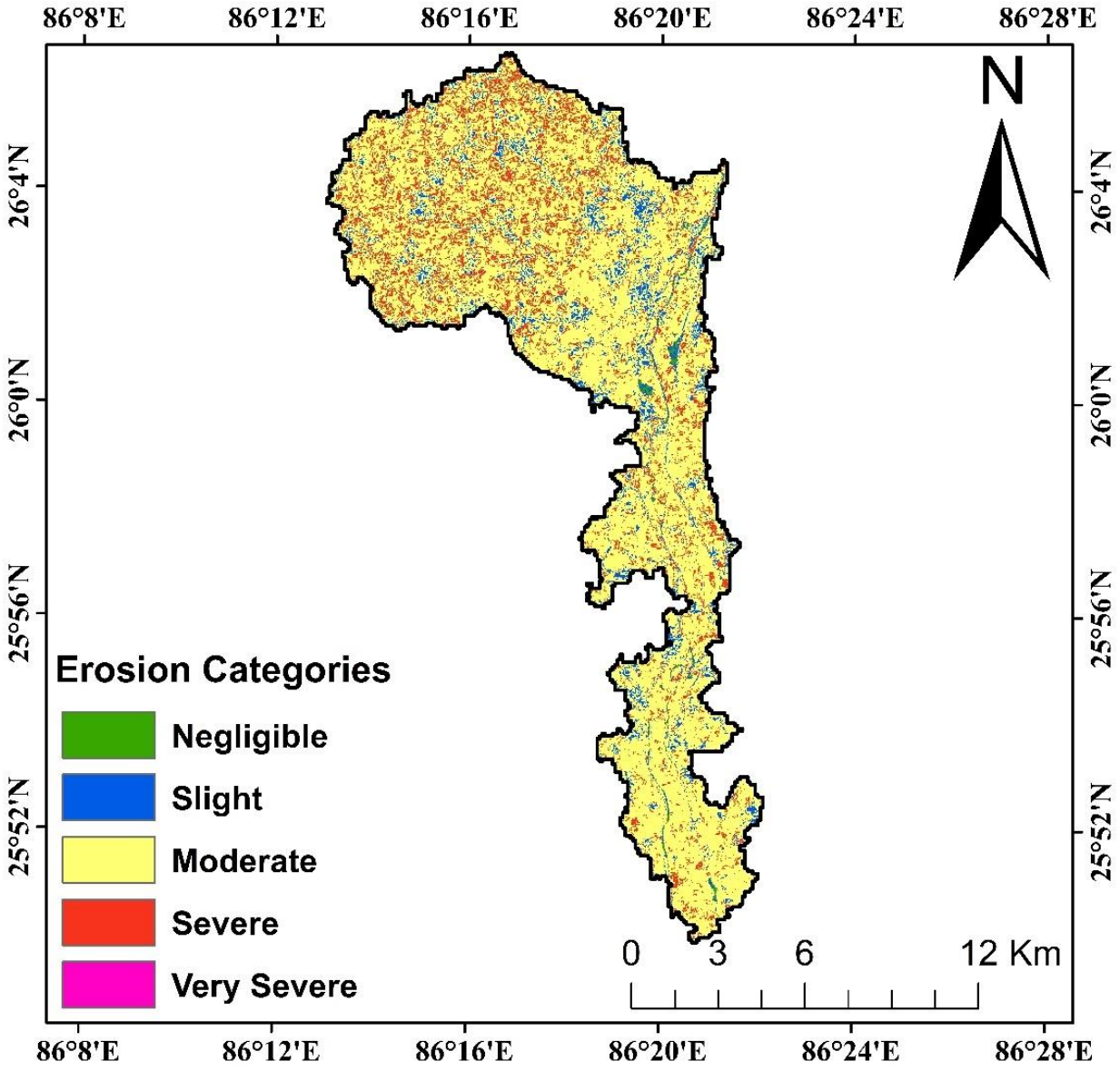

Figure 5.5 (b) Composite Erosion Intensity Unit (CEIU) map of SW-11

5.4.6 Sub-Watershed-12

This sub-watershed 12 has a catchment area of 4905 ha. The land use map is presented in Figure 5.6 (a). In this sub-watershed, the predominant land use is under agriculture (4127.59 ha) followed by tree cover (306.87 ha), herbaceous wetland (189.27 ha), built-up (144.76 ha), grassland (106.54 ha), water body (24.16 ha) and bare/sparse vegetation (5.70 ha). The area requiring treatment under the severe erosion class is about 535.03 ha (10.9%). The erosion areas are mostly concentrated under waste land and agriculture (Figure 5.6 (b)).

A.	**Biological Measures**	**Area (ha)**
1.	Cover Cropping	100
2.	Conservation tillage	100
3.	Mulching	100
4.	NTFP Cultivation	100
	Subtotal	**400**
B.	**Engineering Measures**	**Area (ha)**
1.	Field bunding	50
2.	Contour bunding	50
3.	Veg. Contour Trench	35.03
	Subtotal	**135.03**
	Grand Total (A+B)	**535.03**

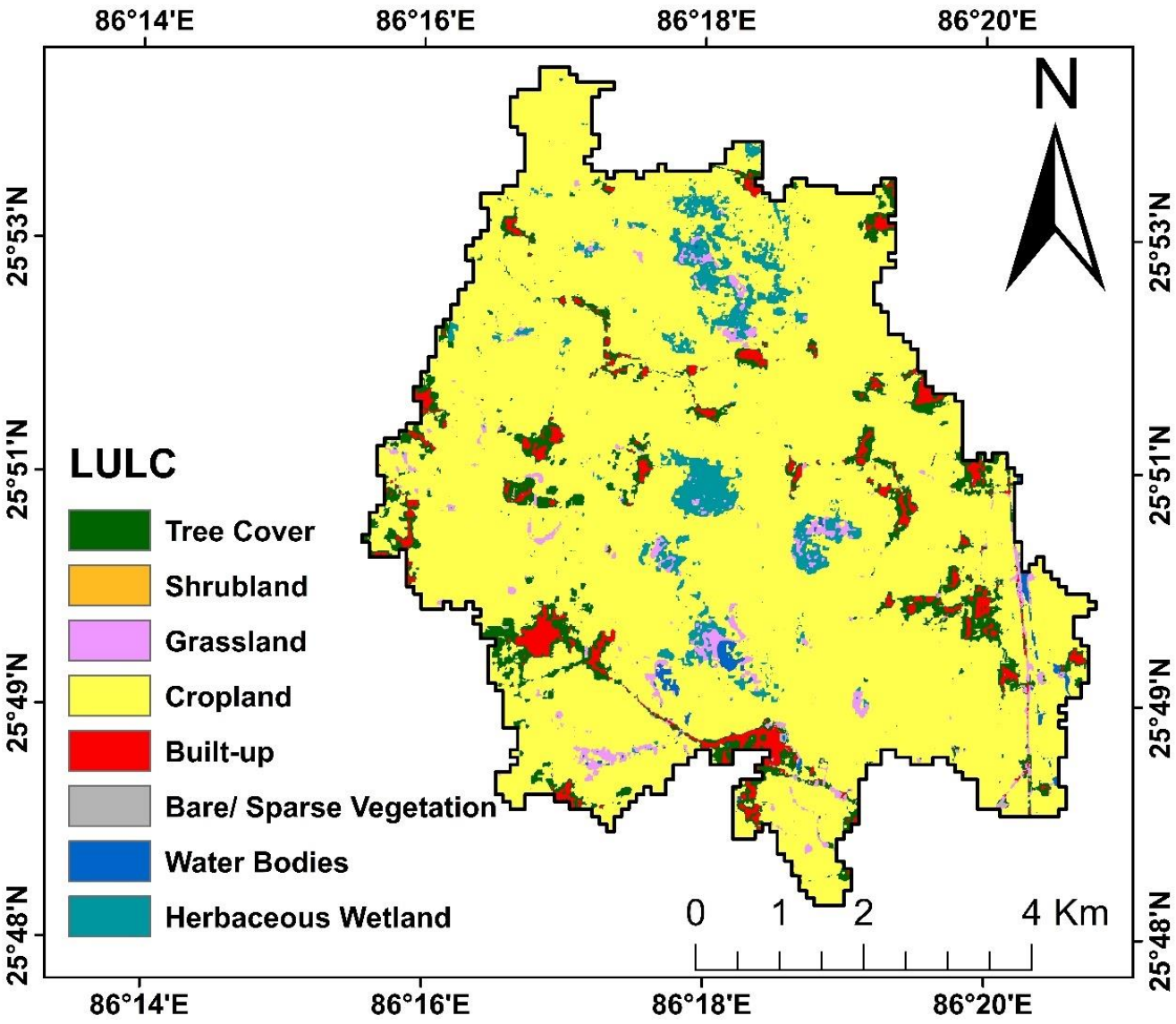

Figure 5.6 (a) Land Use/ Land Cover map of SW-12

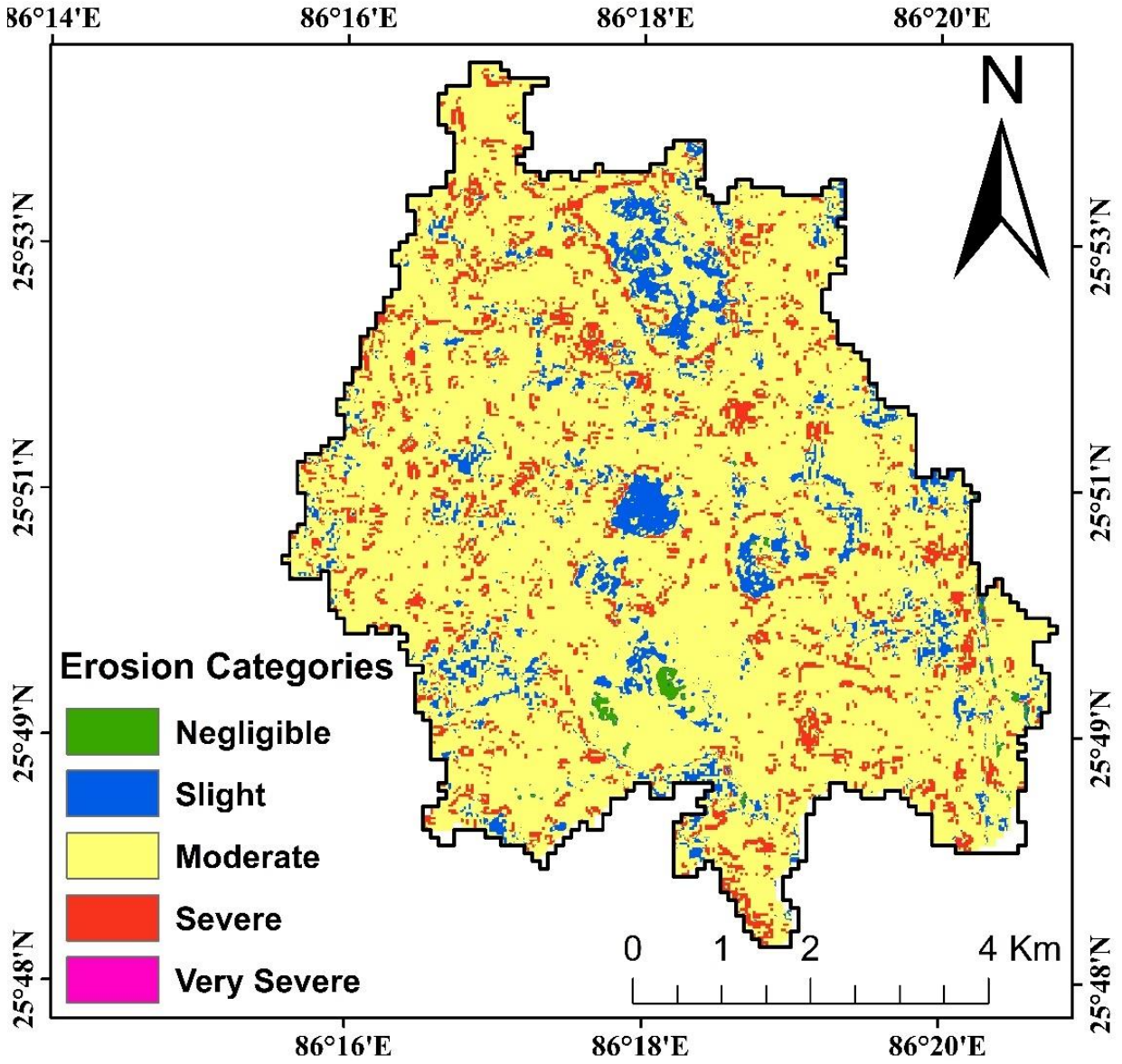

Figure 5.6 (b) Composite Erosion Intensity Unit (CEIU) map of SW-12

By adaptation of the above CAT plan, the sub-watersheds of LKRB will have a sustainable natural resource regime with highly productive resources (crops and trees) managed by the community, and therefore, would contribute significantly to the livelihoods of all the households in the area.

The treatment measures have been designed keeping in view the ecological as well as social dimensions of the project. The treatment measures emphasize the conservation of the catchment through plantation and by supporting engineering works. It envisages the active participation of the local community. Actual patches for plantation shall be earmarked physically by the CAT

implementing agency at the time of execution depending on the accessibility and treatability of the area.

5.5 COST ANALYSIS OF DIFFERENT WORKS UNDER PLAN

5.5.1 Biological Measures

The cost estimates for Cover Cropping, Agroforestry systems, Conservation tillage, Mulching, and NTFP Cultivation are presented in Table 5.3a. The cost estimates for Understory planting, Soil Microbial Inoculation,Riparian Buffer Zones, Regeneration Practices, and Afforestation are presented in Table 5.3b. Total cost estimation for various biological measures is presented in Table 5.4. The cost for these five watersheds falling under very severe and severe priority (SW-5, SW-1, SW-8, SW-10, SW-11, and SW-12) is approximately Rs. 827100000.

5.5.2 Engineering Measures

Engineering measures have been recommended for implementation within high-priority sub-watersheds SW-5, SW-1, SW-8, SW-10, SW-11, and SW-12, encompassing a total area of 11,020.76 hectares. However, due to the absence of requisite field survey data, the precise number and distribution of existing engineering measures remain unknown. Consequently, estimating the potential cost of future engineering interventions within the context of this erosion challenge is currently not feasible. To address this limitation and facilitate informed decision-making, a comprehensive field survey is recommended. This survey would map existing structures and provide crucial data for further analysis and developing a robust and cost-effective erosion mitigation plan.

Table 5.3a Cost estimate for biological measures

	Cover Cropping		Agroforestry systems		Conservation tillage		Mulching		NTFP Cultivation	
	area	cost (Rs 10000/ha)	area	cost (Rs 20000/ha)	area	cost (Rs 8000/ha)	area	cost (Rs 5000/ha)	area	cost (Rs 98200/ha)
SW-5	3000	30000000	3000	60000000	3500	28000000	2500	12500000	3000	294600000
SW-12	100	1000000			100	800000	100	500000	100	9820000
SW-8	500	5000000			500	4000000	500	2500000	250	24550000
SW-10	500	5000000	500	10000000	500	4000000	500	2500000	500	49100000
SW-11	500	5000000			200	1600000	200	1000000	300	29460000
SW-1	500	5000000			500	4000000	500	2500000	500	49100000
Total		51000000		70000000		42400000		21500000		456630000

Table 5.3b Cost estimate for biological measures

	Understory planting		Soil Microbial Inoculation		Riparian Buffer Zones		Regeneration Practices		Afforestation	
	area	cost (Rs 15000/ha)	area	cost (Rs 5000/ha)	area	cost (Rs 15000/ha)	area	cost (Rs 10000/ha)	area	cost (Rs 98200/ha)
SW-5	2500	37500000	2500	12500000	3500	52500000	3500	35000000		
SW-12										
SW-8			250	1250000			400	4000000		
SW-10	500	7500000	500	2500000	500	7500000	500	5000000		
SW-11			200	1000000			300	3000000		
SW-1			500	2500000			400	4000000	100	9820000
Total		45000000		19750000		60000000		51000000		9820000

Table 5.4 Total Cost estimate for biological measures

SW-Code	Total cost Table 5.3a + Table 5.3b (Rs)
SW-5	562600000
SW-12	12120000
SW-8	41300000
SW-10	93100000
SW-11	41060000
SW-1	76920000
Total	**827100000**

Chapter 6: Summary and Conclusions

6.1 Summary

Soil erosion poses significant threats to ecosystems, agricultural lands, and water resources, necessitating sophisticated approaches for assessment and management. In India alone, approximately 5334 million tonnes of soil are detached annually, with erosion rates reaching 16.40 Mg ha^{-1} $year^{-1}$, making it a critical issue not only in India but also in regions like Asia, Africa, and South America. Factors triggering erosion include steep slopes, climate variations, inappropriate land use, and land cover patterns.

Direct field measurements for soil erosion are accurate but time-consuming and costly. Therefore, various models like the Universal Soil Loss Equation (USLE) and the Revised Universal Soil Loss Equation (RUSLE) have been developed. Remote Sensing data and Geographic Information System (GIS) technologies have been increasingly employed for soil erosion estimation and prioritization of sub-watersheds. Advancements in soil erosion modeling, such as integrating sediment delivery ratio (SDR) into (R)USLE models, have enhanced accuracy and applicability. The InVEST-SDR model, for instance, integrates GIS and hydrological modeling, providing valuable insights into erosion risk spatial distribution.

However, limitations exist, such as the inability of the USLE model to estimate storm-wise sediment yields accurately at the watershed scale. The Modified Universal Soil Loss Equation (MUSLE) addresses this limitation and considers additional factors like runoff volume and peak discharge. The MUSLE model is used in conjunction with other established models like the Soil and Water Assessment Tool (SWAT) for better estimation.

Identifying critical erosion-prone areas and implementing best management practices are essential for soil and water conservation. The Catchment Area Treatment (CAT) plan addresses this by incorporating biological and engineering measures, along with social dimensions, to ensure eco-friendly and sustainable development. Spatial variability requires advanced techniques like satellite data and ground truth studies to estimate soil erosion, especially in complex landscapes, accurately.

Overall, the integration of advanced modeling techniques, GIS, and remote sensing data has significantly improved soil erosion assessment and management, enabling more effective erosion control and sustainable land management strategies.

Looking at the above-mentioned, the present study was conducted over a part of the Kamla River Basin (KRB) located within the Indian sub-continent. The prevailing environmental equilibrium in the area has been disrupted due to various factors, leading to extensive soil erosion characterized by the detachment and transportation of soil particles into nearby streams. The primary cause of this erosion can be attributed to the removal of protective soil cover, particularly in the form of forest vegetation, which has significantly contributed to the current erosion patterns observed within the catchment area. In light of these circumstances, this research was conceptualized and carried out to examine three prominent soil erosion assessment methodologies—namely, the Revised Universal Soil Loss Equation (RUSLE), the Integration of Spatially Explicit Watershed Modeling with the Sediment Delivery Ratio (InVEST-SDR), and the Modified Universal Soil Loss Equation (MUSLE). The amalgamation of these models aims not only to evaluate the spatial and temporal distribution of soil loss within the lower region of the KRB but also to establish a foundation for a targeted Catchment Area Treatment (CAT) Plan, facilitating strategic management of soil erosion within the area.

The present study was carried out with the following objectives:

1. The identification of vulnerable areas in the representative catchment of the Kamla River Basin using USLE/RUSLE, GIS, and remote sensing data
    - Soil loss estimation using RUSLE
    - Soil loss estimation using InVEST-SDR model
    - Sediment yield modeling using MUSLE
    - Prioritization of sub-watersheds based on SYI
2. Preparation of Catchment Area Treatment (CAT) plan for recommendation soil conservation measures in the vulnerable areas of the catchment

6.1.1 Soil loss estimation using RUSLE: The R, K, LS, C, and P factors were derived for the Lower Kamla River Basin to estimate the average annual soil loss for 2000, 2010, and 2020 under changing land use cover and uncertain climatic conditions. These estimates were analysed to understand the spatial distribution of soil erosion in the basin. The erosion risk map of the basin indicates that, on average, 58 % area of the basin falls under the slight erosion category, mostly agricultural and plantation areas. It is due to flatter topography, where the slope varies between 27 to 99 m above MSL and agricultural dominant (nearly 75%) land use land cover.

A major part of the basin is approx. 62% (4,510 km^2 out of a total area of 7,232 km2) falls in India, while the rest is in southeast Nepal. As the Kamla River basin has experienced a high sediment issue over the years downstream of the basin. In this study, only the Indian part (62%) of the basin was considered, which shows that a significant percentage of the basin area falls under the high to very severe erosion category. This is due to high annual rainfall, unprotected cultivation practices near the riverbank areas, and a lack of bank stabilization.

Overall, the findings from this approach indicated that significant erosion occurred from the basin, mostly stream bank erosion, is a major issue in the lower KRB, which may be exacerbated by high-intensity rainfall and frequent floods, resulting in a significant contribution of sediments at the lower parts.

6.1.2 Soil Erosion modeling using InVEST-SDR model: The InVEST-SDR model combines RUSLE with a sediment delivery ratio (SDR) to estimate sediment export. In this study, the model was employed to quantify the spatial distribution of soil loss and sediment delivery within the Kamla River Basin at the Jhanjharpur outlet.

The main motive behind employing the InVEST-SDR model in this study was to use observed sediment data and develop an accurate model to simulate and estimate soil loss for LKRB. However, there is a major limitation with this model, particularly in the context of this study. In this study, the observed sediment data was provided at Jhanjharpur station, where the model was calibrated for the catchment area at Jhanjharpur outlet, which encompassed a total area of 3436.43 km^2. Interestingly, of the total area, only 733.19 km^2 falls in India, which accounts for only 21.3 % of the area, and the remaining area lies in Nepal. The calibration parameters obtained for the model were assumed to be valid and applicable for the Lower KRB, which may produce uncertainty in the results. Due to the paucity of data at the outlet of Lower KRB, the InVEST-SDR was run for the LKRB to model the sediment dynamics, and the results obtained are considered to be a representation of critical erosion-prone areas.

The InVEST model results in this study cannot be validated due to a lack of observed data at the outlet. Nonetheless, the modeling results obtained from the InVEST-SDR model highlighted the process of soil loss dynamics (soil erosion, sediment export, and SDR) to distinguish sediment source and sediment delivery rates for the Lower KRB. The model focused only on overland erosion; it does not model gully, bank, or mass erosion. Outputs from the model included the sediment load delivered to the stream at an annual time scale, as well

as the amount of sediment eroded in the catchment and retained by vegetation and topographic features.

The inVEST-SDR model can be the preferred choice for identifying critical soil erosion-prone areas and consequent CAT planning only if data is available at the desired catchment outlet. This is a distributed model which, after calibration, is capable of estimating potential soil loss from each pixel and computing the delivery of sediment from each pixel to the stream.

6.1.3 Sediment Yield Estimation using MUSLE: The development of a Modified Universal Soil Loss Equation (MUSLE)--based model for the catchment area has proven to be highly effective in watershed management. This model excels as a predictive tool, accurately estimating sediment yield from specific storm events. Such precise predictions are vital for implementing efficient soil and water conservation strategies, identifying high erosion zones, and mitigating soil loss while preserving soil fertility.

In this study, our primary focus was on the region-specific variable coefficients of the MUSLE model for the Kamla River basin, utilizing data from the Jhanjharpur gauging station. The comparative analysis of the study demonstrates a strong correlation between the observed and the modeled sediment yield data. Consequently, the MUSLE model, with its optimized, calibrated, and validated parameters (a and b), offers an accurate estimation of sediment yield at the Jhanjharpur outlet. Moreover, this model can be extensively applied to estimate and predict sediment yield for various rainfall events under similar hydrological conditions.

6.1.4 Sub-watershed prioritization using SYI

In this study, the prioritization of sub-watersheds was carried out into twelve sub-watersheds based on the SYI approach documented by the All-India Soil and Land Use Survey (AISLUS). In the SYI method, the composite erosion intensity mapping unit (CEIU) was derived from the spatially varied soil texture, land use/land cover, and topography of the study area. Prioritization of sub-watersheds depicted SW5 as the major source of water-induced soil loss in the lower KRB, followed by sub-watersheds SW1, SW8, SW10, SW11, and SW12 fall under high-priority zones. Furthermore, in these sub-watersheds, improper agricultural activity and the mono-cropping system make it more vulnerable to erosion under extreme climatic conditions. Hence, these sub-watersheds require immediate implementation of conservation practices.

6.1.5 Recommendations for soil conservation measures through a Catchment Area Treatment Plan

To control the rate of soil erosion in the catchment, a sub-watershed-wise Catchment Area Treatment (CAT) plan has been prepared. This comprehensive plan addresses the multifaceted challenges posed by soil erosion within the lower KRB in India. The treatment measures have been suggested for land use classes based on Erosion Severity Classes. As per the need for treatment required under varied land use classes, suitable engineering, as well as vegetative/biological measures, have been proposed. For each sub-watershed, a CAT plan has been proposed, including areas under various engineering measures (field bunds, contour bunds, vegetative trenches, gully plugs) and biological measures (cover cropping, contour farming, agroforestry systems, conservation tillage, mulching, understory planting, soil microbial inoculation, riparian buffer zones).

6.2 Conclusions

The following conclusions are drawn from the present study:

1. Average soil loss rates for 2000, 2010, and 2020 were 19.94, 12.11, and 31.81 t/ha/yr. A significant area (about 30%) falls under Very high to Very severe erosion, mainly rainfall-induced erosion. Most of the severe (40-80 t/ha/yr) to very severe (>80 t/ha/yr) erosion occurred along the major rivers and their networks.
2. The Lower Kamla basin (India Part) has a significant % area falling under the high to very severe erosion category; also, stream bank erosion is a major issue in the lower KRB.
3. The InVEST-SDR model in this study was applied to make use of observed sediment data and develop a model to simulate and estimate soil loss for LKRB. However, its 733.19 km^2 (21.3 %) falls in India, and the remaining area lies in Nepal.
4. Optimized parameter values of a and b for the MUSLE model were found to be 10.7 and 0.429.
5. This model can be used to estimate sediment yield at the Jhanjharpur gauging station for a particular rainfall-runoff event
6. Based on the Silt Yield Index (SYI) values, SW5 Sub-watershed fall under very high priority category. Five sub-watersheds (SW1, SW8, SW10, SW11, SW12) fall under

high priority category. Most of the severe (40-80 t/ha/yr) to very severe (>80 t/ha/yr) erosion occurred along the major rivers and their networks.

7. CAT plans for individual sub-watersheds have been proposed along with tentative expenditure.

6.3 Future Scope

1. The precise number and distribution of existing engineering measures remain unknown. Consequently, estimating the potential cost of future engineering interventions within the context of this erosion challenge is currently not feasible. A comprehensive field survey is recommended to facilitate informed decision-making. This survey would map existing structures and provide crucial data for further analysis and development of a robust and cost-effective erosion mitigation plan.
2. To carry out the Soil and Water Assessment Tool (SWAT) model simulation study for evaluating the sediment yield of a catchment. If data becomes available at the desired outlet.
3. To study long-term changes in hydro-meteorological variables of the basin using the SWAT model.
4. To identify erosion hotspots and prioritize sub-watersheds for soil and water conservation planning using the SWAT model.
5. Evaluation of the effect of Best Management Practices on the hydrological response of the river basin for sustainable basin management.

References

Adhakari, B.R., 2013. Flooding and inundation in Nepal Terai: issues and concerns. Hydro Nepal: Journal of Water, Energy and Environment, 12, pp.59-65.

AISLUS, 1991. All India Soil and Land Use Survey, Ministry of Agriculture and Corporation, Government of India, New Delhi.

Shi, W., Chen, T., Yang, J., Lou, Q. and Liu, M., 2022. An improved MUSLE model incorporating the estimated runoff and peak discharge predicted sediment yield at the watershed scale on the Chinese Loess Plateau. Journal of Hydrology, 614, p.128598.

Barrow, C.J. 1991. Land degradation: development and breakdown of terrestrial environments. Cambridge University Press.

Bhattacharya, R.K., Chatterjee, N.D. and Das, K. 2020. Sub-basin prioritization for assessment of soil erosion susceptibility in Kangsabati, a plateau basin: a comparison between MCDM and SWAT models. Science of the Total Environment, 734, p.139474.

Benavidez, R., Jackson, B., Maxwell, D. and Norton, K., 2018. A review of the (Revised) Universal Soil Loss Equation ((R) USLE): With a view to increasing its global applicability and improving soil loss estimates. Hydrology and Earth System Sciences, 22(11), pp.6059-6086.

Guo, Z., Yan, Z., PaErHaTi, M., He, R., Yang, H., Wang, R. and Ci, H., 2023. Assessment of soil erosion and its driving factors in the Huaihe region using the InVEST-SDR model. Geocarto International, 38(1), p.2213208.

Gashaw, T., Bantider, A., Zeleke, G., Alamirew, T., Jemberu, W., Worqlul, A.W., Dile, Y.T., Bewket, W., Meshesha, D.T., Adem, A.A. and Addisu, S., 2021. Evaluating InVEST model for estimating soil loss and sediment export in data scarce regions of the Abbay (Upper Blue Nile) Basin: Implications for land managers. Environmental Challenges, 5, p.100381.

Borselli, L., Cassi, P. and Torri, D., 2008. Prolegomena to sediment and flow connectivity in the landscape: A GIS and field numerical assessment. Catena, 75(3), pp.268-277.

Cavalli, M., Trevisani, S., Comiti, F. and Marchi, L., 2013. Geomorphometric assessment of spatial sediment connectivity in small Alpine catchments. Geomorphology, 188, pp.31-41.

Chakraborty, T., Kar, R., Ghosh, P. and Basu, S., 2010. Kosi megafan: Historical records, geomorphology and the recent avulsion of the Kosi River. Quaternary International, 227(2), pp.143-160.

CSIRO and WECS, 2021. Water Resources Development Strategy for the Kamala River Basin, Nepal. CSIRO, Australia and Water and Energy Commission Secretariat, Government of Nepal, Singadurbar, Kathmandu. 200 pp.

Dabral, P.P., Baithuri, N. and Pandey, A. 2008. Soil erosion assessment in a hilly catchment of North-Eastern India using USLE, GIS and remote sensing. Water Resources Management, 22(12), 1783-1798.

Desmet, P.J.J. and Govers, G., 1996. A GIS procedure for automatically calculating the USLE LS factor on topographically complex landscape units. Journal of soil and water conservation, 51(5), pp.427-433.

Fox, D.M. and Bryan, R.B., 2000. The relationship of soil loss by inter-rill erosion to slope gradient. Catena, 38(3), pp.211-222.

GoN (Government of Nepal), President Chure-Tarai Madhesh Conservation Development Board, 2017. President Chure-Tarai Madhesh Conservation and Management Master Plan. 267 pp.

Jaafar, H.H. and Ahmad, F., 2019. GCN250, global curve number datasets for hydrologic modeling and design. figshare.

Keesstra, S., Nunes, J., Novara, A., Finger, D., Avelar, D., Kalantari, Z. and Cerdà, A. 2018. The superior effect of nature-based solutions in land management for enhancing ecosystem services. Science of the Total Environment, 610, 997-1009.

Khadse, G.K., Vijay, R. and Labhasetwar, P.K., 2015. Prioritization of catchments based on soil erosion using remote sensing and GIS. Environmental Monitoring and Assessment, 187, pp.1-11.

Mandal, D. and Sharda, V.N. 2013. Appraisal of soil erosion risk in the Eastern Himalayan region of India for soil conservation planning. Land Degradation & Development, 24(5), 430-437.

MFSC (Ministry of Forests and Soil Conservation), 2016. Forest Sector Strategy, 2016–2025. 94 pp. http://mofe.gov.np/ downloadfile/Forestry%20Sector%20 Strategy%20%20(2016-2025)_1526466721.pdf

Narayana, D.V. and Babu, R. 1983. Estimation of soil erosion in India. Journal of Irrigation and Drainage Engineering, 109(4), 419-434.

Nepal Development Research Institute (NDRI) in collaboration with Commonwealth Scientific and Industrial Research Organization (CSIRO) (2016) Kamala Basin [online] Available From:http://www.ndri.org.np/wpcontent/uploads/2017/11/2_Kamala-Basin_FinalReport-19th-Feb.pdf.

Pandey, A., Chowdary, V. M., and Mal, B. C. 2007. Identification of critical erosion prone areas in the small agricultural watershed using USLE, GIS and Remote Sensing. Water Resour. Management, 21(4), 729–746.

Pandey, A., Chowdary, V.M., Mal, B.C. and Dabral, P.P. 2011. Remote sensing and GIS for identification of suitable sites for soil and water conservation structures. Land Degradation & Development, 22(3), pp.359-372.

Quansah, C. 1981. The effect of soil type, slope, rain intensity and their interactions on splash detachment and transport. Journal of Soil Science, 32(2), pp.215-224.

Renard, K.G., 1997. Predicting soil erosion by water: a guide to conservation planning with the Revised Universal Soil Loss Equation (RUSLE). US Department of Agriculture, Agricultural

Research Service.

Renschler, C.S., Mannaerts, C. and Diekkrüger, B. 1999. Evaluating spatial and temporal variability in soil erosion risk—rainfall erosivity and soil loss ratios in Andalusia, Spain. Catena, 34(3-4), 209-225.

Romshoo, S. Altaf, M. Amin, U. 2017. Sediment yield estimation for developing soil conservation strategies in GIS environment for the mountainous Marusudar catchment, Chenab basin, J&K, India. J. Himal. Ecol. Sustain. Dev. 12, 16–32.

Sah, K. and Lamichhane, S. 2019. GIS and remote sensing supported soil erosion assessment of Kamala River Watershed, Sindhuli, Nepal. International Journal of Applied Sciences and Biotechnology, 7(1), 54-61.

Singh, R. and Phadke, V.S. 2006. Assessing soil loss by water erosion in Jamni River Basin, Bundelkhand region, India, adopting universal soil loss equation using GIS. Current Science, 1431-1435.

USDA-Soil Conservation Services (USDA-SCS). 1972. Hydrology in SCS National Engineering Handbook. Science 4, US Department of Agriculture, Washington, D.C.

Wagh, S. and Manekar, V. 2022. Soil Erosion Planning for Reservoir Watershed Using Sediment Yield Index Method: A Case Study of Ujjani Reservoir. Journal of The Institution of Engineers (India): Series A, 103(4), pp.1341-1354.

WECS and CSIRO, 2020. State of the Kamala River Basin, Nepal. 68pp. https://doi.org/10.25919/10mp-bc20

Yang, D., Kanae, S., Oki, T., Koike, T. and Musiake, K., 2003. Global potential soil erosion with reference to land use and climate changes. Hydrological processes, 17(14), pp.2913-2928.

Zanaga, D., Van De Kerchove, R., De Keersmaecker, W., Souverijns, N., Brockmann, C., Quast, R., Wevers, J., Grosu, A., Paccini, A., Vergnaud, S., Cartus, O., Santoro, M., Fritz, S., Georgieva, I., Lesiv, M., Carter, S., Herold, M., Li, Linlin, Tsendbazar, N.E., Ramoino, F., Arino, O., 2021. ESA WorldCover 10 m 2020 v100. (https://doi.org/10.5281/zenodo.5571936)

Annexure A

Field Visit Report -1

1. Introduction

The first field visit was carried out from 29th April 2022 to 5th May 2022 at the project site i.e., Kamla River basin, for collecting the field's hydrological and geological information. The aim of the field visit were (i) to collect the ground truth points at multiple sites of the study area for land use land cover map preparation, (ii) Collection of soil samples for soil texture analysis, and (iii) Basic information collection pertaining to cropping pattern and tillage implements.

The project site is located in the Madhubani district of Bihar State. The livelihood of local people directly depends on agriculture and its allied activities. Farmers of the site usually cultivating paddy in kharif season and wheat in the Rabi season. Hence, the paddy-wheat cropping system is dominated in the project site.

2. Description of project site

The project site is located between 26˚ 12' N to 26˚ 37′ N latitude and 86˚ 08'30″ E to 86˚ 24'15″ E longitude (Figure A.1) and its geographical area is about 707.69 sq. km. The elevation of the project site varies from 33 m to 95 m. The site has a sub-tropical climate with tolerable summer and pleasant winter. The average annual rainfall is 1205.31 mm (1981-2020), of which the south-west monsoon contributes nearly 83% of total rainfall. During the summer season, daily maximum and minimum temperature vary from 36^{0}C to 24 ^{0}C, whereas in winter, temperature ranges from 24^{0}C to 10^{0}C.

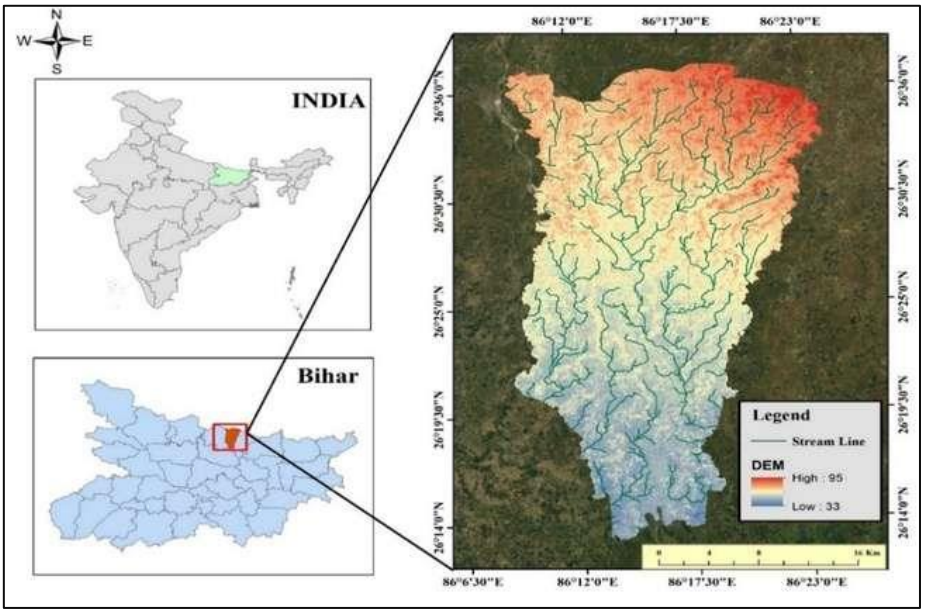

Figure A.1 Location map of the project site

The site is mainly drained by the river Kamla and its tributaries e.g., Soni and Balan. Each year frequent floods occur during monsoon season, particularly along the Kamla river and its tributaries, and is wracked by floods. As a result, several parts of the project site undergo severe soil erosion (Figure A.2).

Figure A.2 Soil erosion prone areas of the project site

3. Task performed at the project site

Collection of ground truth points and soil samples

In order to prepare a highly realistic and accurate land use land cover (LULC), a number of ground truth points throughout the site were collected. Figure A.3 shows some pictures of ground truth points.

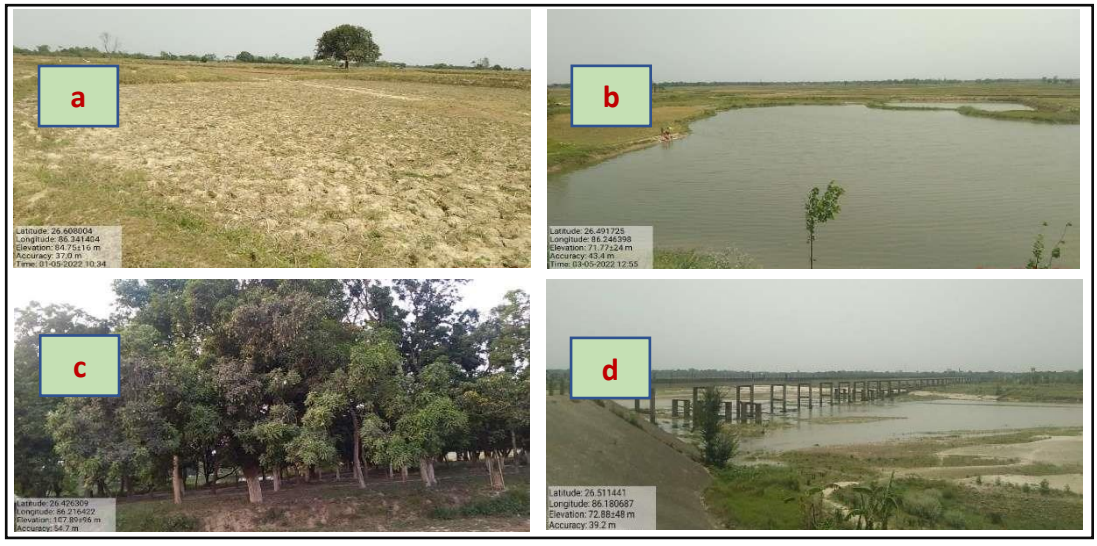

Figure A.3 Ground truth points at project site (a) agricultural land (b) water-bodies (c) plantation (d) Kamla river

Total of 20 soil samples were also collected from different locations in the upper region of the Kamla river basin to conduct soil texture analysis (Figure A.4). All samples were collected below 5-10 cm from the soil surface. Soil texture is directly related to the soil erodibility factor (K), which has a significantly affects soil erosion estimation.

Figure A.4 Soil sample collection from the field

5. Task performed at the IWM Laboratory of the WRD&M lab. after the field trip

Prepared LULC map

Figure A.5 shows the LULC map of the project site. The map is prepared using the LANDSAT 8 imagery of 2022 in the Google Earth Engine (GEE) platform. The classified image is verified with the collected ground truth points and found an overall accuracy of more than 95%. Around 70% area of the total area, falls under cultivation, followed by plantation (21%), built-up (4%), bare land (3%), and water bodies (2%). Paddy and wheat are the major Kharif and Rabi crops of the district. Mango trees are the most common plantation in the site.

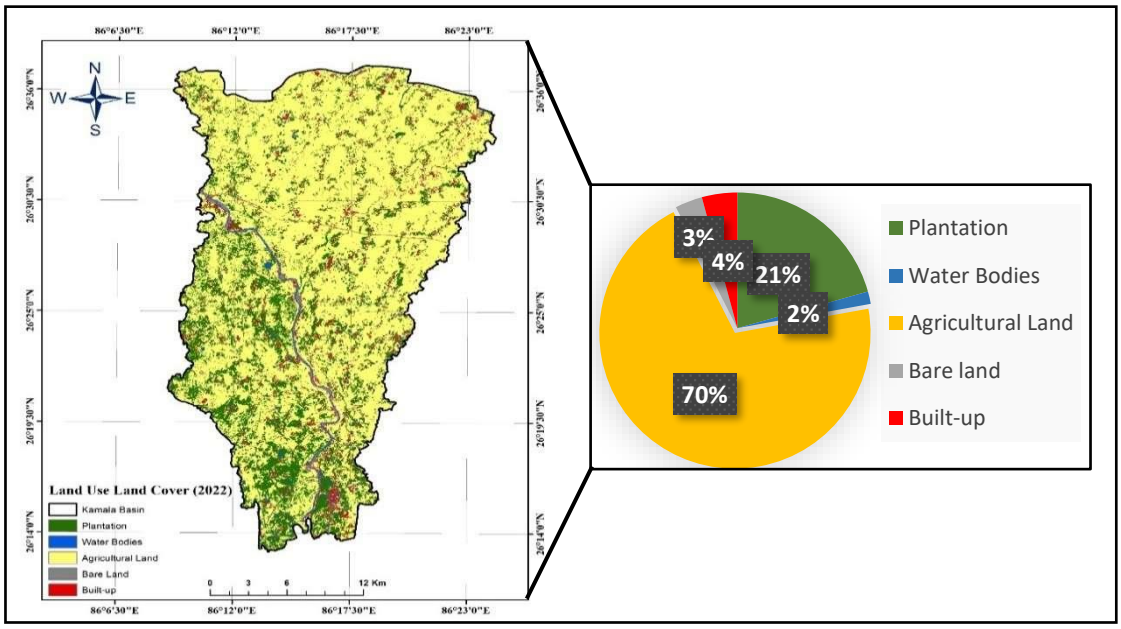

Figure A.5 LULC map of the site

Soil Texture Analysis

Collected soil samples are tested at the Irrigation Water Management (IWM) Laboratory of Deptt. of WRDM, IIT Roorkee using hydrometer method (Figure A.6). Sand, silt, and clay percentage are identified after hydrometer test. Furthermore, soil types are also verified using the textural triangle chart. Analysed results are shown in the Table A.1.

Figure A.6 Soil sample testing at the laboratory

Table A.1 Results of Soil Texture location of sample collection, soil texture and soil type

S. No	**Location**		**Soil Texture**			**Soil Type (Textural Triangle)**
	Latitude	Longitude	Sand (%)	Silt (%)	Clay (%)	
1.	26.43268	86.24158	63.68	32.72	3.60	Sandy loam
	26.43268	86.24158	60.18	35.72	4.10	Sandy loam
2.	26.49793	86.29683	62.68	33.72	3.60	Sandy loam
	26.49793	86.29683	61.58	34.26	4.16	Sandy loam
3.	26.38891	86.3252	55.68	44.32	0	Sandy loam
	26.38891	86.3252	57.68	42.32	0	Sandy loam
4.	26.50565	86.1914	75.68	24.32	0	Loamy Sand
	26.50565	86.1914	76.68	23.32	0	Loamy Sand
5.	26.5454	86.2901	61.68	38.32	0	Sandy loam
	26.5454	86.2901	60.68	39.32	0	Sandy loam

6.	26.60441	86.33841	60.68	33.72	5.6	Sandy loam
	26.60441	86.33841	59.68	32.72	7.60	Sandy loam
7.	26.60448	86.29797	54.68	45.32	0	Sandy loam
	26.60448	86.29797	56.68	43.32	0	Sandy loam
8.	26.506002	86.19206	52.68	47.32	0	Sandy loam
	26.506002	86.19206	53.68	46.32	0	Sandy loam
9.	26.55886	86.29795	53.68	46.32	0	Sandy loam
	26.55886	86.29795	57.68	42.32	0	Sandy loam
10.	26.5717	86.38556	60.68	39.32	0	Sandy loam
	26.5717	86.38556	63.68	36.32	0	Sandy loam

6. Cropping patterns and Tillage operation

Paddy-wheat is the major cropping system in the study area. For Tillage operation, the farmers mainly use secondary tillage implements e.g., rotavator and cultivator.

Annexure B

Field Visit Report -2

1. Introduction

The second field visit was conducted from 23rd August 2022 to 29th August 2022 at the project site, i.e., in the Kamla River Basin, in Bihar, for collecting the field's hydrological and geological Information.

1.1 Purpose of field visit

(i) To collect the ground truth points at multiple locations of the project sites (Darbhanga and Madhubani Districts) to prepare a precise land use map.

(ii) Collection of Soil Samples for Soil texture Analysis.

(iii) Basic information collection pertaining to cropping patterns and tillage implements.

(iv) Measuring the river geometry of major streams.

(v) Measuring the suspended sediment load and surface velocity at the gauging site (Jhanjharpur) in the project area.

(vi) Identification of basin outlets, which drains the whole basin.

(vii) Visiting the CWC office in Patna

2. Field Visit Details

2.1 Collection of Ground Truth Points

In this initial stage of the study, land use classes and land cover (LULC) were identified based on an intensively ground truth survey. The survey was conducted in the whole river basin from 24th August to 28th August 2022. Total of 368 survey points were collected (Figure B.1). In this ground truth survey, equipment (i.e., GPSs, geo-corrected printed image sheet, and cameras) were utilized to facilitate the ground truthing.

Figure B.1 Ground truth points collected in the project site

The main purpose of ground-truthing was to: (i) identify the LULC of the actual location and then compare it to what is shown on the image. (ii) identify colors, tone shape, texture, location, and size (iii) verify and update existing data, especially data on the map sheets or topographic maps and (iv) collect related data/information from local people.

Figure B1 shows generate a map of land use classes and land cover of the lower KRB after verifying ground truthing, which depicts six main land use types: (i) plantation (ii) shrubland (iii) cropland (iv) build-up (v) barren land and (vi) water-bodies. The region with comparatively rich cropland (mostly as a result of Kharif and rabi crops), which is approx. two-thirds of its area. Anthropogenic plantation (mainly mango, bamboo, and banana) is also the most dominant land use. Built-up area is utilized less than 5% (Figure B.2).

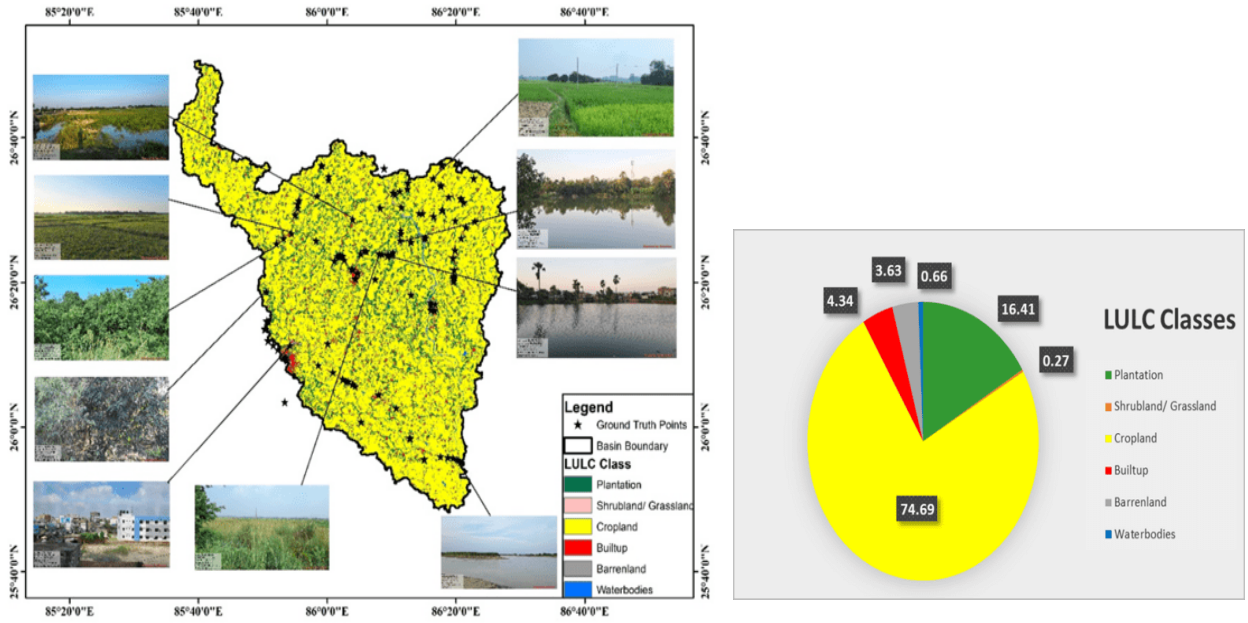

Figure B.2 LULC map of the lower region of KRB

2.2 Soil Samples Collection and Textural Analysis

Soil samples were collected from different locations on the project site. Total of 48 soil samples were collected to perform the textural analysis (Figure B.3). Mostly, topsoil at a depth of 5-10 cm was collected to conduct the soil textural analysis.

Figure B.3 Soil Samples collection in the project area

2.2.1 Soil Sample Analysis

The collected soil samples were analyzed in the IWM Laboratory of the Department of Water Resources Development and Management, IIT Roorkee using soil hydrometers and USDA textural triangle methods (Figure B.4). Analysed results are reported as percentages of % sand, % silt, and % clay (Table B1). Later, soil texture was identified based on the USDA textural triangle. Results show the basin consists of mainly three types of soils: clay, loam, and sandy loam. The dominant soil is loam 62% followed by sandy loam soil (26%) is also distributed along the river banks and clay soil (12%) (Figure B.5)

Figure B.4 Hydrometer Testing of soil sample

Table B.1 Analyzed texture results of collected soil samples

S. No	Latitude	Longitude	Sand (%)	Silt (%)	Clay (%)	Soil Type (Textural Triangle)
1.	26.269	86.268	62.68	34.72	3.60	Sandy Loam
2	26.497	86.296	60.18	35.72	4.10	Sandy Loam
3.	26.571	86.385	62.68	33.72	3.60	Sandy loam
4	26.604	86.297	61.58	34.36	4.16	Sandy loam
5.	26.604	86.297	63.68	44.36	1	Sandy loam
6	26.603	86.2979	57.68	42.32	0	Sandy loam
7.	26.608	86.341	75.68	24.32	0	Sandy loam
8	26.608	86.341	76.68	23.32	0	Sandy loam
9.	26.608	86.340	61.68	38.32	0	Sandy loam
10	26.517	86.353	60.68	39.32	0	Sandy loam
11.	26.548	86.208	60.68	33.72	5.6	Sandy loam
12	26.491	86.245	59.68	32.72	7.60	Sandy loam
13.	26.433	86.251	54.68	45.32	0	Sandy loam
14	26.426	86.216	56.68	43.32	0	Sandy loam
15.	26.159	85.888	52.68	47.32	0	Sandy loam
16	26.460	86.359	53.68	46.32	0	Sandy loam
17.	26.311	85.842	53.68	46.32	0	Sandy loam
18	26.011	86.087	57.68	42.32	0	Sandy loam
19.	26.074	86.132	60.68	39.32	0	Loam
20	26.043	86.178	63.20	36.80	0	Loam
21	25.974	86.213	48.58	38.26	13.16	Loam
22	25.928	86.325	49.36	40.52	10.12	Loam
23	25.931	86.293	46.28	42.68	11.04	Loam
24	26.095	86.072	42.36	40.18	17.46	Loam
25	26.142	85.976	44.72	42.36	12.92	Loam
26	26.601	85.986	45.18	41.72	13.1	Loam
27	26.532	85.974	43.68	45.36	10.96	Loam
28	26.569	86.004	48.32	40.68	11.00	Loam

29	26.503	85.924	47.32	41.72	15.96	Loam
30	26.405	86.101	48.68	41.72	9.6	Loam
31	26.405	86.101	45.18	42.72	12.10	Loam
32	26.191	86.001	47.68	40.72	11.6	Loam
33	26.445	85.907	46.72	42.18	11.1	Loam
34	26.421	85.868	46.68	39.72	13.6	Loam
35	26.429	85.971	48.18	40.72	11.1	Loam
36	26.405	86.101	45.68	41.72	12.6	Loam
37	26.402	86.170	47.18	38.68	14.14	Loam
38	26.478	86.066	42.36	40.18	17.46	Loam
39	26.435	86.346	44.72	42.36	12.92	Loam
40	26.407	86.331	45.18	41.72	13.1	Loam
41	26.343	86.328	43.68	45.36	10.96	Loam
42	26.304	86.218	44.72	42.18	13.1	Loam
43	26.340	86.124	49.42	35.36	15.22	Loam
44	26.354	86.079	46.42	40.22	13.36	Loam
45	26.382	86.019	47.22	39.42	13.36	Loam
46	26.504	86.138	45.92	36.26	17.82	Loam
47	26.539	86.172	60.68	39.32	0	Sandy loam
48	26.473	86.382	63.20	36.80	0	Sandy loam

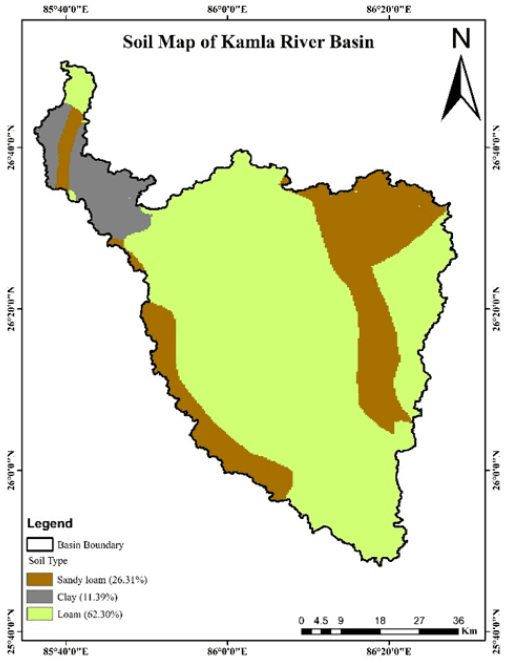

Figure B.5 Soil map of the project site

2.3 Cropping patterns and Tillage operation

The overall cropping pattern of the project site is a typical agricultural economy. Farmers of the site mainly follow the cereal-oriented cropping system. Wheat-rice is the major dominant cropping pattern. Apart from the cultivation, the farmers are also heavily engaged with agricultural allied sectors such as dairy, goatry, and fruits like mango cultivation. For land preparation and sowing of the seasonal crops, the farmers of the district highly depend on the secondary tillage operation. Tractor-operated cultivators and rotavators, and indigenous plows are the major tillage equipment used for tillage operation.

2.4 Measurement of Suspended Sediment and River Cross-section

The monitoring and analysis of Suspended Sediment Concentration (SSC) in a river system are often important to understand hydro-geological processes that are directly connected with soil erosion, land use degradation, extreme hydrological events such as floods, and ecological conditions. Therefore, SSC was also monitored at four locations in the KRB in post-monsoon season of the year 2022 using a suspended sediment analyser (Figure B.6). The result reports that suspended sediment concentration varies from 231 mg/l to 300 mg/l.

Figure B.6 Measurement of suspended sediment concentration and river cross-sections

Table B.2 Estimated SSC values in KRB

S. No	Date of Sampling	Location	Suspended sediment concentrations	Width of the river
1.	25.08.22	Imlighat, Jhagarua	240 mg/l	15 m
2.	26.08.22	U/s Jhanjharpur	231 mg/l	60 m
3.	26.08.22	D/s Jhanjharpur	260 mg/l	64 m
4.	27.08.22	Pakariya	300 mg/l	82 m

2.5 Drainage Pattern and Canal Networks

The Kamla enters India near Jayanagar and flows in the north-eastern direction, finally meeting in Kosi river near Ichwara, Alauli, Khagaria district of Bihar. It crosses four districts of Bihar: Madhubani, Darbhanga, Samastipur, and Khagaria, over a length of 120 km. This basin is situated between Bagmati river basin and the Kosi river basin, and annual flooding is characteristic of the basin. The flood plain is usually 0.5 to 1.5 km wide. To control flood, a system of canals is distributed in the whole basin. It also plays a major role in water resource transport for producing crops. Figure B7 shows the location of major canals and river tributaries passes through the basin. The confluence points of Kamal river with Bagmati river near Pakariya and with river Kosi near Alauli, ultimately joining the Ganga river. The drainage pattern of the basin and distributed major canals are shown in Figure B.7.

2.6 Location of Gauge Site and Identification of Basin Outlet

There are three gauging stations, namely Jaynagar, Jhanjharpur and Jhagarua are available in the lower region KRB where regular flow is being monitored by the CWC, Lower Ganga Basin. Figure B.9 shows the locations of the gauge sites in the lower KRB.

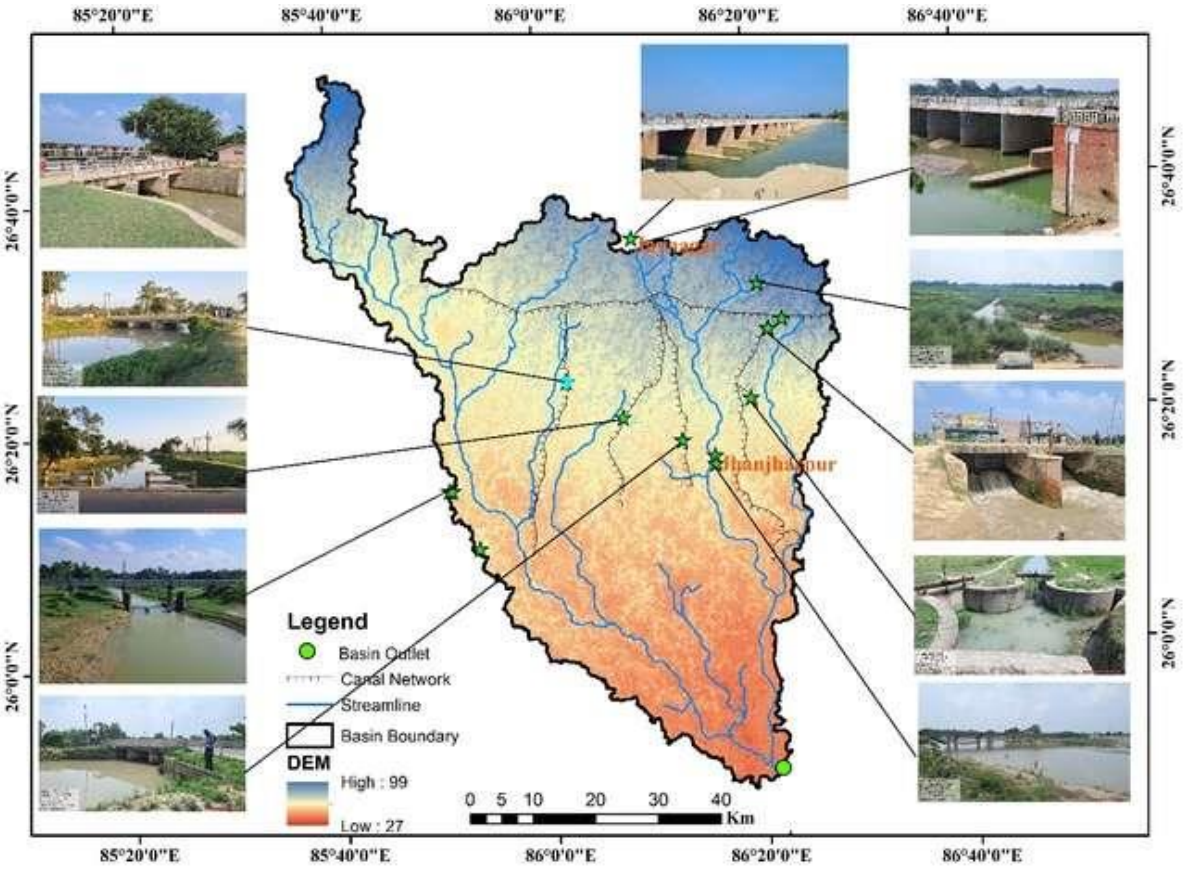

Figure B.7 Location of major canals

Figure B.8 Photographs of gauging sites (Jaynagar and Jhanjharpur) in the basin

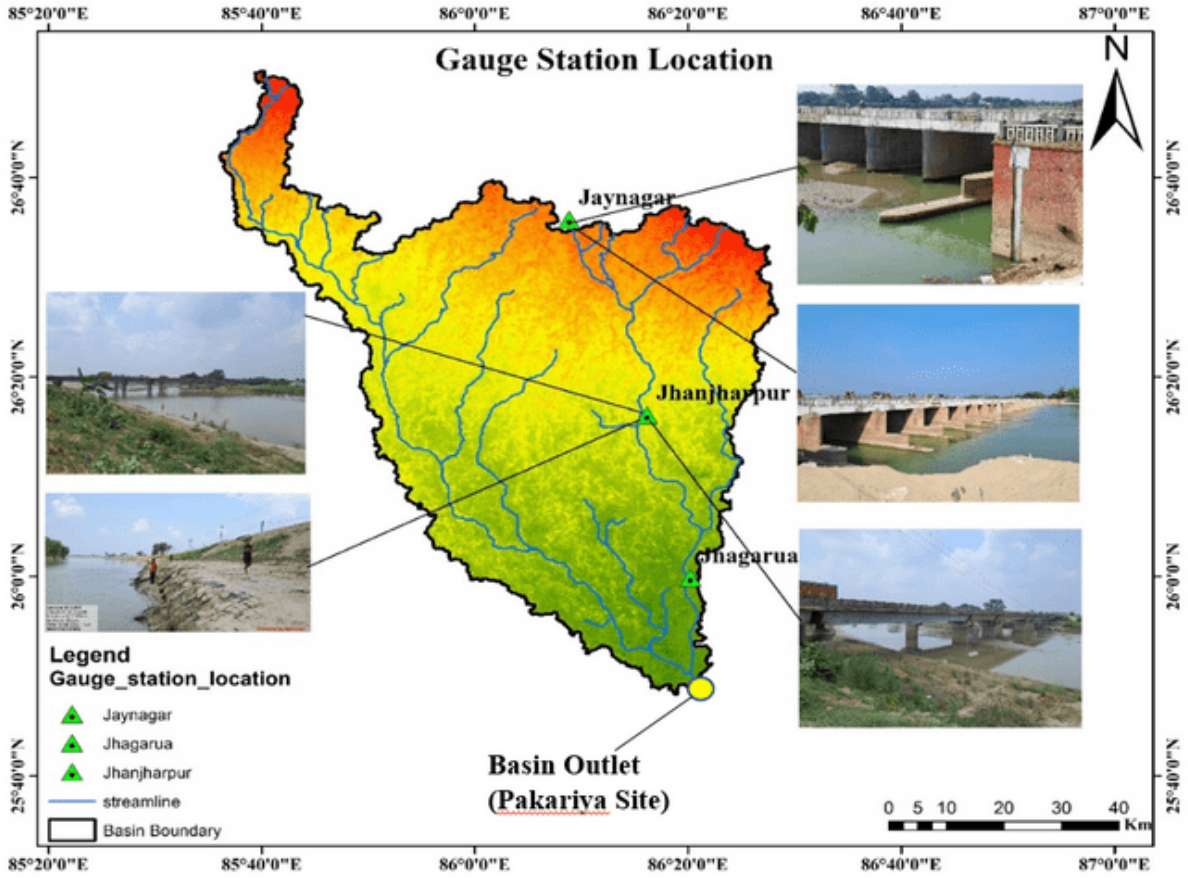

Figure B.9 Location of gauging sites and basin outlet

2.7 Visit of the CWC office

Based on a technical meeting held on 12th August 2022 with CWC officials, project team visited the CWC office, in Patna on 24th August 2022 to discuss about data procurement. They assure to provide daily discharge and sediment data for the mentioned gauging sites.

2.8 Erosion Control Practices

Soil erosion is a common phenomenon in the basin due to high rainfall and frequent occurrence of extreme events like floods. Control measures, i.e., field bunding, are often used to restrict erosion from the agricultural land, and the construction of river bank embankments to protect the bank erosion are practiced in the basin (Figure B.10).

Figure B.10 Erosion control practices in the basin